

# **PHASE II: Experimental Evaluation of Pressure Equalization Factors and Wind Resistance of Vinyl Siding Systems Using a Multi-Chamber Pressure Test Bed**

Project #: P0150335

---

Submitted to:

## **Florida Department of Business and Professional Regulation**

Mo Madani, Program Manager  
Building Codes and Standards  
1940 North Monroe Street  
Tallahassee, Florida 32399

Prepared by:

David O. Prevatt, Ph.D., PE (MA)  
Principal Investigator  
Associate Professor (Structures)

Report No. 08-20  
25 July 2020

David B. Roueche, Ph.D.  
Assistant Professor (Auburn University)

Daniel J. Smith, Ph.D.  
Executive Director, Venrisk Consulting, Boulder CO

Graduate Research Assistants:

Oscar Lafontaine, Xinyang Wu, Dmitrii Golovichev (University of Florida)  
Brandon Rittelmeyer, Brett Davis, Jinyi Wei (Auburn University)

---

Engineering School of Sustainable Infrastructure and Environment  
Department of Civil and Coastal Engineering  
University of Florida  
365 Weil Hall  
P.O. Box 116580  
Gainesville, FL 32611-6580



## **DISCLAIMER**

The material presented in this research report has been prepared in accordance with recognized engineering principles. This report should not be used without first securing competent advice with respect to its suitability for any given application. The publication of the material contained herein does not represent or warrant on the part of the University of Florida or any other person named herein, that this information is suitable for any general or particular use or promises freedom from infringement of any patent or patents. Anyone making use of this information assumes all liability for such use.

## EXECUTIVE SUMMARY

The objective of this research study was to conduct experimental studies identifying the effects of spatio-temporally varying loads on the net pressure distributions on vinyl siding wall systems. Phase I (2019) of this project developed a pressure test chamber and methodology suitable for performing the experimental testing. Phase II (2020) of the project focused on performing the experimental testing on multiple vinyl siding systems, using the Spatio-Temporal Loading Actuator, to explore pressure equalization effects under a range of pressure loading conditions.

Due to health and safety concerns related to the COVID-19 pandemic, the University of Florida's campus was closed, curtailing our experimental research for three months. After resuming on 15 June 2020, we completed a battery of tests using our multi-chamber pressure test device on five of the six planned test specimens. The specimens included vinyl siding products with single-hem, curled hem and double-hem fastening systems. Pressure series included constant pressure, sinusoidal, and stochastic pressure traces produced by up to four pressure chambers. The test results provide good insight into the function and limitations of the multi-chamber test bed and the pressure equalization behavior of vinyl siding systems when subjected to static, and dynamic pressure traces. We reproduced the wind pressure trace from data from Texas Tech's WERFL Building which is real-world wind loading for the side and leeward surfaces of a building. The results are in general agreement with published research by IBHS and Western University. This report reviews the background literature and test standards, presents the experimental setup and test protocol and discusses results for the five vinyl siding specimens.

Key findings from the project include the following:

- A successful multi-chamber pressure box approach to test vinyl siding systems was completed during this experiment. The setup consisted of four pressure chambers, with three of them connected to independent pressure loading actuators and pressure traces controlled via NI Instruments LabVIEW software. Pressure readings in all the chambers were recorded as results.
- Three different types of vinyl siding panels were tested and the results showed no noticeable differences among them. Some of the panels failed prematurely; most failures related to using a punching nail tool on slots in the nail hems.
- Five test sequences were applied to the vinyl siding panels and the highest pressure equalization factors (PEFs) occurred during spatially varying sinusoidal pressure time histories, followed by stochastic wind pressures, and followed by spatially varying static pressures.
- All specimens had very low PEFs values when subjected to synchronized (spatially uniform) pressures in the chambers. This supports our hypothesis that PEFs are a function of the difference in pressures between adjacent chambers (spatial gradients).
- Spatial pressure gradients across a vinyl siding specimen are the dominant drivers in observed PEFs along with the level of correlation between the applied pressures.

## TABLE OF CONTENTS

|   |     |
|---|-----|
| DISCLAIMER.....   | ii  |
| EXECUTIVE SUMMARY .....                                 | iii |
| 1 INTRODUCTION.....                                     | 1   |
| 2 LITERATURE REVIEW.....                                | 2   |
| 2.1 Current Testing Standards for Vinyl Siding.....     | 2   |
| 2.1.1 ASTM D5206.....                                   | 2   |
| 2.1.2 ASTM D3679.....                                   | 2   |
| 2.2 Full-scale Wind Tunnel Testing of Vinyl Siding..... | 3   |
| 2.3 Component Testing of Vinyl Siding.....              | 3   |
| 3 EXPERIMENTAL SETUP.....                               | 7   |
| 3.1 Test Bed .....                                      | 7   |
| 3.2 Spatiotemporal Loading Actuator .....               | 9   |
| 3.2.1 Setup without T Connection.....                   | 10  |
| 3.2.2 Setup with T Connection .....                     | 11  |
| 3.3 Pressure Equalization Factors.....                  | 12  |
| 3.4 Data Collection LabVIEW control software .....      | 14  |
| 3.5 Test Specimens .....                                | 16  |
| 4 TEST PROTOCOL .....                                   | 18  |
| 4.1 Spatially Uniform Static.....                       | 20  |
| 4.2 Spatially Varying Static.....                       | 21  |
| 4.3 Spatially Uniform Sine Waves .....                  | 22  |
| 4.4 Spatially Varying Sine Waves.....                   | 22  |
| 4.5 Stochastic Wind Traces .....                        | 23  |
| 4.6 ASTM D5206 .....                                    | 25  |
| 5 RESULTS.....  | 28  |
| 5.1 Pressure Equalization Factors.....                  | 28  |
| 5.1.1 Spatially Uniform Static.....                     | 29  |
| 5.1.2 Spatially Varying Static .....                    | 30  |
| 5.1.3 Spatially Uniform Sine.....                       | 31  |
| 5.1.4 Spatially Varying Sine .....                      | 32  |
| 5.1.5 Stochastic Wind Trace .....                       | 33  |
| 5.1.6 Comparisons with Previous Studies.....            | 35  |
| 5.2 ASTM D5206 Resistance Tests.....                    | 37  |



6 DISCUSSION .....41

7 CONCLUSIONS .....43

References.....45

Appendix A. PEF Results per Specimen.....46

Appendix B. ASTM D5206 Failure Locations per Specimen.....66

Appendix C. Memorandum of First Meeting.....70

Appendix D. Memorandum of Second Meeting .....72

Appendix E. Memorandum – Stochastic Wind Traces .....74

## List of Tables

| <b>Table</b>   | <b>Page</b> |
|--|-------------|
| Table 1. Identification of pressure chambers, connection to PLAs, and pressure monitoring sensors attached. ....   | 13          |
| Table 2. Summary of primary trace classes utilized. ....   | 19          |
| Table 3. Summary of relevant parameters of the WERFL Building test data. ....  | 24          |
| Table 4. Illustrating the effect of the “T” setup on the magnitudes of the spatial gradients present across the specimen. Values taken from one segment of the spatially varying static pressure trace for Level 3 (peak pressure = $-1.25$ kPa). .... | 31          |
| Table 5. Failure modes and failure pressures recorded during ASTM D5206 for Specimen 4 Partial Roll Over Nail Hem vinyl siding. ....   | 38          |
| Table 6. Failure modes and failure pressures recorded during ASTM D5206 for Specimen 5 Full Roll Over Nail Hem vinyl siding. ....  | 39          |

## List of Figures

| Figure  | Page |
|---|------|
| Figure 1. Test chamber assembly for ASTM D5206-13 (from (ASTM D5206 2013)).....   | 2    |
| Figure 2. Pressure loading actuator system (PLA) (Kopp et al. 2010).....  | 4    |
| Figure 3. Taken from Miller (2020). Pressure equalization factor as a function of the effective wind area for multiple types of air-permeable multilayer systems. ....  | 6    |
| Figure 4. Plan view of multichamber test bed.....   | 8    |
| Figure 5. Details of the Experimental Test bed pressure chamber divisions using latex sheets and HSS frames. Figure 5a – corner detail showing the overlapping and sealing of latex to vinyl siding panel and to test frame; Figure 5b – overview of a single pressure chamber showing installed latex edge seals prior to placing top cover.....   | 8    |
| Figure 6. a) Five port PLA valve individual parts; b) PLAs connected to pressure chambers 2-4 (Miller et al. 2017).....   | 9    |
| Figure 7. Three limiting states of the five-port valve at UF; a) Neutral; b) Full flow out of pressure chamber c) Full flow into pressure chamber.....  | 10   |
| Figure 8. Overall view of test setup without T connection. ....   | 11   |
| Figure 9. Sketch of addition of T connection for chamber 1 and 2.....   | 12   |
| Figure 10. Pressure tap locations for one chamber and schematic of connection to the pressure sensors. ....   | 13   |
| Figure 11. Output file from LabVIEW control software. ....  | 15   |
| Figure 12. Types of vinyl siding panels selected.....   | 17   |
| Figure 13. Example of a full test trace for Level 2 pressures, demonstrating the sequence of spatially uniform static pressure levels, spatially varied static pressure levels, spatially-varied sine waves, and stochastic wind series. In between each trace segment, a benchmark was performed as indicated by the circle with the letter B inscribed. Note that for Level 2, as shown, the peak pressure in each trace segment is $-0.8$ kPa, except for the benchmark and spatially uniform static traces..... | 18   |
| Figure 14. Spatially uniform static pressure traces. Traces are all identical.....  | 21   |
| Figure 15. Spatially varying static pressure traces.....  | 21   |

Figure 16. Spatially uniform sine wave pressure traces. Since all chambers have the same target pressures, the only chamber visible in the plot is the last chamber plotted..... 22

Figure 17. Spatially varying sine wave pressure traces. .... 23

Figure 18. The site of the WERFL building, located in flat, open terrain outside Lubbock, TX at Texas Tech University. .... 24

Figure 19. Stochastic wind pressure time series generated using full-scale measurements from the Texas Tech University WERFL building. .... 25

Figure 20. Test chamber assembly for ASTM D5206-13 (from (ASTM D5206 2013)). .... 26

Figure 21. Illustration indicating leakage across siding and leakage to atmosphere. If the area of leakage to atmosphere is much greater than the area of leakage across the siding, the cavity pressure underneath the siding remains at atmosphere. .... 27

Figure 22. Exposure of vinyl siding edges for ASTM D5206 testing at UF, to eliminate pressure equalization by opening the cavity underneath the vinyl siding to atmosphere through the edges of the specimen such that the area of leakage across the vinyl siding was much less than the area of leakage to atmosphere..... 27

Figure 23. Chamber and cavity pressures in each chamber for the uniform sine wave trace (shown for a single nail-hem specimen). .... 28

Figure 24. Chamber and cavity pressures in each chamber for the spatially-varying sine wave trace (shown for a single nail-hem specimen). .... 29

Figure 25. PEFs resulting from application of spatially uniform static pressure traces. A small portion of the target trace pressures is shown in the top left. .... 30

Figure 26. PEFs resulting from application of spatially varying static pressure traces. A small portion of the target trace pressures is shown in the top left. .... 31

Figure 27. PEFs resulting from application of spatially uniform sine wave pressure traces. A small portion of the target trace pressures is shown in the top left..... 32

Figure 28. PEFs resulting from application of spatially varying sine wave pressure traces. A small portion of the target trace pressures is shown in the top left..... 33

Figure 29. PEFs resulting from application of stochastic wind pressure traces. A small portion of the target trace pressures is shown in the top left. .... 34

Figure 30. PEF values obtained using wind pressure time histories from the **leeward wall** of the WERFL Building Test Run 279 (Pressure Level 3, with “T” test setup)..... 34

Figure 31. PEF values obtained using wind pressure time histories from the **side wall** of the WERFL Building Test Run 279 (Pressure Level 3, with “T” test setup)..... 35

Figure 32. Comparison of instantaneous PEF values between (A) the current UF study and (B) IBHS data from Cope et al. (2013)..... 36

Figure 33. Comparison of envelope PEF values from (top) the current UF study, and (bottom) from the UWO multichamber pressure tests (Miller et al., 2017)..... 37

Figure 34. Typical failure modes encountered during ASTM D5206 testing. Vinyl siding panels stretch as pressure is applied and slide through the fastener (SF) (left image); rupture of the nail hem (NF) (right image)..... 38

Figure 35. Failure of latex in fourth chamber specimen 1 on July 8, 2020; possibly due to fastener penetration through the latex. .... 47

Figure 36. Reinforcement of latex with tape around fastener areas..... 47

Figure 37. Detachment of vinyl siding through nail hem slots created by using punching nail. Failure occurred in chamber 3 in multiple panels. .... 48

Figure 38. Seal of the perimeter of specimen 1 at the fourth pressure chamber with silicon and duct tape. .... 48

Figure 39. Failure of latex in Chamber 4; failure possibly due to latex not being engaged by weatherstripping from below the aluminum plate (weatherstripping only on right side of the angle)..... 50

Figure 40. Secondary layer of weatherstripping to ensure engagement with aluminum plate ..... 50

Figure 41. Static, dynamic, and stochastic test results for Specimen 1 (without T). .... 51

Figure 42. Reinforcement of latex along the frames with duct tape. .... 52

Figure 43. Static, dynamic, and stochastic test results for Specimen 2 without T..... 53

Figure 44. Static, dynamic, and stochastic test results for Specimen 3 without T..... 55

Figure 45. Static, dynamic, and stochastic test results for Specimen 3 with T..... 57

Figure 46. Static, dynamic, and stochastic test results for Specimen 4 without T..... 59

Figure 47. Static, dynamic, and stochastic test results for Specimen 4 with T..... 61

Figure 48. Static, dynamic, and stochastic test results for Specimen 5 without T..... 63

Figure 49. Static, dynamic, and stochastic test results for Specimen 5 with T..... 65

Figure 50. Vinyl Siding panel failures in specimen 4 during ASTM D5206. Pressure chambers are indicated by the red boxes, labeled from left to right as Chamber 1, 2, 3, and 4. ... 66

Figure 51. Vinyl Siding panel failures in specimen 5 during ASTM D5206. Pressure chambers are indicated by the red boxes, labeled from left to right as Chamber 1, 2, 3, and 4. ... 67

Figure 52. Exploration of failures in vinyl siding panels after ASTM 5206 testing of specimen 4..... 67

Figure 53. Observed vinyl siding panel deflections during ASTM D5206 testing (Chamber 3) ..... 68

Figure 54. Observed vinyl siding panel deflections during ASTM D5206 testing (Chamber 4) ..... 69

Figure 55. Tap layout and wind angle of attack for the TPU WERFL building, with side wall pressure zones for each test run highlighted..... 76

Figure 56. Example time histories for each pressure zone (data taken from Run 2079, side wall case)..... 76

# 1 INTRODUCTION

Vinyl siding systems are among a class of discontinuous cladding systems, whereby open joints between individual vinyl cladding panels allow air flow from outside to inside and vice versa, enabling pressure equalization to occur. This pressure equalization (PEF) modifies the net pressure loading on the cladding system and is defined as the ratio of the net pressure to the external wind pressure. The PEF value can be used as a modifier to the external design wind pressure, for example as determined from the ASCE 7 minimum design load provisions or from wind tunnel tests. The current wind resistance test standard for vinyl siding systems is the ASTM D5206 test protocol. Recent research by the Insurance Institute for Business and Home Safety (IBHS), Florida International University and others have provided new data on the variability of PEFs on buildings, summarized in the following section.

The aim of this research is to conduct experimental studies identifying the effects of spatio-temporal wind pressure variations on the pressure distributions on vinyl siding wall systems, using the vinyl siding pressure test chamber that has been built in Project Phase I. Specifically, the project aims to evaluate PEFs for a variety of vinyl wall cladding systems, using a robust range of spatially and temporally varying pressure load scenarios. An experimental device consisting of four pressure chambers was developed in Phase I of this project and is used herein to recreate the spatio-temporal pressure distributions.

The Research Team assembled a Research Advisory Group that included members with expertise in research related areas, as well as industry and manufacturing of vinyl siding panels. The input provided by the Research Advisory Group was instrumental in the development of the test setup and test procedures. We gratefully acknowledge their contributions. The members of the Research Advisory Group are listed below.

| <b>NAME</b>         | <b>AFFILIATION</b>                                    |
|---------------------|---|
| Matthew Dobson      | Vinyl Siding Institute                                |
| Sara Krompholz      | Vinyl Siding Institute                                |
| Stan Hathorn        | Royal Building Products                               |
| Zach Priest         | PRI Construction Materials Technologies               |
| Dr. Anne Cope       | Institute for Business and Home Safety                |
| Dr. Murray Morrison | Institute for Business and Home Safety                |
| T. Eric Stafford    | T. Eric Stafford & Associates, LLC, (IBHS consultant) |
| Dr. Greg A. Kopp    | Western University                                    |
| Neil J. Sexton      | CertainTeed LLC                                       |

## 2 LITERATURE REVIEW

### 2.1 Current Testing Standards for Vinyl Siding

#### 2.1.1 ASTM D5206

The resistance of vinyl siding panels is tested following ASTM D5206. The loading methodology consists of applying a uniform pressure difference across the test specimen in increments of 5 psf, holding it for 30 seconds before each increment, and continuing until the specimen fails. The pressure at which the specimen fails (ultimate pressure) and the failure mode are recorded. The highest pressure that was sustained for 30 seconds is the maximum sustained static pressure. Pressure equalization on the vinyl siding panels is eliminated by installing an airtight barrier between the vinyl siding panel and the wall substrate or insulating layer.

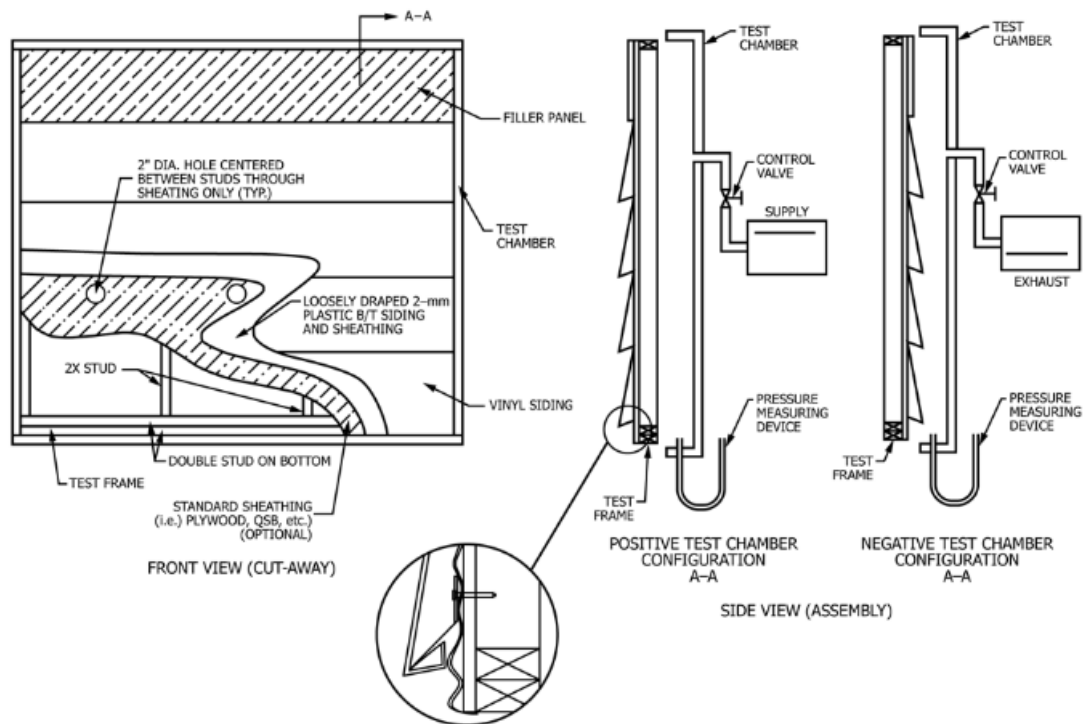


Figure 1. Test chamber assembly for ASTM D5206-13 (from (ASTM D5206 2013))

#### 2.1.2 ASTM D3679

ASTM D3679 establishes the requirements and test methods for materials, dimensions, shrinkage, warp, impact strength, expansion, appearance and wind loads of vinyl siding panels (ASTM D3679 2017). Annex A1 of the design standard shows an example of how



the wind load resistance is calculated from design pressure values obtained from ASCE 7 Components and Cladding methodology. The design pressure is multiplied by a pressure equalization factor (PEF) of 0.5, a ratio of net pressures to total external pressures, and a safety factor from ASD (American Society of Civil Engineers 2019). The result of this multiplication is referred to as the required test pressure. The limit-state pressures obtained from ASTM D5206 must be equal or less than the required test pressure for a safe design.

## **2.2 Full-scale Wind Tunnel Testing of Vinyl Siding**

Cope et al. (2013) conducted full-scale testing of residential structures with multilayer wall systems with vinyl siding cladding. The walls had both wood and foam sheathing and the testing was conducted at the Insurance Institute for Business & Home Safety (IBHS). The tests were performed on a 30 ft wide by 40 ft long structure with a mean roof height of 17 ft, and a gable/hip roof configuration. Pressures were monitored at both the exterior surface of the vinyl siding panels and in the inside surface of the panel. Vinyl siding experienced 75 percent to 80 percent of the applied external pressures.

Morrison et al. (2015) also performed testing at IBHS on a single story building. Each of the four walls of the building were divided into two sections separated both structurally and aerodynamically by using an air seal as the dividing line. The divisions allowed for the testing of different siding products (vinyl, foam backed vinyl, wood siding, cement siding). The pressures on the walls were measured similar to Cope et al. (2012). Results showed that an optimal value for design pressure for vinyl siding should be around 55 percent to 60 percent of the external pressure (PEF of 0.55- 0.6).

Moravej et al. (2016) conducted an experimental study to observe wind effects on vinyl siding installed on low-rise buildings. The study was conducted at the Wall of Wind (WOW) facility at Florida International University and the low-rise building had dimensions of 8 ft wide by 9 ft long and 7.5 ft eave height (exact dimensions were on SI units). PEFs were calculated by measuring pressures in the exterior and interior surfaces of the vinyl siding cladding. Results suggested a 0.75 PEF for a vinyl siding wall with a 1 m<sup>2</sup> tributary areas, and a 0.85 for smaller tributary areas (0.2 m<sup>2</sup>) to prevent localized failures of connections.

## **2.3 Component Testing of Vinyl Siding**

One example of initial component testing systems was the BRERWULF by. Cook et al. (1988) which allowed the application of realistic fluctuating surface pressures of a nominally airtight building component or cladding material via pressure chamber testing. More recently, Kopp et. al (2010) developed a testing methodology focused on replicating the surface pressure distributions created when wind flows over a structure. The methodology focused on

being able to replicate realistic wind pressure fluctuations (temporal variation) which led to the development of Pressure Loading Actuators (PLA). A PLA mainly consists of a blower fan, a valve with a rotating disk, and a servomotor which regulates pressure (Figure 2). The PLA approach allowed (i) better frequency response of the pressure controlling valve, (ii) high fidelity even with leakage through the building component or cladding, (iii) multiple units to be mounted in close proximity due to the reduction in size of each unit (Kopp et al. 2012). According to Kopp et al. (2010) the limitations of the PLA methodology are:

- The PLA approach replicates only pressure fields, not the flow field.
- Use of pressure chambers.
  - When very flexible cladding needs to be tested, like vinyl siding, the need of mechanical attachment requires that only one pressure chamber is used, and that it must surround the test area without contacting the surface of the cladding (no spatial variation).
- Maximum displacement of the cladding is limited by the depth of the pressure chamber.
  - Small elements cannot be tested due to minimum size limitations for the pressure chamber.
- Visual limitations of the experiment since mostly the pressure chambers can be observed rather than the actual building component or cladding.

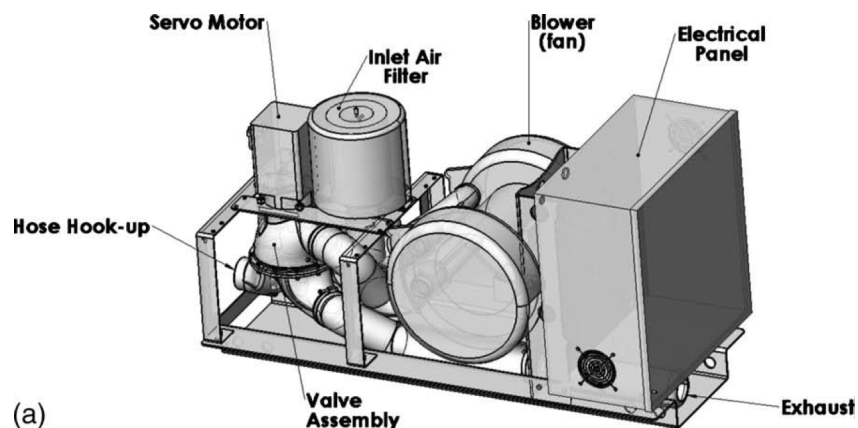


Figure 2. Pressure loading actuator system (PLA) (Kopp et al. 2010)

Kopp and Gavanski (2011) utilized PLAs to conduct an experimental study of full-scale wood-framed residential component wall sections to determine failure capacities under suction loads. Realistic fluctuating loads (dynamic) were applied to single and multilayer wood-framed residential structure walls. The level of pressure equalization was highly dependent on the details of the wall construction of the various layers (i.e. presence of housewrap). In general,

vinyl siding equalized almost perfectly under temporally-varying loads only ( $PEF = 0$ ). Spatial variation however was not considered in this study.

Some of the limitations of the PLA approach were overcome with the development of flexible air-box system that attached to the building surface (Kopp et al. 2012). Each air-box consisted of a steel-frame, an inlet duct with an air-filter, rigid modular lid and a flexible vinyl membrane glued to the lid and the surface of the specimen and allowing it to displace. Miller et al. (2017) extended the experimental setup to utilize a latex barrier glued to the surface of a multilayer vinyl siding cladding wall. In this approach, divisions were created between five adjacent air-boxes minimizing the unloaded surfaces on the surface of vinyl siding panels. The latex material was nominally air-tight, strong enough to resist test pressures, flexible, easily installed, and repeatable. Pressure traces from full-scale experiments at IBHS were replicated in each air-box or pressure chamber. Thus, spatial variation without altering external pressure gradients and appropriate dynamic fluctuating pressures were applied to the vinyl siding wall. Results from this experiment showed PEF values close to 0.7 which agreed with the full-scale experiments at IBHS.

Miller (2020) performed a comprehensive review of PEFs for a variety of air-permeable cladding systems, including vinyl siding, foam-back vinyl siding, roof pavers, solar panels, and more, calculated using both full-scale wind tunnel studies and component-level studies. He enveloped the PEFs as a function of the effective wind area, resulting in the relationship shown in Figure 3. Note that the convention used for calculating the PEF here is defined as the ratio of the peak enveloped net pressure (occurring at any location, time, or wind angle) to the peak enveloped external pressure (also occurring at any location, time, or wind angle). In other words, the PEF is not directly measured, since the numerator and denominator are calculated independently. The resulting PEFs better compare with the design approaches of ASCE 7.

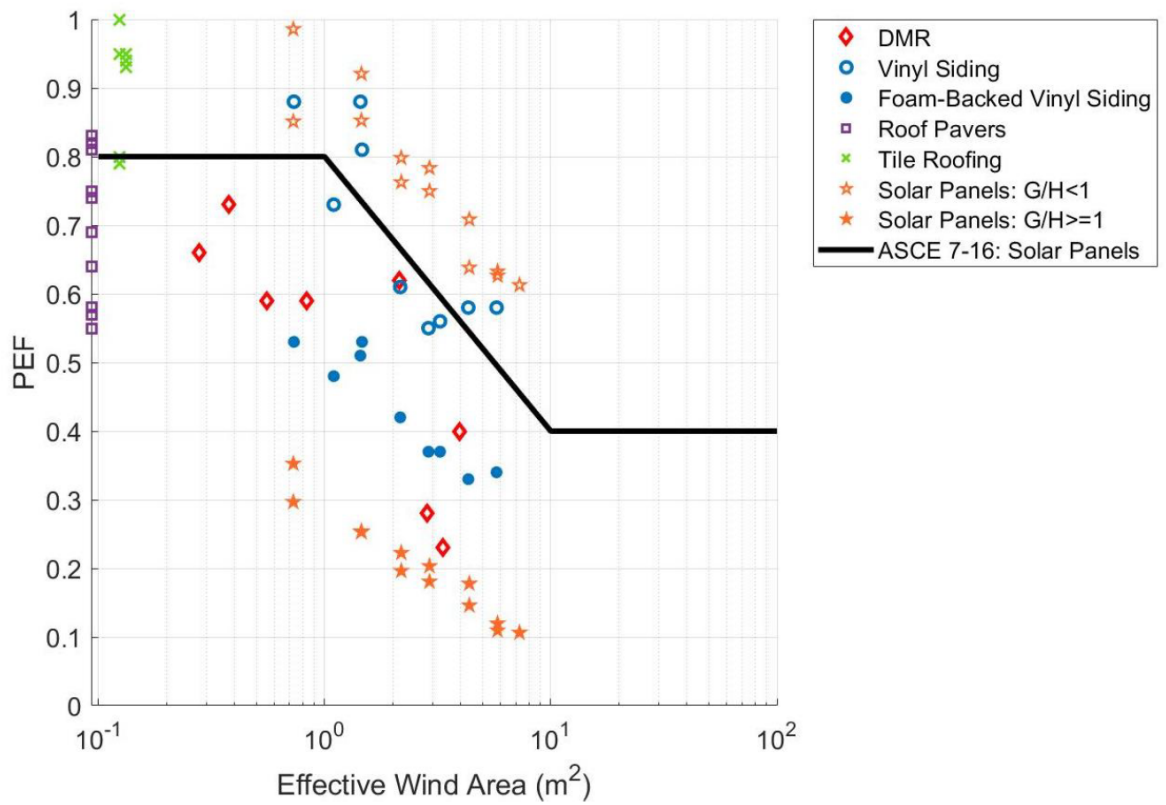


Figure 3. Taken from Miller (2020). Pressure equalization factor as a function of the effective wind area for multiple types of air-permeable multilayer systems.

### 3 EXPERIMENTAL SETUP

This experiment was designed to explore a feasible laboratory-based experimental method that will reproduce the spatial pressure distribution and simultaneous temporal changes that occur on vinyl cladding systems installed on real residential-scale buildings. A test bed was designed to accommodate vinyl siding wall specimens and instrumentation and software were selected and designed to collect the necessary experimental data. The test specimens were subjected to different pressure variations along the length of the wall, and pressure data were collected as the vinyl siding panels reacted to each test protocol.

#### 3.1 Test Bed

The experimental testing was conducted at the University of Florida's Powell Family Structures & Materials Laboratory, using the Spatio-temporal Pressure Loading Actuator (SPLA). The multi-chamber pressure test bed was constructed in Phase 1 of this project during FY2018-2019. A link to the final report for that work can be found here (<https://bit.ly/ufWIND-02-2020>).

The experiment test bed can create four separate pressure chambers on a vinyl siding wall. The first two chambers have 24 in by 96 in dimensions and the other two chambers are 48 in by 96 in. The chamber sizes are based on spatial distributions of pressures in which the first two chambers were subjected to higher magnitude of pressure gusts over smaller length, and the next two chambers generally have lesser magnitude pressures. The Powell Family Structures & Materials Laboratory "Murphy Bed" was utilized as the support frame for the wood walls, which were installed horizontally. This test bed consists of a steel frame with diagonal beams running across its length. The wood frame walls are placed on top of diagonal steel beams of the test bed and 2 in by 4 in wood studs are placed in the bottom of the test bed diagonal beams with 12-Gauge galvanized steel heavy strip ties to connect the wood frame to the bottom wood members; the wall is fixed to the test bed preventing it from displacing due to the applied pressures.

Aluminum Hollow Structural Section (HSS) frames are used as the framing supports for the sides and top of each pressure chamber. The HSS cross section size is 4 in by 4 in and were designed using SAP 2000 for shear, moment, and deflection criteria. The HSS frames are connected to the test bed with aluminum plates. U-bolts are used to connect the HSS sections to the base plate providing the advantage of being able removable when needed or removing individual frames when a different configuration of pressure chambers is desired. The HSS frame sections have a total height of 11 in, leaving sufficient space (4 in) for the vinyl siding panels to deflect freely. Latex sheets are attached from the aluminum frames to the

vinyl siding panels to seal the sides of each pressure chamber without preventing the panels' natural deflection patterns. Each pressure chamber is closed with removable plywood and plexiglass sheets which rest on aluminum angles that were welded to the frames.

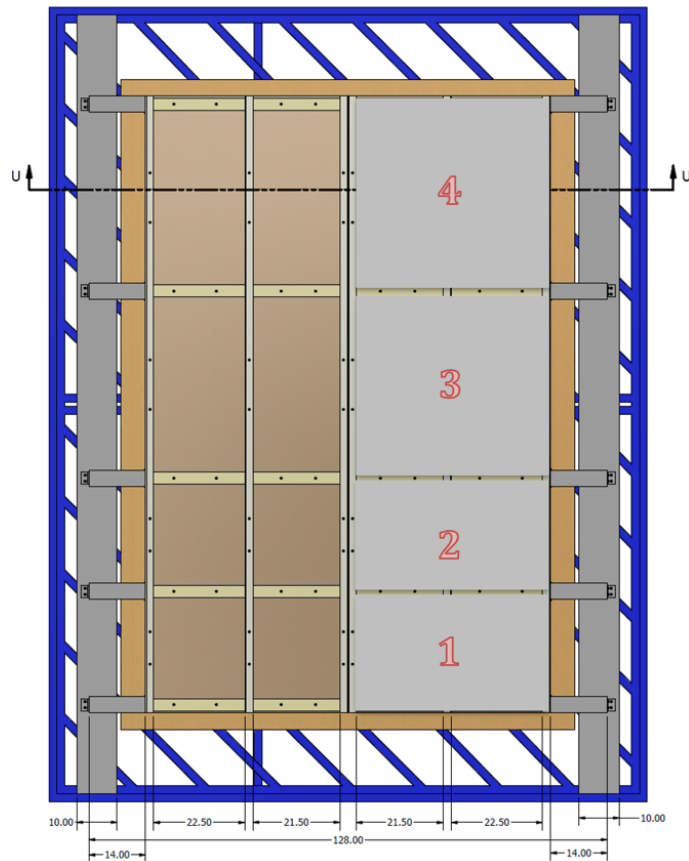
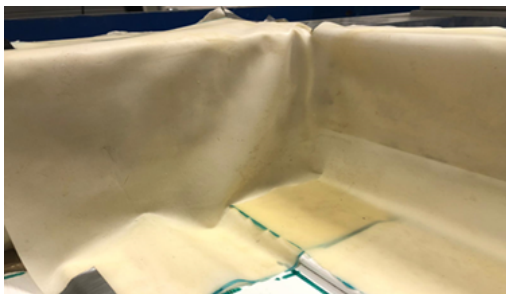


Figure 4. Plan view of multichamber test bed

a)



b)

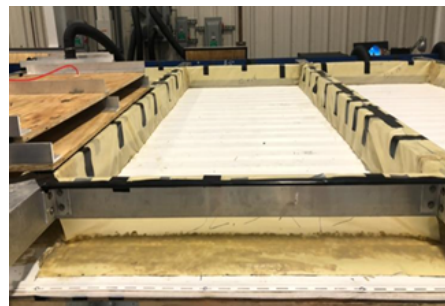


Figure 5. Details of the Experimental Test bed pressure chamber divisions using latex sheets and HSS frames. Figure 5a – corner detail showing the overlapping and sealing of latex to vinyl siding panel and to test frame; Figure 5b – overview of a single pressure chamber showing installed latex edge seals prior to placing top cover.

### 3.2 Spatiotemporal Loading Actuator

The University of Florida's Spatiotemporal Loading Actuator (SPLA) consists of a four Pressure Loading Actuator (PLA) array powered by a 40 HP centrifugal blower whose output is controlled with an ABB ACS550 variable frequency drive (VFD). Pressure or suction configurations can be achieved with each individual PLA by manipulating the position of a slotted disk controlled with a servomotor controller. The slotted disk is found between two parts of a 5-port valve in each PLA. In the top part of the valve, two ports are present, connecting the valve to the inlet "i" (low pressure side) and outlet "o" (high pressure side) of the fan. In the bottom part of the valve, three ports are present, connecting to (1) inflow from atmosphere, (2) the pressure chamber, and (3) outflow to the ambient atmosphere. Figure 6 shows the valve configuration.

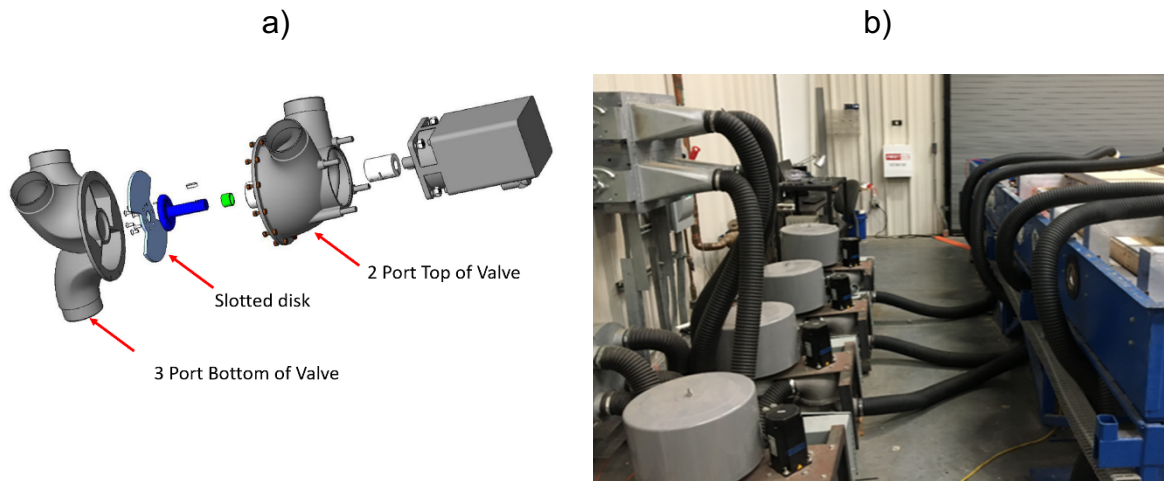


Figure 6. a) Five port PLA valve individual parts; b) PLAs connected to pressure chambers 2-4 (Miller et al. 2017)

The slotted disk between the ports is rotated as desired to create three different valve limiting states. The first is the "neutral position" where there is no flow in or out of the pressure chamber. The second is the "full flow out of pressure chamber". During this limiting state, the port connecting to inflow from atmosphere is completely closed, thus the flow is from the pressure chamber into the fan inlet, across the fan and out to the atmosphere (causes pressures lower than atmosphere- suction). The third valve limiting state is the "full flow into pressure chamber". In this case, the outflow to the atmosphere port is completely closed and the airflow is from the outlet of the fan, across the fan and into the chamber. This configuration causes pressures that are higher than atmospheric pressure.

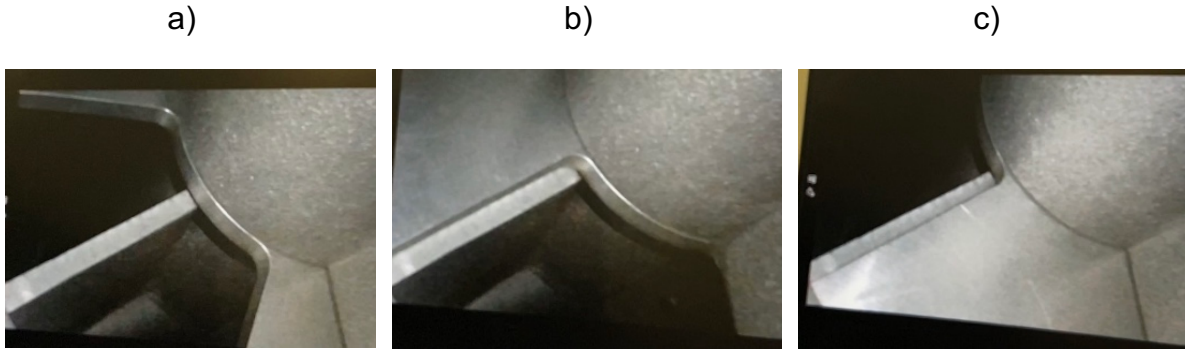


Figure 7. Three limiting states of the five-port valve at UF; a) Neutral; b) Full flow out of pressure chamber c) Full flow into pressure chamber

### **3.2.1 Setup without T Connection**

PLA 1 was not operational for this project due to an electrical issue in the system. For the initial test setup Chambers 2, 3 and 4 were each connected to an individual PLA and were fully operational. Chamber 1 remained open to atmospheric pressures since PLA 1 was not operational. The experimental plans and applied pressures continued as planned for pressure Chambers 2-4. The resultant effect of this setup was that whenever Chambers 2-4 had an applied pressure differing from atmospheric, Chamber 1 induced a pressure gradient across the specimen, even if Chambers 2-4 had identical pressures, since the cavity pressure was responding to atmospheric pressure input from Chamber 1 in combination with some other (identical or not) pressures from Chambers 2 through 4. The ramifications from this are discussed in the presentation of the results, as the effect on the PEFs is noticeable.





Figure 8. Overall view of test setup without T connection.

### **3.2.2 Setup with T Connection**

To better control the spatial gradients across the specimens, a PVC T-connection was used to divide the airflow from PLA 2 to both Chamber 1 and Chamber 2 (Figure 9). When applying identical pressures in all chambers, this setup effectively eliminated any pressure gradient across the specimen. This in turn allowed the application of uniform pressures in all the chambers in accordance to ASTM D5206. Also, pressurization of Chamber 1 allowed allow for comparisons between setups with and without the T to determine any effects caused by different spatial gradients. The T connection was installed after testing the third specimen (a single nail hem vinyl siding). The remaining test specimens were tested with and without the T-connection.

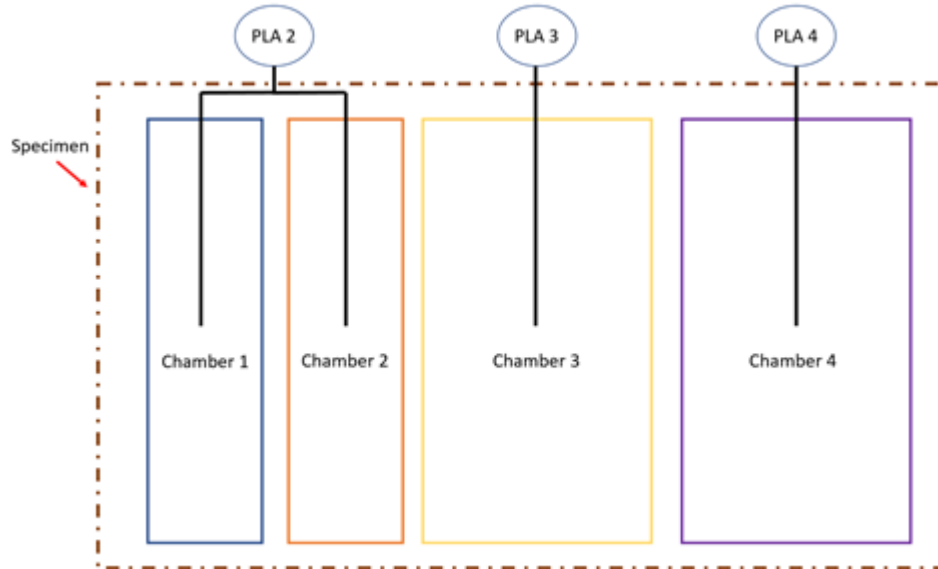


Figure 9. Sketch of addition of T connection for chamber 1 and 2.

### 3.3 Pressure Equalization Factors

During the experiment, pressures were monitored at eight different locations for each wood frame wall. Each pressure chamber has two pressure taps in its center (Figure 10). One pressure tap monitors the pressure within the pressure chambers which is referred to as “external pressure” experienced by the outer surface of the vinyl siding panel. The other pressure tap is located under the vinyl siding panel and monitors the cavity pressure. Two types of pressure transducers are used to monitor these locations. For the external pressures, four OMEGA PX409 pressure transducers with a 6.9 kPa range and <1 ms response time are used. The cavity pressures are monitored with four Setra 264 differential pressure transducers (15-50 ms response time, +/- 2.5 kPa range) with the high-pressure port connected to the external pressure via a manifold and the low-pressure port measuring the cavity pressure underneath the vinyl siding.

Pressure Equalization Factors (PEFs) are defined as a ratio of net pressures to external pressures experienced by the vinyl siding panels. Each Setra sensor measured the differential between external chamber pressure and the cavity pressure (net pressure), while the Omega sensors measure the external chamber pressure. External pressure and cavity pressure data are recorded every 50 milliseconds. The PEF is calculated in two ways, the first defining an instantaneous PEF, based on Cope et al. (2013):

$$PEF(t) = \left( P_{external}(t) - P_{cavity}(t) \right) / P_{external}(t) \quad 1$$

An envelope PEF can also be calculated by referencing the instantaneous differential pressure to the peak external pressure, which has more relevance to comparisons with design pressures. This variation of the PEF is calculated as follows:

$$PEF(t) = (P_{external(t)} - P_{cavity(t)}) / \hat{P}_{external} \quad 2$$

where  $\hat{P}_{external}$  is the peak external pressure occurring in the given pressure time series. A more thorough discussion of various conventions for calculating the PEFs is provided in Miller (2020). The above conventions are suitable for discussing the results of the testing within this current project.

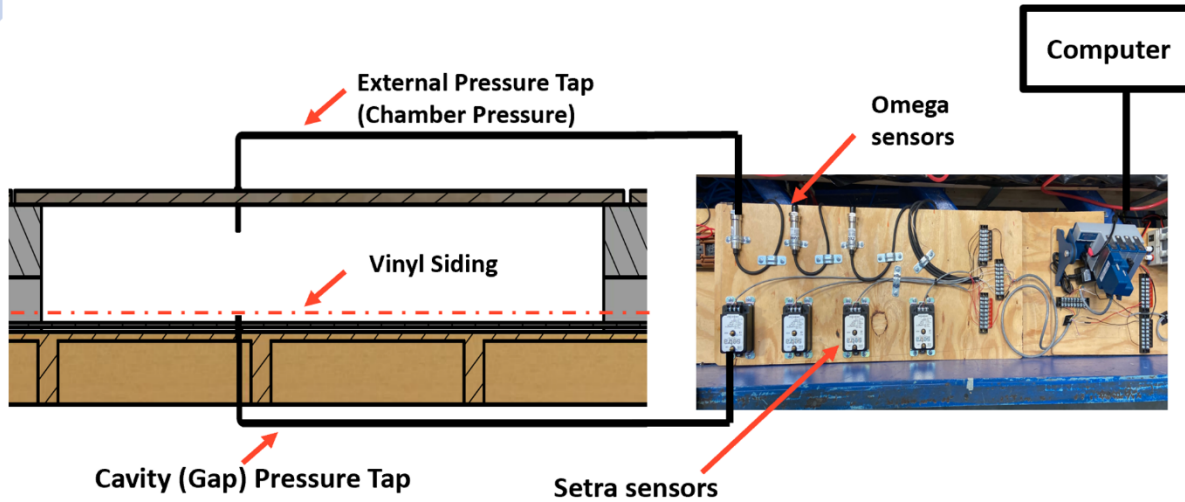


Figure 10. Pressure tap locations for one chamber and schematic of connection to the pressure sensors.

Table 1. Identification of pressure chambers, connection to PLAs, and pressure monitoring sensors attached.

| Chamber | PLA | Size        | External Pressure | Cavity Pressure |
|---------|-----|-------------|-------------------|-----------------|
| 1       | 1   | 2 ft x 8 ft | Omega-1           | Setra-1         |
| 2       | 2   | 2 ft x 8 ft | Omega-2           | Setra-2         |
| 3       | 3   | 4 ft x 8 ft | Omega-3           | Setra-3         |
| 4       | 4   | 4 ft x 8 ft | Omega-4           | Setra-4         |

\*PLA 1 in chamber 1 was not operational

### 3.4 Data Collection LabVIEW control software

National Instruments LabVIEW control software was used for instrumentation control, and data acquisition. Input target pressures/set points were read by the software (via input text file) for various wind traces. These target pressures are the pressure values in time that the vinyl siding is subjected to (a time series). Data is collected for time, VFD voltage, PLAs valve position, Omega sensor pressure readings, and the Setra sensors pressure readings. The software provides an output text file with 18 columns where:

- Columns 1 and 2 correspond to time in seconds and VFD voltage
- Columns 3-6 correspond to valve count (used to control the valve positions to achieve any desired state)

Columns 7-18 correspond to set point values (SP) which are target pressures, Omega and Setra sensor readings for each chamber. Instrumentation control is achieved with the use of a Proportional- Integrative- Derivative (PID) controller. This closed loop control algorithm continuously calculates an error value  $e(t)$  as the difference between a desired target pressure/ set point and a measured process variable (PV). The process variable is defined as the measured value of a process that is being controlled; external/chamber pressure in this experiment (measured with Omega sensors). Thus, the goal is to read the input target pressures and subject the vinyl siding specimens to these pressures by manipulating the PLA valve limiting states. Each PLA valve is adjusted in time between the neutral (no pressure) state and its full vacuum state regulating the amount of airflow flowing out of the chambers to create the target pressures. The PLA valve position in this experiment is the manipulated variable (MV); what is manipulated to obtain the desired PV (external pressure in each chamber).

| Time (s) | Voltage (V) | Valve Count | Valve Count | Valve Count | Valve Count | Target Pressure 1 | External Pressure 1 | Target Pressure 2 | External Pressure 2 | Target Pressure 3 | External Pressure 3 | Target Pressure 4 | External Pressure 4 | Cavity Pressure 1 | Cavity Pressure 2 | Cavity Pressure 3 | Cavity Pressure 4 |
|----------|-------------|-------------|-------------|-------------|-------------|-------------------|---------------------|-------------------|---------------------|-------------------|---------------------|-------------------|---------------------|-------------------|-------------------|-------------------|-------------------|
| 46.716   | 10.0        | 2900        | 2074        | 2080        | 2110        | -0.019867         | 0.019639            | -0.006945         | -0.003982           | -0.003664         | -0.006705           | -0.003666         | -0.002444           | 0.083262          | 0.049713          | 0.040579          | 0.036631          |
| 46.783   | 10.0        | 2900        | 2073        | 2077        | 2111        | -0.020552         | 0.020193            | -0.007184         | -0.004069           | -0.003790         | -0.006525           | -0.003792         | -0.002458           | 0.084274          | 0.050337          | 0.040558          | 0.037207          |
| 46.850   | 10.0        | 2900        | 2073        | 2076        | 2111        | -0.021237         | 0.020263            | -0.007424         | -0.004613           | -0.003916         | -0.007168           | -0.003919         | -0.002701           | 0.084899          | 0.049533          | 0.039938          | 0.037475          |
| 46.916   | 10.0        | 2900        | 2075        | 2076        | 2111        | -0.021922         | 0.020577            | -0.007663         | -0.004846           | -0.004043         | -0.008798           | -0.004045         | -0.003088           | 0.084600          | 0.049363          | 0.039426          | 0.036831          |
| 46.982   | 10.0        | 2900        | 2076        | 2076        | 2111        | -0.022607         | 0.020005            | -0.007903         | -0.003883           | -0.004169         | -0.006861           | -0.004171         | -0.003138           | 0.084332          | 0.049753          | 0.039805          | 0.037334          |
| 47.048   | 10.0        | 2900        | 2078        | 2078        | 2111        | -0.023293         | 0.021059            | -0.008142         | -0.003800           | -0.004295         | -0.005495           | -0.004298         | -0.003029           | 0.084908          | 0.049020          | 0.040536          | 0.036601          |
| 47.114   | 10.0        | 2900        | 2077        | 2076        | 2110        | -0.023978         | 0.020353            | -0.008382         | -0.004763           | -0.004422         | -0.008148           | -0.004424         | -0.004056           | 0.083506          | 0.048761          | 0.040357          | 0.035861          |
| 47.180   | 10.0        | 2900        | 2078        | 2073        | 2108        | -0.024663         | 0.020236            | -0.008621         | -0.004610           | -0.004548         | -0.008780           | -0.004551         | -0.003536           | 0.085503          | 0.051444          | 0.040782          | 0.036680          |
| 47.245   | 10.0        | 2900        | 2075        | 2069        | 2108        | -0.025348         | 0.020572            | -0.008860         | -0.007150           | -0.004674         | -0.008977           | -0.004677         | -0.003527           | 0.086235          | 0.049516          | 0.039363          | 0.037120          |
| 47.312   | 10.0        | 2900        | 2075        | 2068        | 2107        | -0.026033         | 0.020339            | -0.009100         | -0.007573           | -0.004801         | -0.007411           | -0.004803         | -0.003399           | 0.087445          | 0.049183          | 0.039852          | 0.037107          |
| 47.379   | 10.0        | 2900        | 2077        | 2076        | 2107        | -0.026718         | 0.020070            | -0.009339         | -0.006867           | -0.004927         | -0.005689           | -0.004930         | -0.003288           | 0.085255          | 0.047278          | 0.041897          | 0.034595          |
| 47.446   | 10.0        | 2900        | 2078        | 2074        | 2108        | -0.027403         | 0.020346            | -0.009579         | -0.007010           | -0.005053         | -0.006906           | -0.005056         | -0.003279           | 0.084451          | 0.047642          | 0.042317          | 0.034500          |
| 47.513   | 10.0        | 2900        | 2080        | 2077        | 2109        | -0.028088         | 0.020426            | -0.009818         | -0.006809           | -0.005180         | -0.004935           | -0.005183         | -0.003270           | 0.085293          | 0.046216          | 0.041511          | 0.035210          |
| 47.579   | 10.0        | 2900        | 2079        | 2077        | 2109        | -0.028773         | 0.020626            | -0.010058         | -0.007434           | -0.005306         | -0.004793           | -0.005309         | -0.003261           | 0.084048          | 0.046928          | 0.043665          | 0.034501          |
| 47.646   | 10.0        | 2900        | 2079        | 2078        | 2109        | -0.029458         | 0.020755            | -0.010297         | -0.007498           | -0.005432         | -0.004347           | -0.005435         | -0.003252           | 0.085103          | 0.046445          | 0.043888          | 0.035045          |
| 47.713   | 10.0        | 2900        | 2082        | 2080        | 2110        | -0.030143         | 0.019894            | -0.010537         | -0.006495           | -0.005559         | -0.002998           | -0.005562         | -0.004690           | 0.084189          | 0.047514          | 0.043847          | 0.034889          |
| 47.779   | 10.0        | 2900        | 2083        | 2082        | 2112        | -0.030828         | 0.020445            | -0.010776         | -0.006516           | -0.005685         | -0.002342           | -0.005688         | -0.004085           | 0.084861          | 0.046153          | 0.044499          | 0.034439          |
| 47.845   | 10.0        | 2900        | 2082        | 2086        | 2114        | -0.031513         | 0.020622            | -0.011016         | -0.007992           | -0.005811         | -0.000842           | -0.005815         | -0.002986           | 0.084232          | 0.044740          | 0.045762          | 0.034571          |
| 47.911   | 10.0        | 2900        | 2084        | 2089        | 2114        | -0.032198         | 0.020954            | -0.011255         | -0.007041           | -0.005938         | 0.000709            | -0.005941         | -0.002986           | 0.083406          | 0.045104          | 0.046365          | 0.034644          |
| 47.977   | 10.0        | 2900        | 2084        | 2087        | 2114        | -0.032884         | 0.020503            | -0.011495         | -0.007694           | -0.006064         | -0.000893           | -0.006067         | -0.003530           | 0.083873          | 0.045528          | 0.046632          | 0.035851          |
| 48.043   | 10.0        | 2900        | 2087        | 2090        | 2115        | -0.033569         | 0.020820            | -0.011734         | -0.006612           | -0.006190         | 0.000219            | -0.006194         | -0.003521           | 0.083832          | 0.044862          | 0.046497          | 0.035543          |
| 48.112   | 10.0        | 2900        | 2084        | 2088        | 2115        | -0.034254         | 0.020381            | -0.011974         | -0.009120           | -0.006317         | -0.002383           | -0.006320         | -0.003519           | 0.083587          | 0.044811          | 0.045273          | 0.035853          |
| 48.179   | 10.0        | 2900        | 2085        | 2089        | 2116        | -0.034939         | 0.020300            | -0.012213         | -0.008849           | -0.006443         | -0.001660           | -0.006447         | -0.003817           | 0.084163          | 0.044550          | 0.045245          | 0.036084          |
| 48.245   | 10.0        | 2900        | 2086        | 2090        | 2116        | -0.035624         | 0.020920            | -0.012453         | -0.008864           | -0.006569         | -0.001563           | -0.006573         | -0.003971           | 0.085178          | 0.044630          | 0.045988          | 0.035409          |
| 48.312   | 10.0        | 2900        | 2085        | 2089        | 2114        | -0.036309         | 0.019973            | -0.012692         | -0.010326           | -0.006696         | -0.002816           | -0.006699         | -0.005436           | 0.083935          | 0.044345          | 0.045517          | 0.035921          |
| 48.378   | 10.0        | 2900        | 2088        | 2089        | 2115        | -0.036994         | 0.020254            | -0.012932         | -0.008726           | -0.006822         | -0.003517           | -0.006826         | -0.005194           | 0.085512          | 0.045564          | 0.044911          | 0.036084          |
| 48.445   | 10.0        | 2900        | 2083        | 2087        | 2115        | -0.037679         | 0.019850            | -0.013171         | -0.012265           | -0.006948         | -0.005155           | -0.006952         | -0.005584           | 0.085118          | 0.043543          | 0.044758          | 0.035967          |
| 48.511   | 10.0        | 2900        | 2085        | 2085        | 2114        | -0.038364         | 0.020123            | -0.013410         | -0.011577           | -0.007075         | -0.006754           | -0.007079         | -0.006290           | 0.087005          | 0.045140          | 0.043357          | 0.036161          |
| 48.577   | 10.0        | 2900        | 2084        | 2085        | 2113        | -0.039049         | 0.020363            | -0.013650         | -0.012410           | -0.007201         | -0.007281           | -0.007205         | -0.006973           | 0.088430          | 0.044971          | 0.042480          | 0.036475          |
| 48.643   | 10.0        | 2900        | 2081        | 2085        | 2113        | -0.039734         | 0.020205            | -0.013889         | -0.014558           | -0.007327         | -0.007266           | -0.007331         | -0.007374           | 0.087098          | 0.041967          | 0.043959          | 0.036173          |
| 48.710   | 10.0        | 2900        | 2086        | 2081        | 2113        | -0.040419         | 0.020095            | -0.014129         | -0.012328           | -0.007454         | -0.009906           | -0.007458         | -0.007408           | 0.087445          | 0.045598          | 0.041621          | 0.036784          |
| 48.776   | 10.0        | 2900        | 2086        | 2083        | 2114        | -0.041104         | 0.019779            | -0.014368         | -0.012091           | -0.007580         | -0.008876           | -0.007584         | -0.006444           | 0.087589          | 0.045338          | 0.042033          | 0.036907          |
| 48.843   | 10.0        | 2900        | 2087        | 2079        | 2114        | -0.041789         | 0.020264            | -0.014608         | -0.012398           | -0.007706         | -0.010739           | -0.007711         | -0.007328           | 0.087862          | 0.045069          | 0.040308          | 0.036417          |
| 48.910   | 10.0        | 2900        | 2089        | 2084        | 2116        | -0.042475         | 0.020314            | -0.014847         | -0.011793           | -0.007833         | -0.007485           | -0.007837         | -0.005838           | 0.087642          | 0.044092          | 0.041364          | 0.036774          |
| 48.976   | 10.0        | 2900        | 2088        | 2083        | 2116        | -0.043160         | 0.020871            | -0.015087         | -0.013668           | -0.007959         | -0.009099           | -0.007963         | -0.007506           | 0.087417          | 0.043312          | 0.041287          | 0.036626          |
| 49.042   | 10.0        | 2900        | 2090        | 2087        | 2114        | -0.043845         | 0.020510            | -0.015326         | -0.012087           | -0.008085         | -0.005810           | -0.008090         | -0.007626           | 0.087937          | 0.042800          | 0.043608          | 0.035736          |
| 49.108   | 10.0        | 2900        | 2087        | 2086        | 2115        | -0.044530         | 0.020715            | -0.015566         | -0.014437           | -0.008212         | -0.006889           | -0.008216         | -0.007253           | 0.086414          | 0.042990          | 0.044018          | 0.035194          |
| 49.175   | 10.0        | 2900        | 2087        | 2082        | 2114        | -0.045215         | 0.019948            | -0.015805         | -0.013418           | -0.008338         | -0.010581           | -0.008343         | -0.008282           | 0.088895          | 0.044630          | 0.041549          | 0.036869          |
| 49.242   | 10.0        | 2900        | 2090        | 2082        | 2114        | -0.045900         | 0.020449            | -0.016045         | -0.013077           | -0.008464         | -0.009867           | -0.008469         | -0.008249           | 0.088563          | 0.044883          | 0.040818          | 0.036895          |
| 49.309   | 10.0        | 2900        | 2089        | 2081        | 2115        | -0.046585         | 0.020048            | -0.016284         | -0.014155           | -0.008591         | -0.010166           | -0.008595         | -0.007904           | 0.089364          | 0.044070          | 0.042082          | 0.035743          |
| 49.375   | 10.0        | 2900        | 2089        | 2079        | 2115        | -0.047270         | 0.020754            | -0.016524         | -0.013705           | -0.008717         | -0.011480           | -0.008722         | -0.008809           | 0.089065          | 0.043996          | 0.041043          | 0.036412          |
| 49.441   | 10.0        | 2900        | 2091        | 2077        | 2115        | -0.047955         | 0.020130            | -0.016763         | -0.013799           | -0.008843         | -0.013012           | -0.008848         | -0.008101           | 0.088607          | 0.045756          | 0.040495          | 0.037124          |
| 49.507   | 10.0        | 2900        | 2089        | 2078        | 2116        | -0.048640         | 0.020485            | -0.017003         | -0.015990           | -0.008970         | -0.011779           | -0.008975         | -0.008190           | 0.089970          | 0.042420          | 0.039482          | 0.037137          |
| 49.573   | 10.0        | 2900        | 2090        | 2081        | 2116        | -0.049325         | 0.020477            | -0.017242         | -0.015518           | -0.009096         | -0.010609           | -0.009101         | -0.007776           | 0.088321          | 0.042114          | 0.041500          | 0.035803          |
| 49.639   | 10.0        | 2900        | 2090        | 2077        | 2118        | -0.050010         | 0.019972            | -0.017481         | -0.016060           | -0.009222         | -0.011975           | -0.009227         | -0.006954           | 0.088440          | 0.043316          | 0.041324          | 0.036846          |
| 49.705   | 10.0        | 2900        | 2092        | 2079        | 2118        | -0.050695         | 0.020409            | -0.017721         | -0.015263           | -0.009349         | -0.011011           | -0.009354         | -0.007377           | 0.089560          | 0.043107          | 0.039598          | 0.037703          |
| 49.771   | 10.0        | 2900        | 2091        | 2080        | 2118        | -0.051381         | 0.019899            | -0.017960         | -0.015574           | -0.009475         | -0.008861           | -0.009480         | -0.007907           | 0.087934          | 0.041797          | 0.041558          | 0.036811          |
| 49.838   | 10.0        | 2900        | 2095        | 2086        | 2120        | -0.052066         | 0.020960            | -0.018200         | -0.014554           | -0.009601         | -0.006605           | -0.009607         | -0.006902           | 0.087849          | 0.041999          | 0.043248          | 0.035690          |
| 49.905   | 10.0        | 2900        | 2094        | 2084        | 2120        | -0.052751         | 0.020436            | -0.018439         | -0.015378           | -0.009728         | -0.007871           | -0.009733         | -0.007428           | 0.086693          | 0.041917          | 0.043739          | 0.035375          |
| 49.971   | 10.0        | 2900        | 2094        | 2085        | 2119        | -0.053436         | 0.019895            | -0.018679         | -0.015408           | -0.009854         | -0.006655           | -0.009860         | -0.007938           | 0.088454          | 0.041280          | 0.043927          | 0.036193          |
| 50.038   | 10.0        | 2900        | 2091        | 2082        | 2119        | -0.054121         | 0.021105            | -0.018918         | -0.018140           | -0.009980         | -0.009833           | -0.009986         | -0.008189           | 0.088638          | 0.040857          | 0.043788          | 0.036404          |

Figure 11. Output file from LabVIEW control software.



### 3.5 Test Specimens

Three vinyl siding systems were selected following input from the Vinyl Siding Institute. These systems represent typical products used in Florida for both standard zones and Hurricane High Velocity Zones and each have a Florida product approval number on file. The products vary in thickness and nail hem shape. The vinyl siding systems were installed following directions from a Certified Vinyl Siding installer using remote technologies.



Single Nail- Hem

- FL# XXXXX
- 0.04 in. panel thickness and ½ in. panel projection
- VSI SDPR 55.6 psf



Partial Roll-over Nail- Hem

- FL# XXXXX; FL HVHZ# XXXXX
- 0.044 in. panel thickness
- VSI SDPR 55.1 psf



Full Roll-over Nail- Hem

- FL# XXXXX; NOA XX-XXXX.XX
- 0.046 in. panel thickness
- VSI SDPR 89.4 psf

Figure 12. Types of vinyl siding panels selected.

## 4 TEST PROTOCOL

Each specimen underwent a series of static and dynamic, uniform and spatially varying pressure traces to explore a wide range of temporal and spatial pressure gradients from which to evaluate Pressure Equalization Factors (PEFs). A summary of the various traces is provided in Table 2. An example trace is shown in Figure 13 with annotations of the major components of the trace.

Traces were organized into three different pressure levels, which defined the peak pressure achieved in each trace. The chosen pressure levels were set at peak pressures of -0.5 kPa, -0.8 kPa, and -1.25 kPa in order to explore the relationship between external pressure magnitude and PEF, while avoiding pressures that could induce failures in the vinyl siding specimens or test bed. The various traces were connected with several intermediate traces that served to provide benchmarks for the system to evaluate any changes in leakage, and ramp up and down segments from and to trace start points to minimize overshooting of the target trace by the PLAs. The various trace types are described in more detail in the following sections.

Each test chamber was assigned a separate trace. However, only traces for Chambers 2 through 4 were actually applied to the specimens due to PLA-1 being out of commission. In some of the tests, the T-setup was used whereby the Chamber 2 pressures were applied to Chamber A as well. When applied to the specimens, the complete pressure trace for each pressure level was segmented into static (spatially uniform static and spatially varying static), dynamic (spatially uniform and spatially varying sine waves), and stochastic (measured wind pressure time histories).

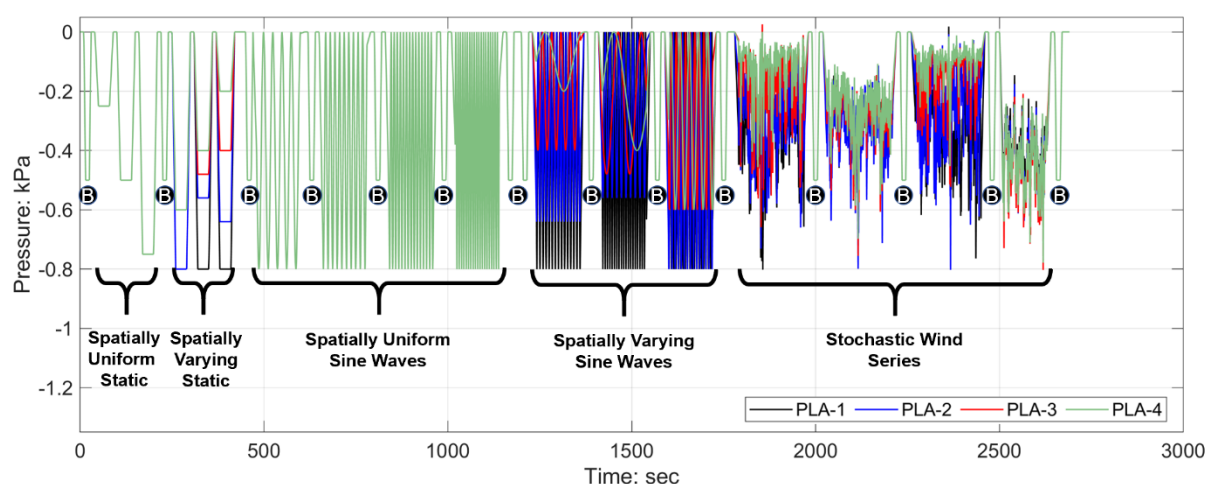
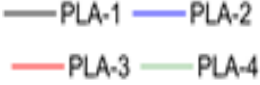

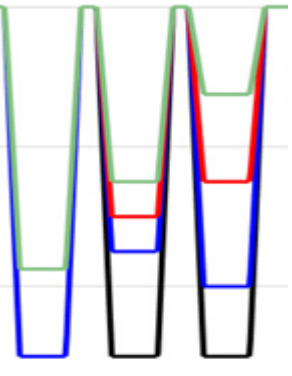
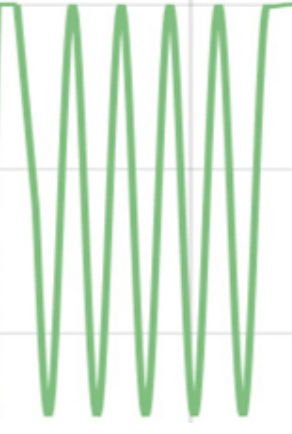
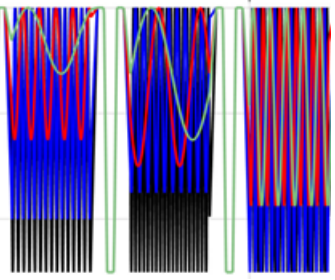
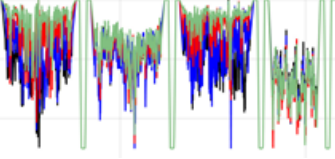


Figure 13. Example of a full test trace for Level 2 pressures, demonstrating the sequence of spatially uniform static pressure levels, spatially varied static pressure levels, spatially-varied sine waves, and stochastic wind series. In between each trace segment, a benchmark was performed as indicated by the circle with the letter B inscribed. Note that for Level 2, as shown, the peak pressure in each trace segment is -0.8 kPa, except for the benchmark and spatially uniform static traces.



Table 2. Summary of primary trace classes utilized.

| Test Run                            | Description                          | Visualization of Trace<br> | Peak Target Pressure (kPa) | Levels |
|-------------------------------------|--------------------------------------|--|----------------------------|--------|
| <b>Uniform Static Tests</b>         |                                      |  |                            |        |
| 1.1                                 | Uniform Static- (US-1)               |                            | 0.5                        | 1      |
| 1.2                                 | Uniform Static- (US-2)               |  | 0.8                        | 2      |
| 1.3                                 | Uniform Static- (US-3)               |  | 1.25                       | 3      |
| <b>Spatially Varying Static</b>     |                                      |  |                            |        |
| 2.1                                 | Varied Static- (VS-1)                |                           | 0.5                        | 1      |
| 2.2                                 | Varied Static- (VS-2)                |  | 0.8                        | 2      |
| 2.3                                 | Varied Static- (VS-3)                |  | 1.25                       | 3      |
| <b>Uniform Sine Waves</b>           |                                      |  |                            |        |
| 3.1                                 | Uniform Sine Waves (US-1)            |                          | 0.5                        | 1      |
| 3.2                                 | Uniform Sine Waves (US-2)            |  | 0.8                        | 2      |
| 3.3                                 | Uniform Sine Waves (US-3)            |  | 1.25                       | 3      |
| <b>Spatially Varying Sine Waves</b> |                                      |  |                            |        |
| 4.1                                 | Spatially Varying Sine Waves (SVS-1) |  | 0.5                        | 1      |

|                                  |                                      |  |      |   |
|----------------------------------|--------------------------------------|--|------|---|
| 4.2                              | Spatially Varying Sine Waves (SVS-2) |  | 0.8  | 2 |
| 4.3                              | Spatially Varying Sine Waves (SVS-3) |  | 1.25 | 3 |
| <b>Stochastic Wind Pressures</b> |                                      |  |      |   |
| 5.1                              | Stochastic Wind Series (S-1)         |  | 0.5  | 1 |
| 5.2                              | Stochastic Wind Series (S-2)         |  | 0.8  | 2 |
| 5.3                              | Stochastic Wind Series (S-3)         |  | 1.25 | 3 |

#### 4.1 Spatially Uniform Static

The spatially uniform static pressure traces loosely follow that of ASTM D5206, which consists of applying a uniform pressure difference across the specimen in increments of 5 lbf/ft<sup>2</sup> (0.25 kPa), holding for 30 seconds before increasing the next 5 lbf/ft<sup>2</sup> (0.25 kPa) until the specified pressure for the given level (e.g., 0.5 kPa for Level 1, 0.8 kPa for Level 2, 1.25 kPa for Level 3) is achieved. A difference between these traces and D5206 was that the system was allowed to return to neutral (0 kPa) prior to ramping up to the next step pressure change. The peak pressure in this trace series was capped by the three pressure levels, while pressures were decreased by  $-0.25$  kPa at each pressure step, resulting in two pressure steps for Level 1, three for Level 2, and five for Level 3.

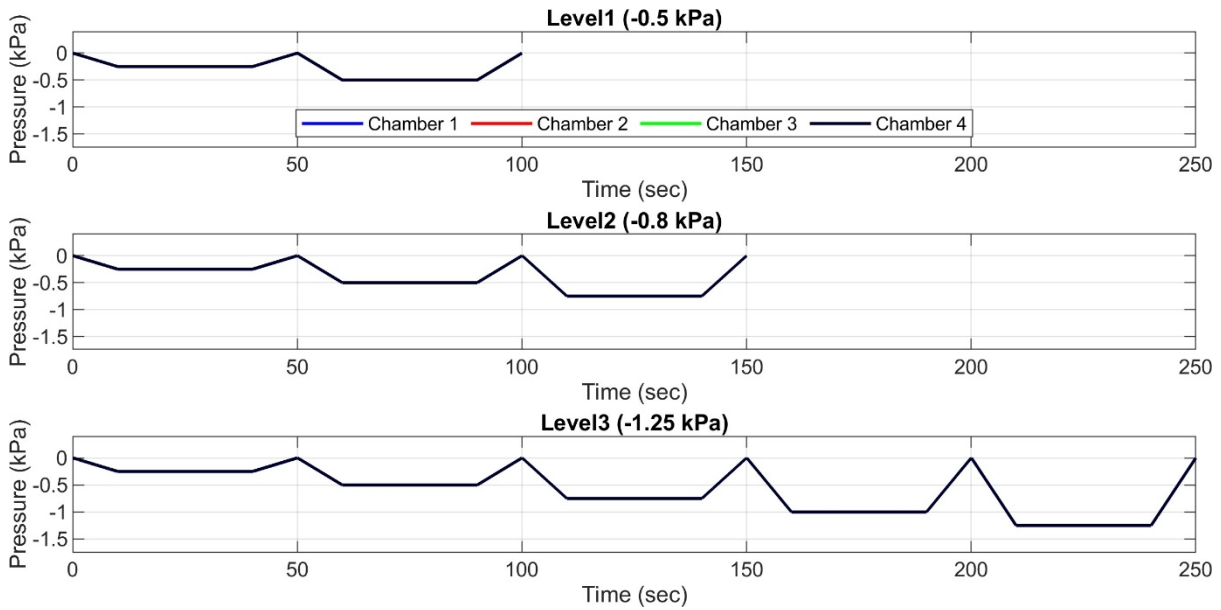


Figure 14. Spatially uniform static pressure traces. Traces are all identical.

## 4.2 Spatially Varying Static

The spatially varying pressures pressure traces consisted of pressures being held constant in each chamber, but at different magnitudes in each chamber (Figure 15). The spatially-varying static pressure patterns include (1) Peak pressure level (e.g., 1.0 kPa) in Chambers 1 and 2, with 75% in Chamber 3 and 75% in Chamber 4; (2) Peak pressure in Chamber 1 with 70% of the peak pressure in Chamber 2, 60% in Chamber 3 and 50% in Chamber 4; and (3) Peak pressure in Chamber 1 with 80% of the peak pressure in Chamber 2, 50% in Chamber 3 and 25% in Chamber 4. Pressures were held constant at each step for 30 seconds.

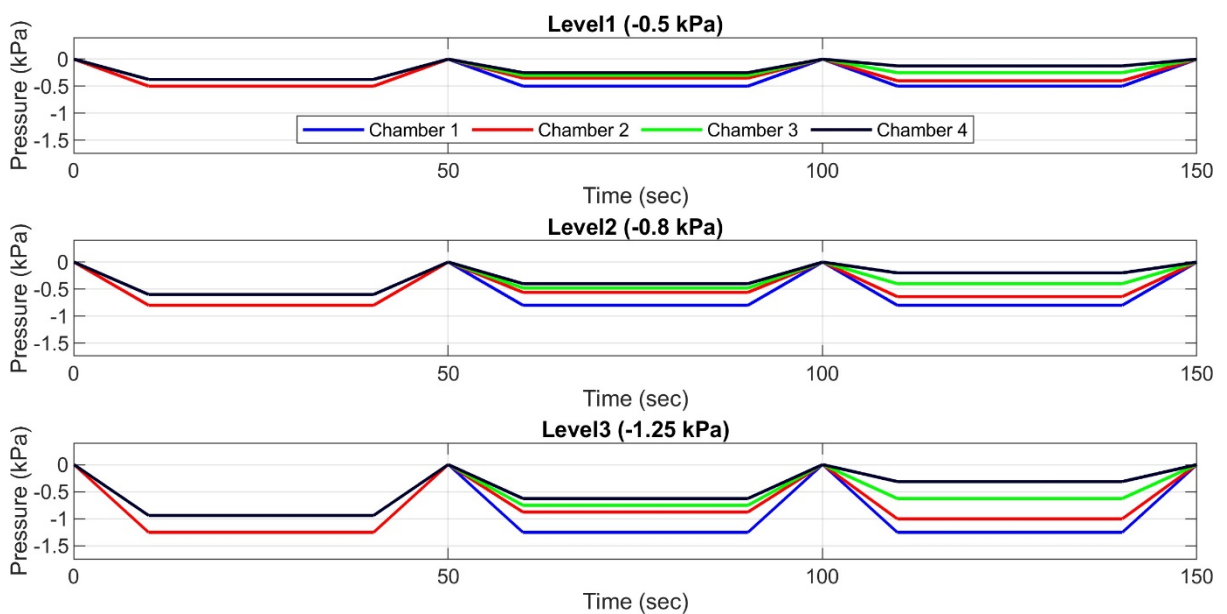


Figure 15. Spatially varying static pressure traces.

### 4.3 Spatially Uniform Sine Waves

These traces consisted of three segments of identical sine waves in each pressure chamber. For each segment, the angular frequency was changed to alter how rapidly the pressures changed in each chamber. The peak pressure was always equal to the peak pressure associated with the given pressure level. Figure 16 demonstrates the various uniform sine pressure traces utilized.

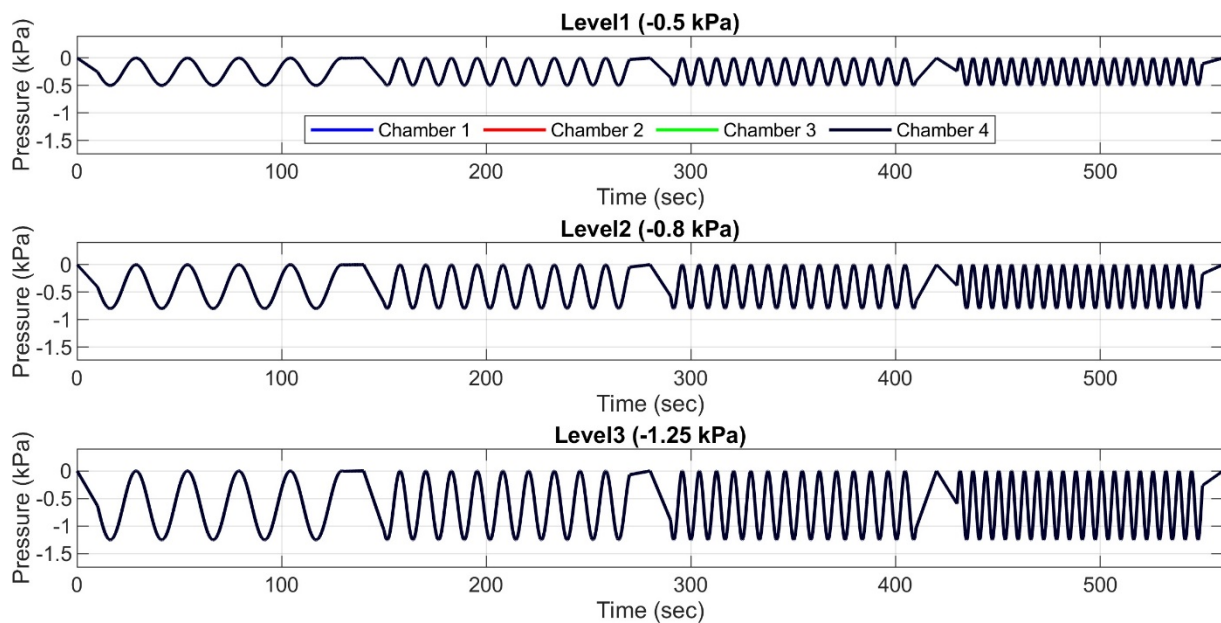


Figure 16. Spatially uniform sine wave pressure traces. Since all chambers have the same target pressures, the only chamber visible in the plot is the last chamber plotted.

### 4.4 Spatially Varying Sine Waves

These pressure traces consisted of sine waves with varying magnitudes, phase shifts, and angular frequencies ( $< 1$  Hz) in each chamber. The highest magnitude pressures and angular frequencies were assigned in Chamber 1, with decreasing pressures in Chamber 2 and decreasing pressures and angular frequencies in Chambers 3 and 4. For each combination of magnitude, phase shift, and angular frequency, the sine wave traces had a duration of 2 minute. A total of three combinations were used.

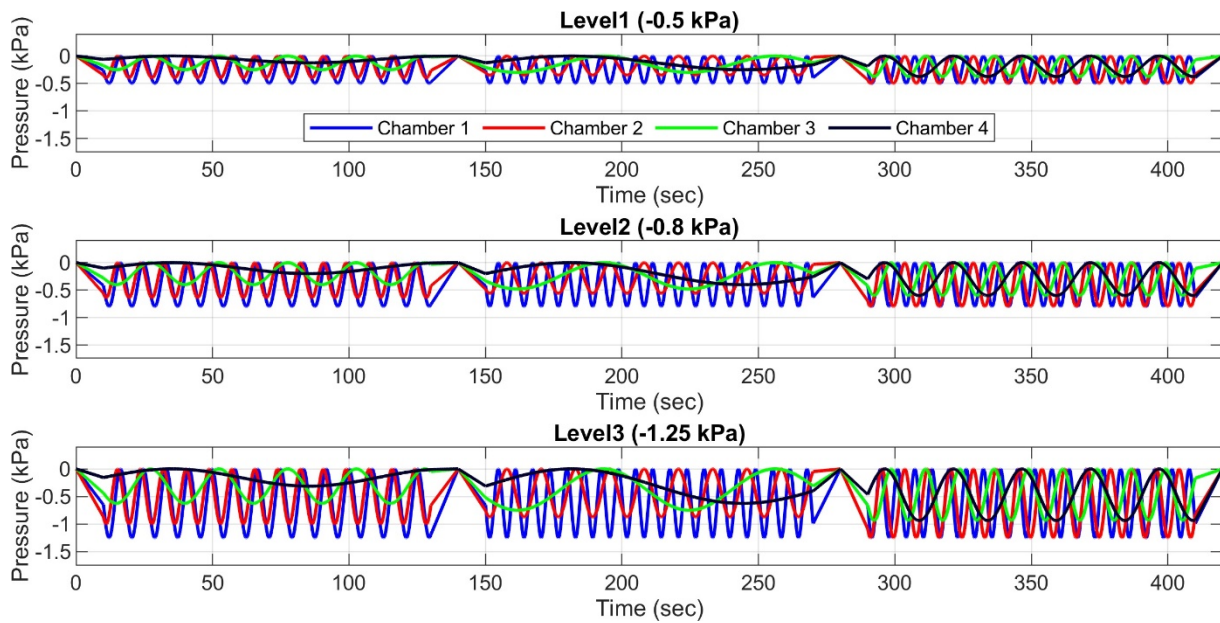


Figure 17. Spatially varying sine wave pressure traces.

#### 4.5 Stochastic Wind Traces

Stochastic wind traces were generated using full-scale wind pressure data from the Wind Engineering Research Field Laboratory (WERFL) at Texas Tech University, publicly available through the NSF DesignSafe-CI platform (Smith et al., 2018). An overview of the test site is shown in Figure 18, taken from Smith et al. (2018). The facility consists of a 160 ft meteorological tower instrumented at 5 heights and a flat roof test structure with outside dimensions 30'-3" x 45'-3" x 12'-10" high, similar in scale to a residential building. Two test cases were pulled from the dataset (identified as Run 2071 and Run 279). Parameters of these test cases are provided in Table 3, along with the provided parameters from the IBHS testing (Cope et al, 2013) for comparison. The turbulence parameters were similar albeit slightly lower relative to those of IBHS. The WERFL building data and IBHS data all were collected in nominally open terrain with between 17-20% longitudinal turbulence intensity. Only the WERFL building pressures were used for this study.

The wind pressures for the WERFL cases were published as non-dimensional pressure coefficient time histories, referenced to the mean roof height wind speed. The pressure coefficient time histories were converted to pressure time histories as described in Appendix E. For each test run, the output was four pressure traces representing spatially averaged pressures within adjacent zones on the walls of the WERFL building, with the peak pressure observed across all of the four zones equaling each of the pressure levels (e.g., -0.5 kPa for Level 1). The spatial averaging was performed over zones on one side wall and one leeward wall in each test run, resulting in a total of four wind series for each pressure level, each containing four separate pressure traces corresponding to the four pressure chambers of the

SPLA. The resulting pressure traces are shown in Figure 19. The sidewall traces generally had correlation coefficients between the four traces ranging from 0.5 to 0.9, while leeward wall traces generally had correlation coefficients ranging from 0.8 to 0.9.

Table 3. Summary of relevant parameters of the WERFL Building test data.

| Test Run           | Test Duration                  | Mean Roof Height Wind Speed (mph) | Wind Angle of Attack | Roughness Length (ft) | Turbulence Intensity ( $I_u$ ) |
|--------------------|--------------------------------|-----------------------------------|----------------------|-----------------------|--------------------------------|
| 2071               | 15 minutes                     | 30                                | 355                  | 0.025                 | 17%                            |
| 279                | 15 minutes                     | 18                                | 10                   | 0.042                 | 17%                            |
| Cope et al. (2013) | 15 minutes per angle of attack | 40-110                            | 0-360                | 0.03                  | ~20%                           |



Figure 18. The site of the WERFL building, located in flat, open terrain outside Lubbock, TX at Texas Tech University.



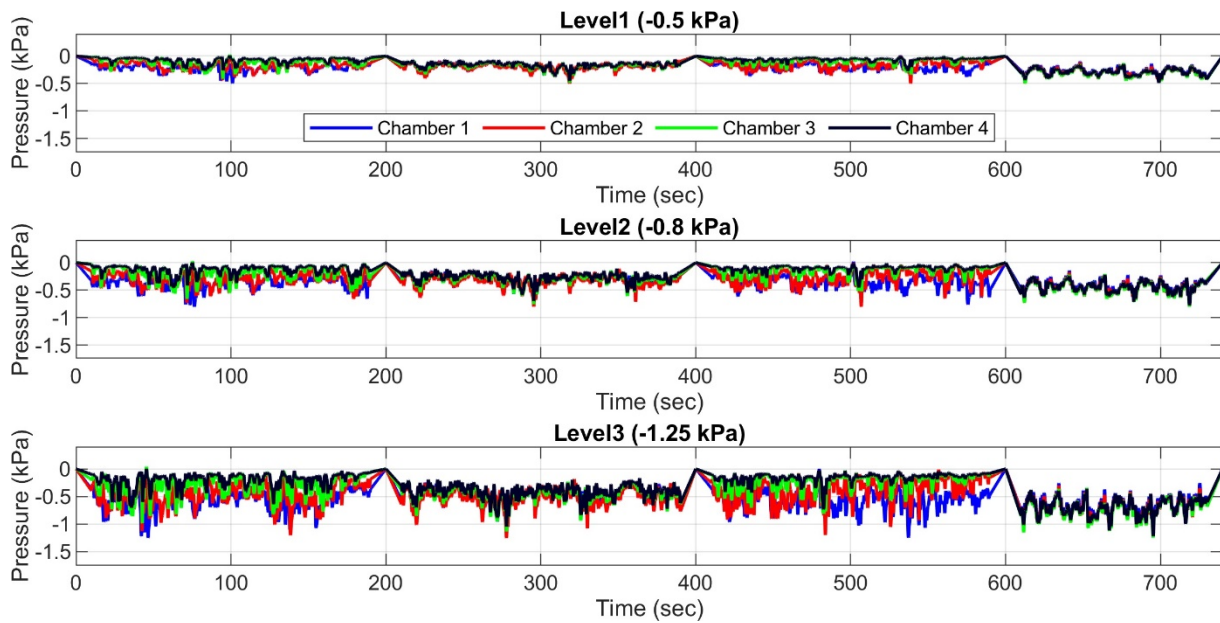


Figure 19. Stochastic wind pressure time series generated using full-scale measurements from the Texas Tech University WERFL building.

#### 4.6 ASTM D5206

The resistance of vinyl siding panels is tested following ASTM D5206. The loading methodology consists of applying a uniform pressure difference across the test specimen in increments of 0.239 kPa (5 psf), holding it for 30 seconds before each increment, and continuing until the specimen fails. The pressure at which the specimen fails (ultimate pressure) and the failure mode are recorded. The highest pressure that was sustained for 30 seconds is the maximum sustained static pressure. Pressure equalization on the vinyl siding panels is eliminated by installing an airtight barrier between the vinyl siding panel and the wall substrate or insulating layer.

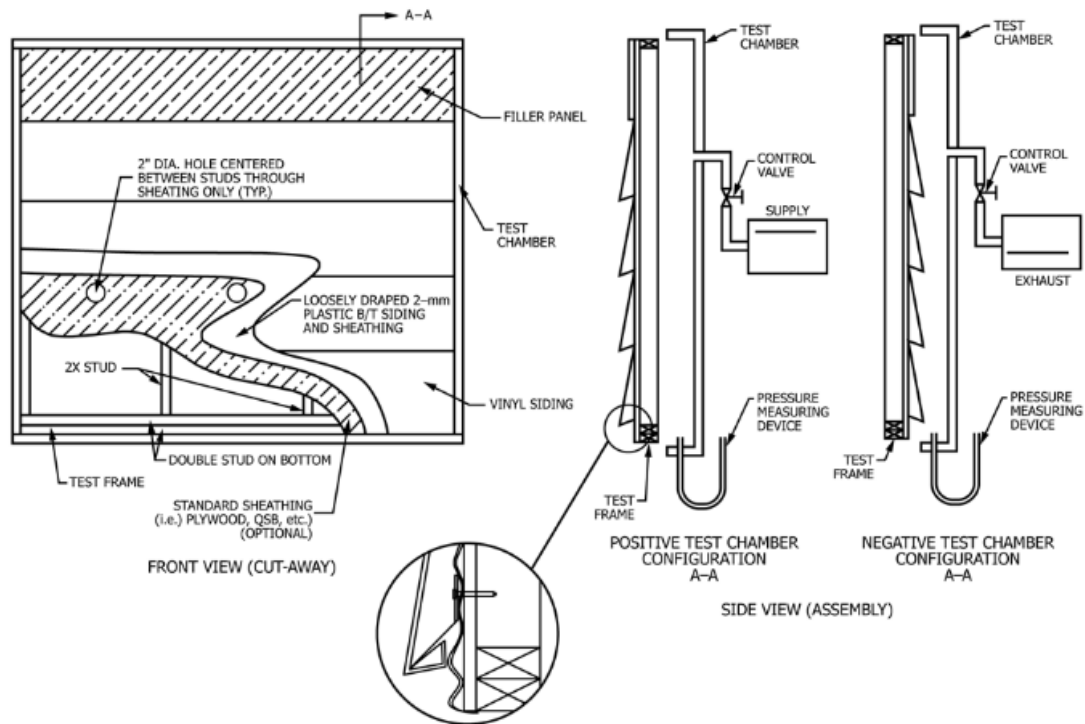


Figure 20. Test chamber assembly for ASTM D5206-13 (from (ASTM D5206 2013))

In the University of Florida experimental setup, it was not possible to eliminate pressure equalization effects by installing plastic sheeting between the vinyl siding and wood wall sheathing, since PEF testing was being performed on the same specimens that were subjected to ASTM D5206. With PEF testing, as described above, the plastic sheeting was installed between the wood sheathing and wood stud framing in order to create a sealed chamber yet allow for pressure equalization across the vinyl siding layer. Therefore, for ASTM D5206 testing at UF, pressure equalization was eliminated by opening the cavity underneath the vinyl siding to atmosphere through the edges of the specimen such that the area of leakage across the vinyl siding was much less than the area of leakage to atmosphere (Figure 21, Figure 22). By doing so, the cavity pressure remained at atmospheric while the chamber pressure was increased in magnitude in stepwise manner until failure occurred. Cavity pressures were measured throughout to ensure that the differential pressure across the vinyl siding was equal to the chamber pressure, i.e., no pressure equalization occurred.



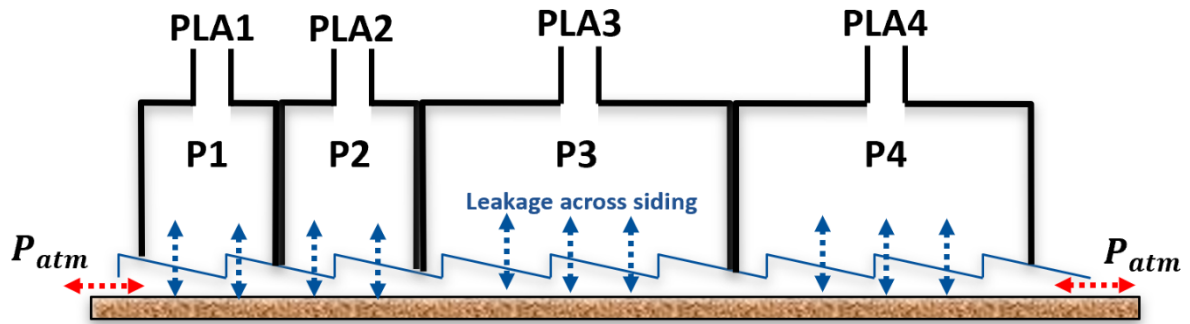


Figure 21. Illustration indicating leakage across siding and leakage to atmosphere. If the area of leakage to atmosphere is much greater than the area of leakage across the siding, the cavity pressure underneath the siding remains at atmosphere.

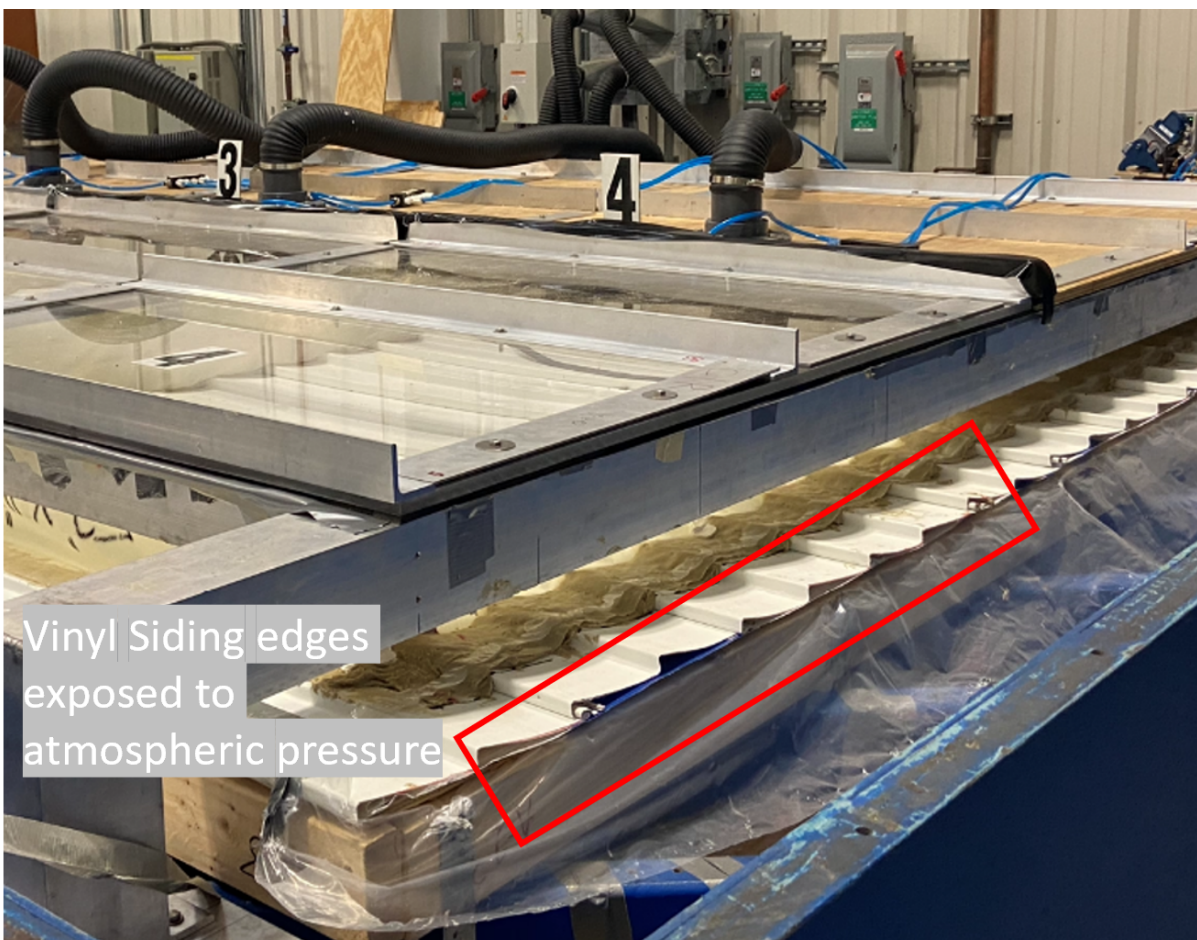


Figure 22. Exposure of vinyl siding edges for ASTM D5206 testing at UF, to eliminate pressure equalization by opening the cavity underneath the vinyl siding to atmosphere through the edges of the specimen such that the area of leakage across the vinyl siding was much less than the area of leakage to atmosphere.

## 5 RESULTS

A summary of results is presented below for (1) PEF values and (2) failure pressures and mechanisms stemming from the ASTM D5206 testing. Additional data on each test is provided in Appendix A and Appendix B.

### 5.1 Pressure Equalization Factors

The test results demonstrated that the cavity pressure between the vinyl siding and wood sheathing responds to the pressures on top of the siding in each of the four pressure chambers as expected. This is illustrated by comparing Figure 23 and Figure 24. In Figure 23 (uniform sine wave trace), the cavity pressure follows closely with the identical sine wave pressures in each chamber, which results in nearly complete pressure equalization and PEFs close to 0 as the chamber pressure increases. In contrast, when a spatial gradient is added (Figure 24; spatially varying sine wave trace), the effect of the pressure trace in each chamber can be clearly seen in the response of the cavity pressure, which retains elements of the frequencies of all pressure traces, akin to summing the various sine waves present. Stemming from this main observation, results are summarized below by comparing PEFs obtained from each specimen for each major trace class.

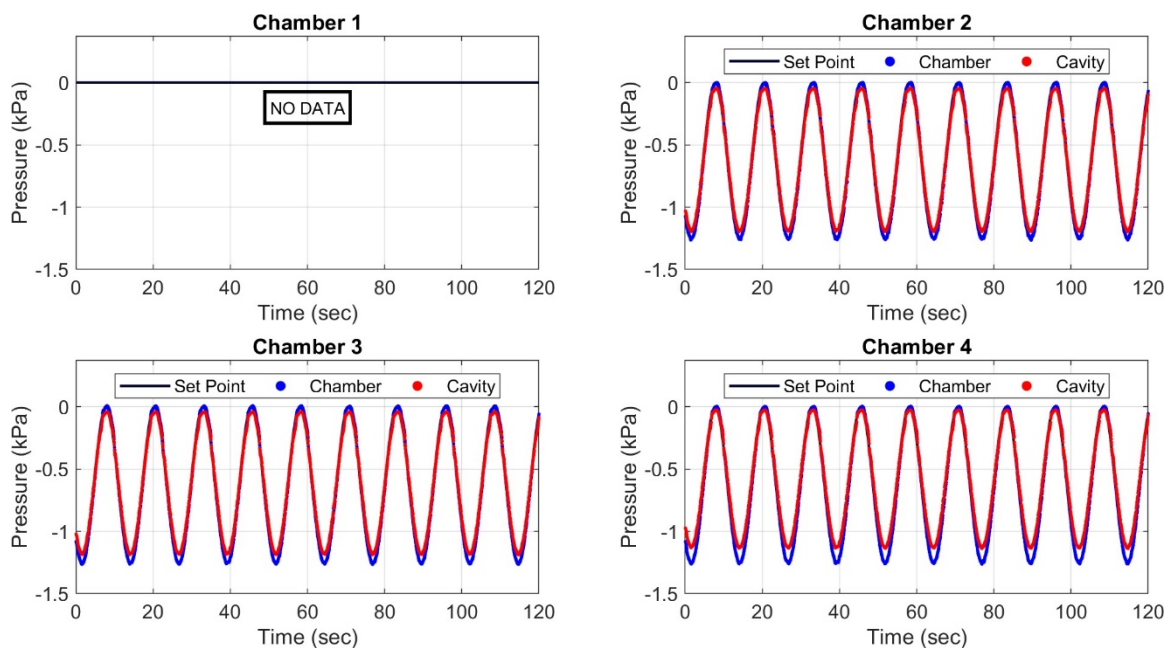


Figure 23. Chamber and cavity pressures in each chamber for the uniform sine wave trace (shown for a single nail-hem specimen).

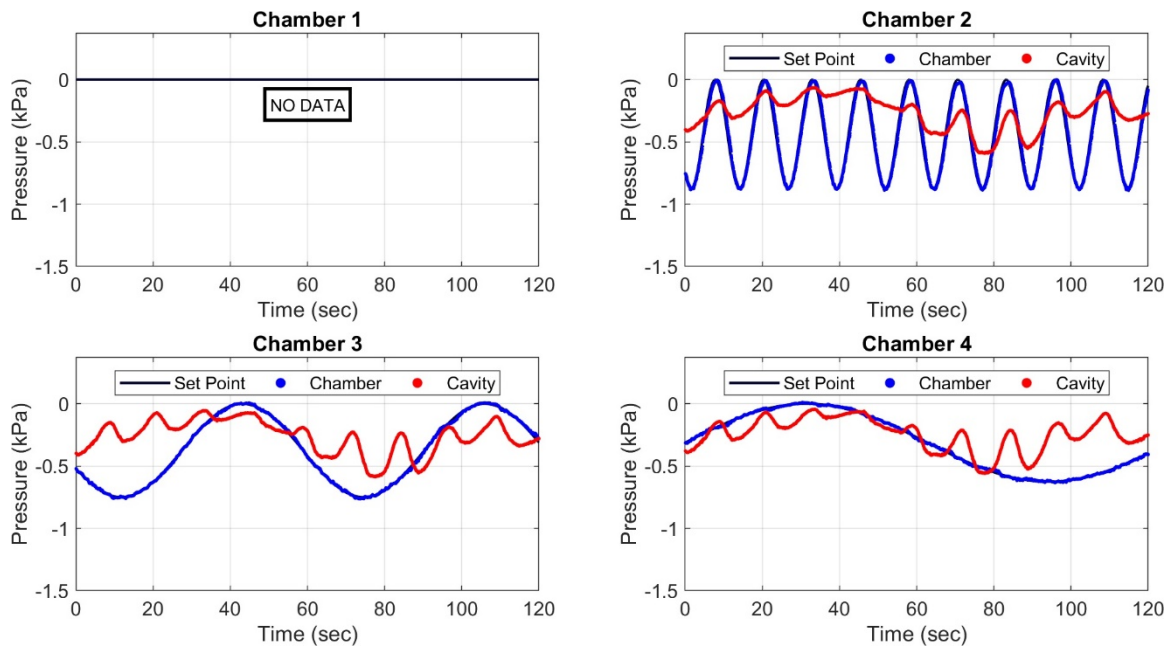


Figure 24. Chamber and cavity pressures in each chamber for the spatially-varying sine wave trace (shown for a single nail-hem specimen).

### 5.1.1 Spatially Uniform Static

Under spatially uniform static pressure loading, PEFs remained low, especially with the “T” setup, which ensured external pressures were truly uniform across all four chambers. Without the “T”, external pressures in Chambers 2-4 were identical, but Chamber 1 remained at atmospheric, inducing a small but noticeable pressure gradient across the specimen. The result is that without the T, PEFs under “uniform” pressures were as high as approximately 0.35 in some specimens. With the T, PEFs remain at or very close to 0 for all specimens. No conclusive trends with respect to product type are evident from these pressure traces.

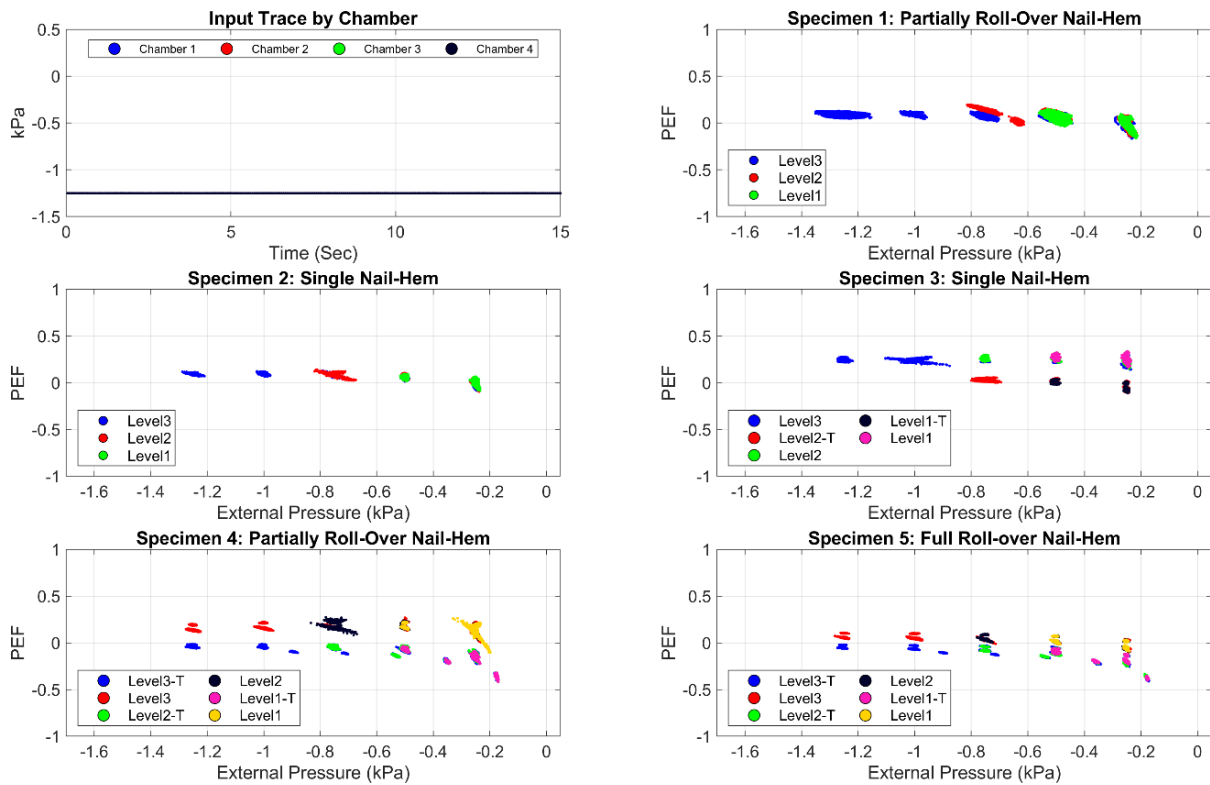


Figure 25. PEFs resulting from application of spatially uniform static pressure traces. A small portion of the target trace pressures is shown in the top left.

### 5.1.2 Spatially Varying Static

Under spatially varying static pressure loading, PEFs exhibited an asymptotic relationship, approaching a PEF value of approximately 0.6-0.7 for most specimens. Again, with the “T” setup, the PEF values were slightly lower, likely because a larger spatial gradient is present when Chamber 1 remains at atmosphere in comparison to being set equal to Chamber 2. For example, Table 4 illustrates the maximum spatial pressure gradient in one configuration of the spatially varying static traces both with and without the “T” setup. The larger spatial pressure gradient is present without the “T”, again suggesting that spatial pressure gradients are the dominant driver of PEF values. Again, no significant difference in PEF values was observed between specimens.

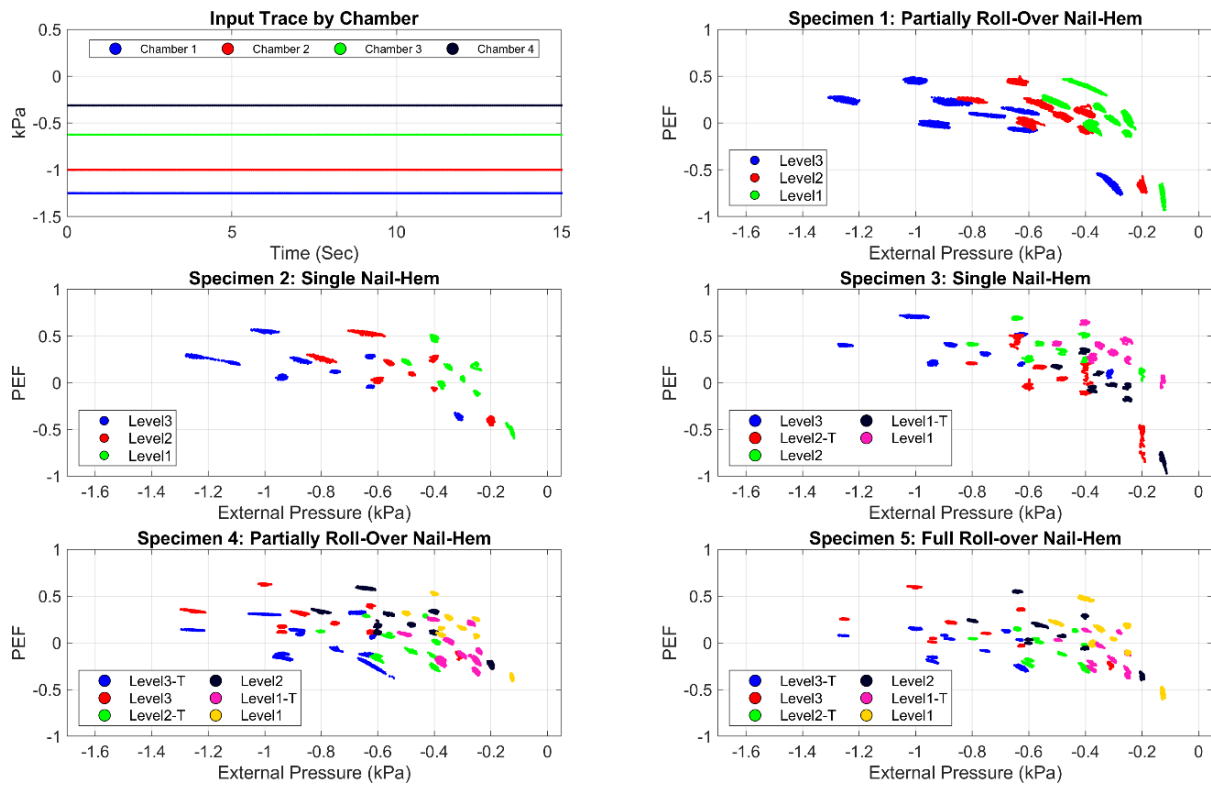


Figure 26. PEFs resulting from application of spatially varying static pressure traces. A small portion of the target trace pressures is shown in the top left.

Table 4. Illustrating the effect of the “T” setup on the magnitudes of the spatial gradients present across the specimen. Values taken from one segment of the spatially varying static pressure trace for Level 3 (peak pressure =  $-1.25$  kPa).

|                               | Pressure (No “T”), kPa | Pressure (with “T”), kPa |
|-------------------------------|------------------------|--------------------------|
| Chamber 1                     | 0                      | -1.25                    |
| Chamber 2                     | -1.25                  | -1.25                    |
| Chamber 3                     | -0.94                  | -0.94                    |
| Chamber 4                     | -0.94                  | -0.94                    |
| Maximum Differential Pressure | 0.94                   | 0.31                     |
| Maximum PEF (All Specimens)   | 0.75                   | 0.5                      |

### 5.1.3 Spatially Uniform Sine

Under spatially uniform sine wave pressure traces, PEF values were of similar magnitude to the uniform static, less than approximately 0.2 for the highest external pressures. The exception was the first partially roll-over nail-hem replicate (shown in top right of Figure 23)Figure 27. PEFs resulting from application of spatially uniform sine wave pressure traces. A small portion of the target trace pressures is shown in the top left., where the PID controls for the SPLA were not well tuned, leading to high overshoots and poor tracking of the target traces. This resulted in pressures not truly being uniform across the specimen, with significant



pressure gradients occurring as the various chambers tried to match the target trace, in turn driving larger PEF values. Once the system was better tuned to follow the traces, PEF values remained low, particularly with the T setup.

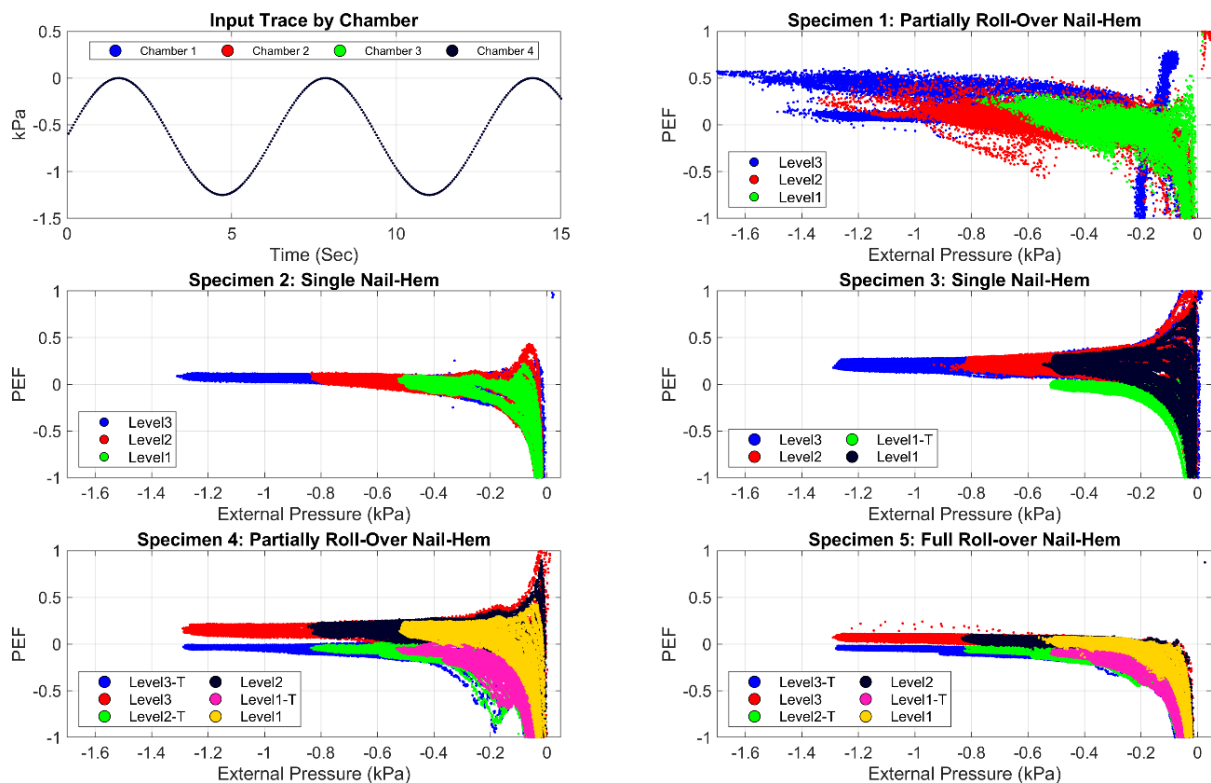


Figure 27. PEFs resulting from application of spatially uniform sine wave pressure traces. A small portion of the target trace pressures is shown in the top left.

### 5.1.4 Spatially Varying Sine

PEF values under spatially varying sine waves were much larger compared to the uniform sine wave pressure traces, approaching maximums greater than 0.8 for all specimens (Figure 28). Figure 28. PEFs resulting from application of spatially varying sine wave pressure traces. A small portion of the target trace pressures is shown in the top left. Considering tests run with the “T” setup only, the maximum PEF approached values between 0.6 and 0.7. In all tests, the highest PEF values again appeared to be driven by the magnitude of the instantaneous pressure gradient (i.e., the magnitude of the pressure differentials across the chambers at a given moment in time), with the highest pressure differentials driving the greatest PEF values.

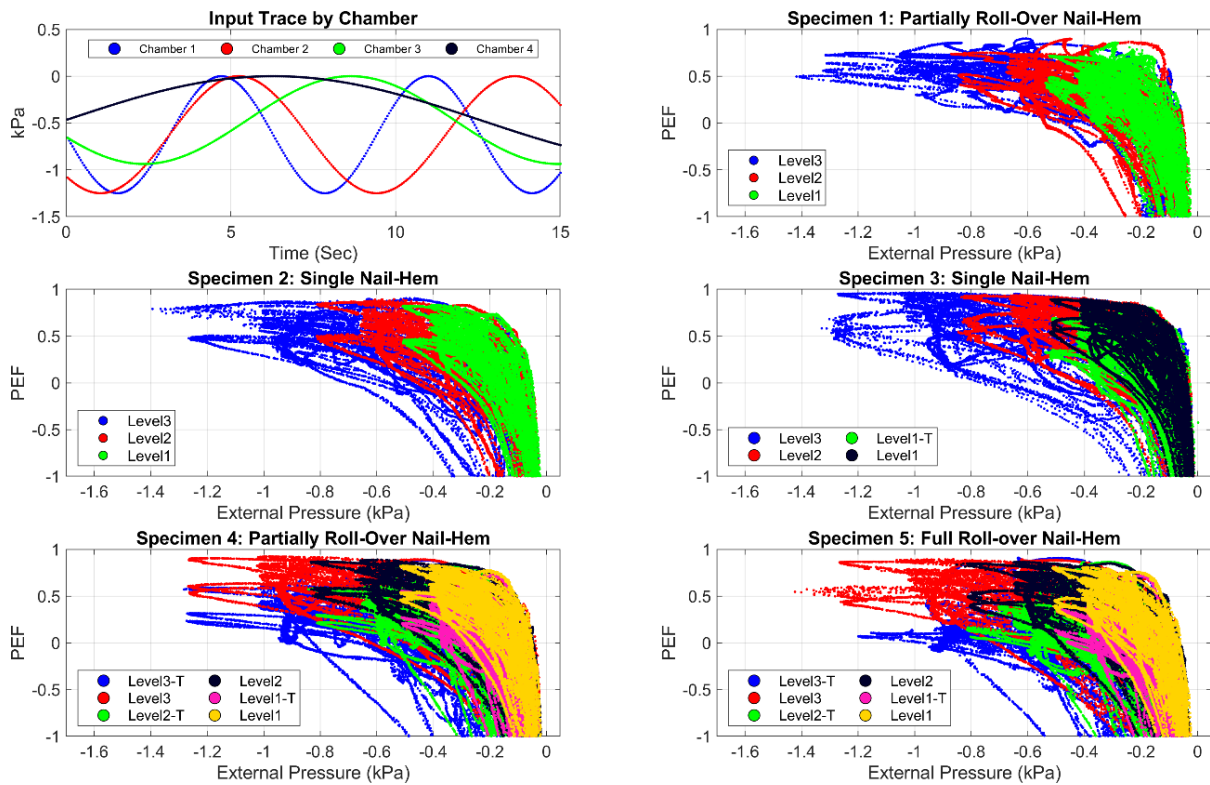


Figure 28. PEFs resulting from application of spatially varying sine wave pressure traces. A small portion of the target trace pressures is shown in the top left.

### 5.1.5 Stochastic Wind Trace

The stochastic wind traces (Figure 29) showed the greatest variability in the PEF values, with a dense array of PEF values for the range of external pressures tested. Similar trends were observed with the stochastic wind traces compared to the spatially varying sine wave traces, albeit with slightly lower PEF values overall, nominally approaching maximum values between 0.6 and 0.9, again with lower PEF values for the “T” test setup than without. The slightly lower PEF values in the realistic wind traces as compared to the spatially varying sine wave traces indicate that the wind loads on the residential-scale building used in this study were more highly correlated than what was represented by some of the sine wave traces generated. This is best illustrated by comparing the PEF values obtained using wind pressure traces from the leeward side of a building (where pressures within zones on the scale of the SPLA are highly correlated) to those obtained from a side wall (where flow separation and possibly reattachment occur and pressures are less correlated). As illustrated in Figure 30, for the leeward wall case, PEFs are nearly 0 with the “T” test setup (Level 3 pressures, WERFL Building Run 279), while for the side wall case (Figure 31) PEFs approach 0.5. This again reinforces that spatial gradients are the primary driver of PEF values, as the more correlated the pressure traces are the greater the pressure equalization that occurs.

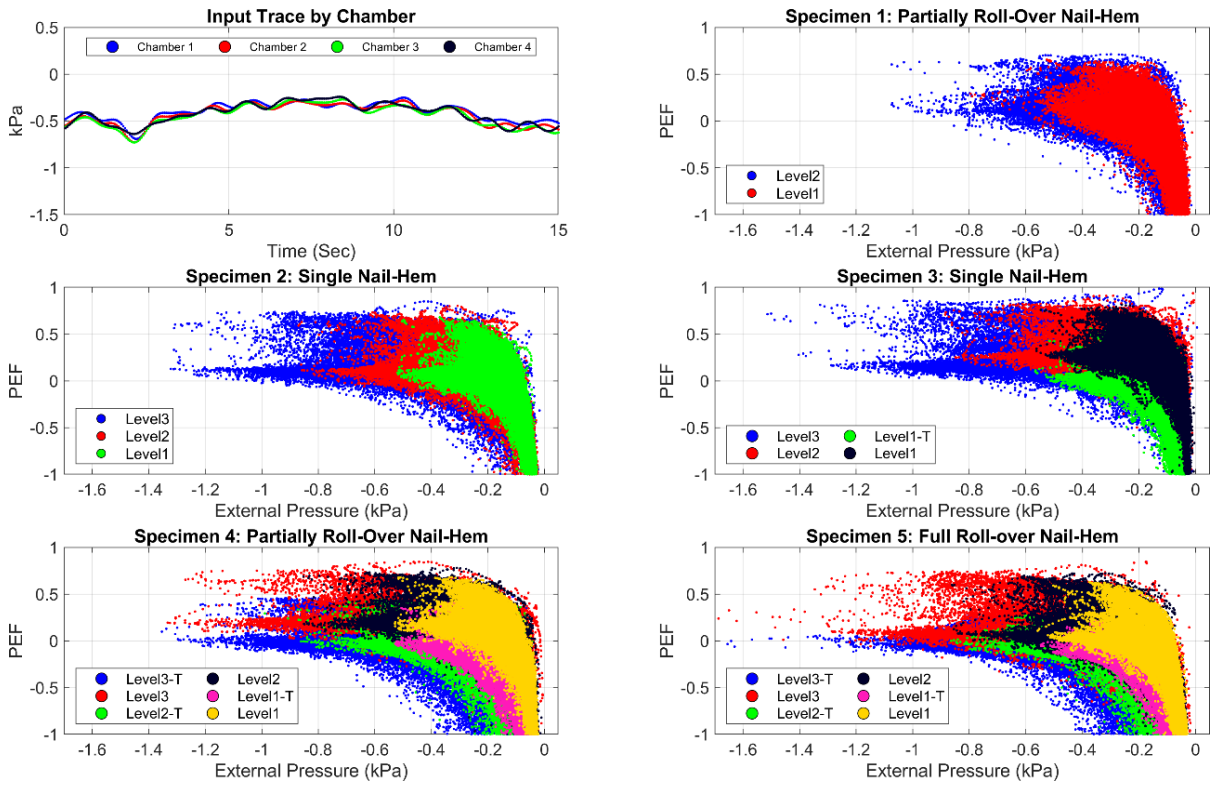


Figure 29. PEFs resulting from application of stochastic wind pressure traces. A small portion of the target trace pressures is shown in the top left.

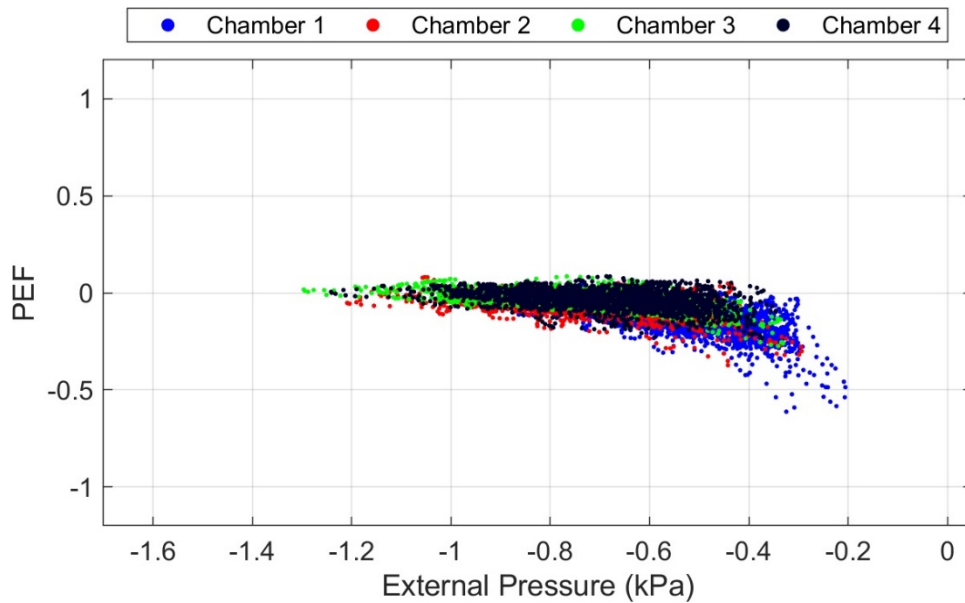


Figure 30. PEF values obtained using wind pressure time histories from the **leeward wall** of the WERFL Building Test Run 279 (Pressure Level 3, with "T" test setup).



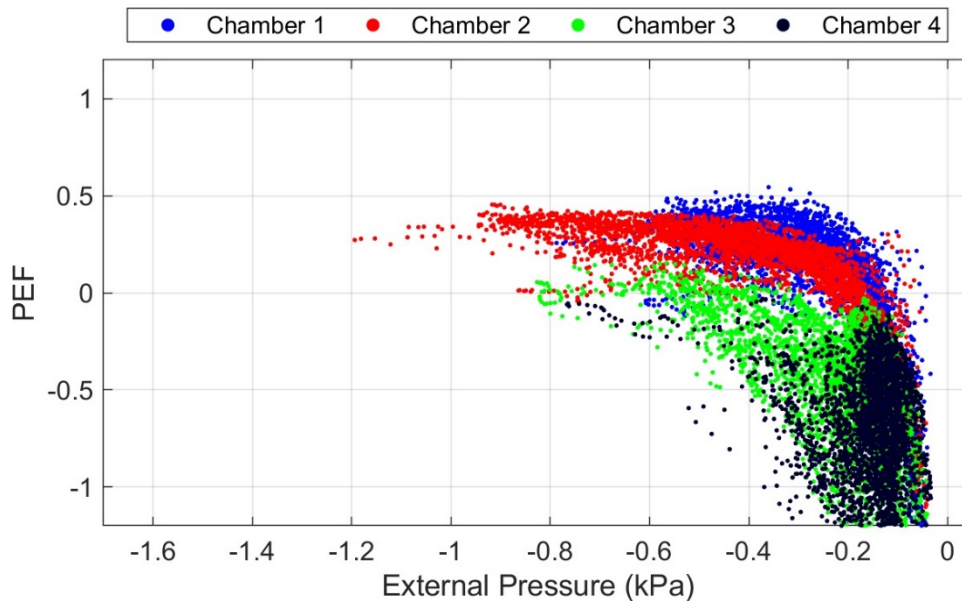


Figure 31. PEF values obtained using wind pressure time histories from the **side wall** of the WERFL Building Test Run 279 (Pressure Level 3, with “T” test setup).

### 5.1.6 Comparisons with Previous Studies

The PEFs generated using stochastic wind pressure traces are compared against both IBHS results (Cope et al. 2013) and UWO results (Miller et al. 2017) in Figures 32 and 33. Comparisons with the IBHS results use the instantaneous PEF convention shown in equation (1), where the instantaneous PEF is defined as the ratio of the instantaneous differential pressure across the vinyl siding in a given chamber to the instantaneous external or chamber pressure for the same chamber. For comparison with the UWO results, we use the envelope PEF convention shown in equation (2), where the PEF is taken as the ratio of the instantaneous differential pressure across the vinyl siding to the peak external pressure occurring in the given chamber during the entire time series. We use all data from all stochastic wind traces, and plot by maximum pressure level.

The comparisons overall show reasonably good agreement. Comparing instantaneous PEF values between UF and IBHS show maximum PEF values generally remaining less than 0.8 at larger magnitude external pressures. The descending asymptotic trend of PEF with external pressure present in the IBHS data is not present in the UF data, as the UF PEF values do not extend above 1. Recall however, that the UF PEF values represent just two different wind angles of attack and two regions of a building, whereas the IBHS data represents a full 360° of wind angles of attack and multiple regions of a building. Also of note is that the IBHS pressures presented were induced by wind speeds as high as 105 mph in their testing. This gives some scale to the pressures generated on the vinyl siding specimens in the UF study.

Envelope PEF values between UF and UWO test results showed similar patterns overall. The UF testing extended to higher external pressures but had slightly lower PEF values than the UWO testing. Note that the UWO tests were based on pressure traces directly obtained from the IBHS full-scale wind tunnel, while the UF tests used wind pressure traces from full-scale, in-situ measurements at the Texas Tech University WERFL building. All in all, the results are reasonably consistent, albeit with much higher variability in the UF PEF results as compared to UWO. Maximum PEF values approached 0.75 for each pressure level tested in the UF testing.

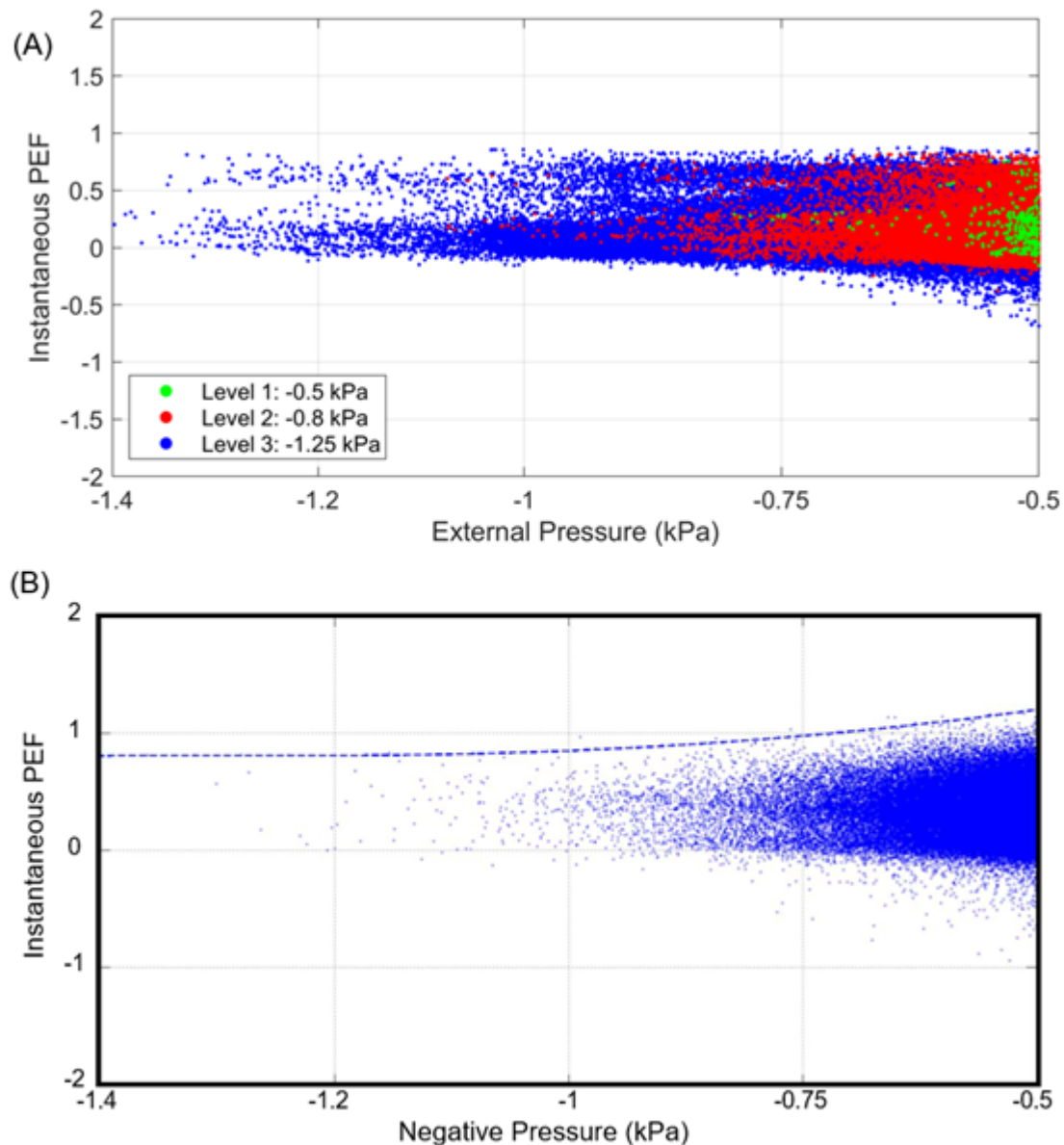


Figure 32. Comparison of instantaneous PEF values between (A) the current UF study and (B) IBHS data from Cope et al. (2013).

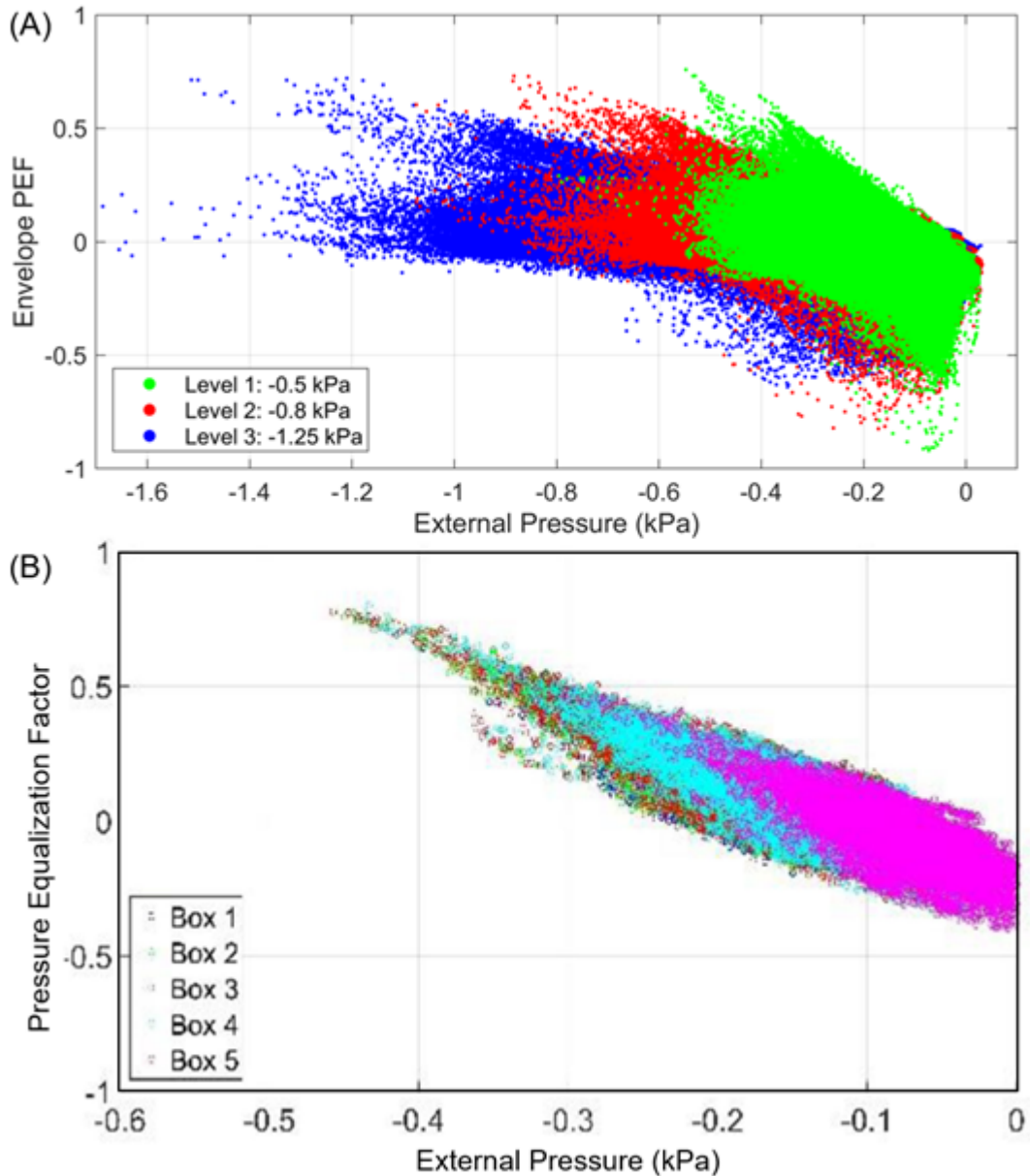


Figure 33. Comparison of envelope PEF values from (top) the current UF study, and (bottom) from the UWO multichamber pressure tests (Miller et al., 2017).

## 5.2 ASTM D5206 Resistance Tests

Two specimens (one Partial Roll-over Nail-Hem and one Full Roll-Over Nail-Hem) were subjected to ASTM D5206 testing with the vinyl siding edges exposed to atmospheric pressure. Both specimens had already been subjected to the full suite of wind traces used to generate PEF values as described in the preceding sections.

For both specimens, typical failures modes included stretching of the vinyl siding panels nail hem causing it to slide across the fastener at multiple locations (SF). Rupture of the nail hem (NF) was also observed. Figure 34 illustrates these failure mechanisms. Table 5 summarizes the specific failures and the pressures at which they occurred for each specimen.

For the Partial Roll-Over Nail-Hem, 39 SF failures occurred, initiating at -1.25 kPa, and ten NF failures occurred, initiating at -2.125 kPa. For the Full Roll-Over Nail-Hem, nine SF failures were observed, initiating at -1.25 kPa. Exact locations of each failure are provided in Appendix B.

In general, actual design failure pressures were not able to be reached in the pressure chambers (minimum applied pressure was -2.5 kPa) due to limitations of the test setup. Under the UF modified D5206 test setup, pressure equalization was negated by opening the edges of the vinyl siding panels, such that the areas of leakage across the vinyl siding were much less than the area of leakage to atmosphere as previously discussed. However, when the failures begin to occur at higher pressures, the vinyl siding panels start to deflect excessively (~5 in) upwards increasing the area of leakage across the siding and into the chamber. The PLAs were able to overcome this leakage until a maximum pressure point which was -2.5 kPa during the testing of specimen 4 (Chamber 3) and -2.125 kPa during the testing of specimen 5 (Chamber 4), at which point the area of leakage across the siding (internal cavity to pressure chamber) is of similar magnitude to the area of leakage to atmosphere (internal cavity to open edges). At this point, the system was no longer able to achieve the desired pressures in the chambers as the chambers themselves were now open to atmosphere via a leakage path through the deflected vinyl siding panels and on to the open edges of the specimen.



Figure 34. Typical failure modes encountered during ASTM D5206 testing. Vinyl siding panels stretch as pressure is applied and slide through the fastener (SF) (left image); rupture of the nail hem (NF) (right image).

Table 5. Failure modes and failure pressures recorded during ASTM D5206 for Specimen 4 Partial Roll Over Nail Hem vinyl siding.

| <b>Failure Modes</b> | <b>Failure Pressure (-kPa)</b> | <b>Failure Modes</b> | <b>Failure Pressure (-kPa)</b> |
|----------------------|--------------------------------|----------------------|--------------------------------|
| SF-1                 | 1.25                           | SF-30                | 1.5                            |
| SF-2                 | 2.125- 2.5                     | SF-31                | 2.125- 2.5                     |
| SF-3                 | 2.125- 2.5                     | SF-32                | 2.125- 2.5                     |
| SF-4                 | 2.125- 2.5                     | SF-33                | 2.125- 2.5                     |
| SF-5                 | 2.125-2.5                      | SF-34                | 2.125- 2.5                     |
| SF-6                 | 2.125-2.5                      | SF-35                | 2.125- 2.5                     |
| SF-7                 | 2.125-2.5                      | SF-36                | 2.125- 2.5                     |
| SF-8                 | 2.125-2.5                      | SF-37                | 1.25                           |
| SF-9                 | 2.125-2.5                      | SF-38                | 1.25                           |
| SF-10                | 2.125- 2.5                     | SF-39                | 1.25                           |
| SF-11                | 2.125- 2.5                     | NF-1                 | 2.125- 2.5                     |
| SF-12                | 2.125- 2.5                     | NF-2                 | 2.125- 2.5                     |
| SF-13                | 2.125- 2.5                     | NF-3                 | 2.125- 2.5                     |
| SF-14                | 2.125- 2.5                     | NF-4                 | 2.125- 2.5                     |
| SF-15                | 2.125- 2.5                     | NF-5                 | 2.125- 2.5                     |
| SF-16                | 2.125- 2.5                     | NF-6                 | 2.125- 2.5                     |
| SF-17                | 2.125- 2.5                     | NF-7                 | 2.125- 2.5                     |
| SF-18                | 2.125- 2.5                     | NF-8                 | 2.125- 2.5                     |
| SF-19                | 2.125- 2.5                     | NF-9                 | 2.125- 2.5                     |
| SF-20                | 2.125- 2.5                     | NF-10                | 2.125- 2.5                     |
| SF-21                | 2.125- 2.5                     |                      |                                |
| SF-22                | 2.125- 2.5                     |                      |                                |
| SF-23                | 2.125- 2.5                     |                      |                                |
| SF-24                | 2.125- 2.5                     |                      |                                |
| SF-25                | 2.125- 2.5                     |                      |                                |
| SF-26                | 2.125- 2.5                     |                      |                                |
| SF-27                | 2.125- 2.5                     |                      |                                |
| SF-28                | 2.125- 2.5                     |                      |                                |
| SF-29                | 2.125- 2.5                     |                      |                                |

Table 6. Failure modes and failure pressures recorded during ASTM D5206 for Specimen 5 Full Roll Over Nail Hem vinyl siding.

| <b>Failure ID</b> | <b>Pressure kPa</b> |
|-------------------|---------------------|
| SF-1              | 1.2                 |
| SF-2              | 2.125               |
| SF-3              | 2.125               |
| SF-4              | 2.125               |

|      |       |
|------|-------|
| SF-5 | 2.125 |
| SF-6 | 2.125 |
| SF-7 | 2.125 |
| SF-8 | 2.125 |
| SF-9 | 2.125 |

## 6 DISCUSSION

The main takeaway from the results thus far is that the spatial pressure gradient is the driving factor behind Pressure Equalization Factors (PEFs). Our results show that uniform static pressures, uniform dynamic pressures, or highly correlated stochastic wind pressures all produce low PEF values. In contrast, spatial pressure gradients caused by multi-chamber application of static pressures, weakly or uncorrelated sine wave pressure time series, or weakly or uncorrelated stochastic wind pressure time series all produced higher PEF values, approaching 0.9 with certain sine wave pressure time series. The maximum PEFs are reasonably consistent in our testing for all specimens and major trace classes once negative external pressure magnitudes exceed approximately -0.5 kPa. More negative pressure magnitudes tended to show little variation in the maximum PEFs beyond this value. These findings agree well with those of previous studies (Cope et al. 2013, Miller et al. 2017) as discussed previously. Our study tended to produce slightly lower PEF values with stochastic wind pressure traces than comparable studies, but this may in part be due to the differences in the wind pressures themselves. While each of the UF, IBHS and UWO studies nominally used wind pressure data measured in full-scale in open terrain, the data used from the WERFL building in this project were generated by lower wind speeds than IBHS, and had slightly lower turbulence levels than those reported by IBHS. There may be some dependence of the PEFs on the level of turbulence in the upwind flow, which is primarily driven by the terrain (more suburban or urban terrain generates higher turbulence levels), but this hypothesis would require further exploration.

With regards to the potential for future test standards to assess PEF values, the testing showed that nearly any PEF value can be generated with the right combination of spatial and temporal pressure gradients. Even static pressure gradients were able to produce meaningful PEF values over a wide range (0 – 0.75). It will therefore be up to the industry, governing bodies, and other stakeholders to come to a consensus on (1) what is the appropriate PEF for any of the vinyl siding systems that have been tested thus far under pressure gradients either at UF or other facilities; and (2) the proper test approach to reproduce those PEFs using a test standard that can be applied to a wide range of vinyl siding systems. Our data clearly demonstrates that such a standard is possible using multi-chamber test setups, but other options also exist for directly measuring through-gap and along-gap leakage area as discussed in Miller (2020), and may already be under consideration by industries and stakeholders for other air-permeable cladding systems.

With respect to observed failures, the chamber pressures never exceeded the listed design pressures for the specific vinyl siding products used during the PEF testing, but a handful of failures were still observed. Most failures occurred during the spatially varying sine waves portions of the testing, when PEFs were generally the highest, and most occurred in the single nail-hem product testing. In the modified ASTM D5206 testing, failures were more widespread, being observed at 58 different fastener locations in the two specimens tested, despite not reaching the full design pressure. Failures primarily consisted of nail slippage through the nail hem (83% of all observed failures), but rupture of the nail hem was also observed (27% of failures). It should be noted that the ASTM D5206 tests for both specimens were completed after the full run of PEF testing was completed on the same samples. Fatigue-related failures could have played a role in the failures, but if so, then fatigue-related issues would also be of concern during long duration loading from a hurricane.



## 7 CONCLUSIONS

Tests conducted on three vinyl siding products using a multi-chamber pressure test bed simulated uniform and spatially varying static, dynamic, and stochastic pressure distributions. Those external pressures generated a broad range of net pressures within the gap between the vinyl siding and wall sheathing, reflected in a wide range of pressure equalization factors (PEFs). Key findings from the project are summarized as follows:

- In general, the spatial pressure gradients across the pressure chambers were the dominant drivers in the observed PEFs.
- We observed PEF values using 3-chamber (called “without T-section” in report) and 4-chamber test beds. PEF values at or near peak negative pressures were higher when using the 3-chamber test bed since the 4<sup>th</sup> chamber remained at atmospheric, creating a larger pressure gradient. These results reinforced our theory that spatial pressure gradients drive the PEF values.
- The cavity pressures, (i.e. measured pressures within the gap between vinyl siding and wood sheathing), respond directly to the external pressures applied above (or on the top surface of) the vinyl siding specimen in all pressure chambers.
- The magnitude of the PEFs, which is a measure of the difference between external pressure and the cavity pressure, is increased as the spatial pressure gradients (i.e. differences in pressure levels between chambers) is increased. When the spatial pressure gradient is zero (i.e. all chambers are held at the same pressure), the PEF values at peak negative chamber pressure were also nominally zero ( $< 0.05$ ).
- When a varying static pressure trace is applied to vinyl siding specimens, the PEF results asymptotically approaches the highest PEF values, at or near peak negative pressures. The trends in these results are in general agreement with previous observations of similar studies conducted by Institute for Business and Home Safety and Western University.
- Results from the uniform sinusoidal pressure time series were similar to the behavior observed with the static uniform pressures (PEF values less than 0.2 for the most negative external pressure) resulting in almost perfect pressure equalization when no spatial gradients were present, despite the temporal variations.
- Maximum PEF values were observed for specimens subjected to spatially varying sinusoidal pressure time series. This is the expected result as this pressure time history is the least correlated among all chamber pressure test sequences used. The larger the pressure difference between chambers, the greater the differences that potentially

exist between the cavity pressure and the external pressure in any given chamber, producing a higher PEF.

- As expected, the stochastic pressure time histories (of actual wind pressure traces) show the greatest variability in the PEF values. The PEF values from stochastic traces show similar trends to the spatially varying sine waves, although with slightly lowered overall PEF values. The slightly lowered PEF values observed with the actual wind traces indicate that the wind pressure time-history from the residential-scale building used in this study is better correlated than the time-history of the artificial spatially varying sine wave.
- Results of two ASTM D5206 protocol tests produced specimen ultimate failures at 1.25 kPa and 2.5 kPa, respectively. These ultimate failure pressures are substantially lower than the certified wind uplift pressure capacity for the systems. It is reasonable to expect a low failure pressure because the D5206 tests were run following very experimental arduous pressure test series to develop our PEF results. Typical observed failure modes were rupture of the nail hem and sliding of the panels nail hem across the fastener due to stretching of the vinyl siding panels.
- It is possible to reproduce the spatial and temporal characteristics of observed PEF values produced during the stochastic wind pressure testing by using a simplified static pressure test sequence. It is important that the spatial pressure gradients within the simplified test sequence matches the pressure gradients of the stochastic pressure trace.

This study has provided guidance and it can be used as a resource document for developing standard pressure test protocols to evaluate pressure equalization factors on vinyl siding systems. Careful interpretation of the results is required; including the selection of chamber pressure levels, how specimens are installed and sealed and selecting the spatial pressure gradients. The next step recommended for this research is to study appropriate test sequences to replicate stochastic pressure distributions using the simplified uniform pressure sequences. This should be done in collaboration with certified test laboratories in order to work with the level of equipment sophistication that is commonly available to them.

## REFERENCES

- ASTM (2013). "ASTM D5206-13 Standard Test Method for Wind Load Resistance of Rigid Plastic Siding." ASTM International.
- ASTM (2017). "ASTM D3679-17 Standard Specification for Rigid Poly(Vinyl Chloride) (PVC) Siding." ASTM International.
- Baradaranshoraka, M., Pinelli, J.-P., Gurley, K., Peng, X., and Zhao, M. (2017). "Hurricane wind versus storm surge damage in the context of a risk prediction model." *Journal of Structural Engineering*, 143(9), 04017103.
- American Society of Civil Engineers (2019). *Design Loads on Structures during Construction*, ASCE Library.
- ASTM D3679 (2017). "Standard Specification for Rigid Poly(Vinyl Chloride) (PVC) Siding." West Conshohocken, PA; ASTM International.
- ASTM D5206 (2013). "Standard Test Method for Windload Resistance of Rigid Plastic Siding." West Conshohocken, PA; ASTM International.
- Cook, N. J., Keevil, A. P., and Stobart, R. K. (1988). "Brewulf-the big bad wolf: I'll huff and I'll puff and I'll blow your house down!" *Journal of Wind Engineering and Industrial Aerodynamics*, 29(1-3), 99-107.
- Cope, A. D., Crandell, J. H., Johnston, D., Kochkin, V., Liu, Z., Stevig, L., and Reinhold, T. A. (2013). "Wind loads on components of multi-layer wall systems with air-permeable exterior cladding." *Advances in Hurricane Engineering: Learning from Our Past*, 238-257.
- Kopp, G. A., and Gavanski, E. (2011). "Effects of pressure equalization on the performance of residential wall systems under extreme wind loads." *Journal of Structural Engineering*, 138(4), 526-538.
- Kopp, G. A., Morrison, M. J., and Henderson, D. J. (2012). "Full-scale testing of low-rise, residential buildings with realistic wind loads." *Journal of Wind Engineering and Industrial Aerodynamics*, 104-106, 25-39.
- Kopp, G. A., Morrison Murray, J., Gavanski, E., Henderson David, J., and Hong Han, P. (2010). "'Three Little Pigs' Project: Hurricane Risk Mitigation by Integrated Wind Tunnel and Full-Scale Laboratory Tests." *Natural Hazards Review*, 11(4), 151-161.
- Miller, C. S. (2020). "Design Wind Loads for Air-Permeable Multilayer Cladding Systems."
- Miller, C. S., Kopp, G. A., Morrison, M. J., Kemp, G., and Drought, N. (2017). "A Multichamber, Pressure-Based Test Method to Determine Wind Loads on Air-Permeable, Multilayer Cladding Systems." *Frontiers in Built Environment*, 3, 7.
- Moravej, M., Zisis, I., Gan Chowdhury, A., Irwin, P., and Hajra, B. (2016). "Experimental Assesment of Wind Loads on Vinyl Wall Siding." *Frontiers in Built Environment*, 2(35).
- Morrison, M. J., and Cope, A. D. "Wind performance and evaluation methods of multi-layered wall assemblies." 2735-2748.

## Appendix A. PEF Results per Specimen

### Specimen 1- Partially Roll-over Nail Hem

Test Specimen 1 (July 8, 2020- 11:00 am to 1:00 pm)

Present

UF Team:

- Oscar Lafontaine
- Xinyang Wu
- Dmtrii Golovichev
- David O. Prevatt
- Irina Afanasyeva
- Keith Mungal

Advisory Group via Zoom:

- Mo Madani
- Matt Dobson
- Sara Krompholz
- Neil Sexton
- Fernando Pages
- Anne Cope

Specimen:

- First specimen selected for testing was the Partially Folded Roll- over nail hem.
- Specimen is 112 in by 160 in and was installed under the direction of Eric Cotterman, Certified Vinyl Siding Installer/ Trainer.

Issues:

- The PLA attached to chamber 1 number is not working – we determined to conduct experiment with remaining 3.
- This is first time the control software was run. The experiment was used to iron out bugs – such as
  - Establishing appropriate running time
  - Latex failure in the fourth pressure chamber
  - Vinyl siding excessive expansion due to a suspected fastener withdrawal failure
  - Excessive leakage at the edges of the fourth pressure chamber



Figure 35. Failure of latex in fourth chamber specimen 1 on July 8, 2020; possibly due to fastener penetration through the latex.

- The UF team took the rest of the day to address these issues:
  - The latex failure was patched by gluing another piece and reinforced with duct tape
  - Furthermore, latex is now reinforced with tape around the areas where fasteners are inserted ensuring the fastener does not damage the sheet when being drilled into the aluminum beams or angles.



Figure 36. Reinforcement of latex with tape around fastener areas.

- Inspection of the vinyl siding panels showed that the panels were sliding through fasteners at locations where a nail puncher was used.
  - The nail puncher was used to be able to fasten at the wood stud locations

- Some of the panels were able to be separated from the interlocked panel and fasteners were installed at regular nail slot locations
- However, at other locations, face nailing had to be done as a correction
- The edges of the vinyl siding were carefully sealed by using silicon and duct tape at leakage locations



Figure 37. Detachment of vinyl siding through nail hem slots created by using punching nail. Failure occurred in chamber 3 in multiple panels.

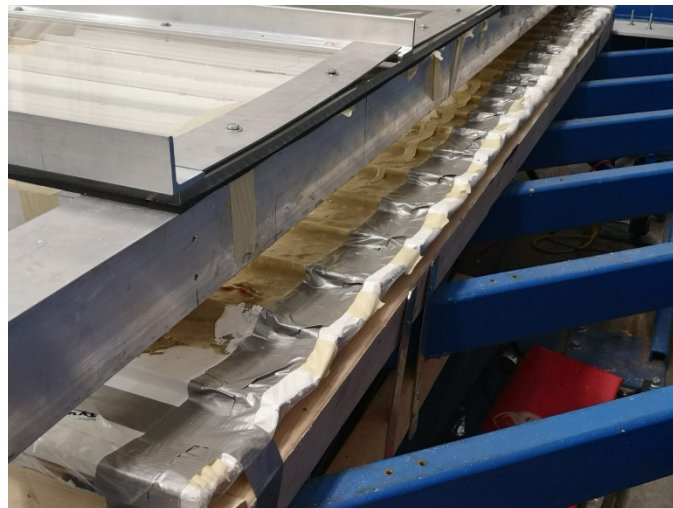


Figure 38. Seal of the perimeter of specimen 1 at the fourth pressure chamber with silicon and duct tape.

## Test Specimen 1 (continuation July 9, 2020- 11:00 am to 5 pm)

Present

UF Team:

- Oscar Lafontaine
- Xinyang Wu
- Dmtrii Golovichev
- David O. Prevatt
- Irina Afanasyeva
- David B. Roueche
- Daniel Smith
- Keith Mungal

Advisory Group via Zoom:

- Matt Dobson
- Sara Krompholz
- Fernando Pages
- Murray Morrison

Issues:

- The testing was briefly stopped during the morning to correct the output of the Omega-4 sensor which was reporting positive pressure values, instead of the negative values (vacuum) that we are applying.
- Problem was troubleshooted and testing resumed at 2:30 pm.

Testing outcome:

- Results for level 1 and level 2 of pressures were recorded with no significant damage to the vinyl siding or the chambers.
- Static results for level 3 were recorded with no significant damage to the vinyl siding or the chambers.
- During the level 3 dynamic test, the latex in the fourth chamber failed initially at 1.25 kPa but the chamber maintained the applied pressure (leakage was not significant)
  - At a later stage of the test, the chamber the failure of the latex progressed until the chamber pressure was remaining atmospheric
  - Stochastic level 3 test was not performed for this reason



Figure 39. Failure of latex in Chamber 4; failure possibly due to latex not being engaged by weatherstripping from below the aluminum plate (weatherstripping only on right side of the angle).

- A second layer of weatherstripping will be added on the side of the aluminum plate to ensure the latex is engaged

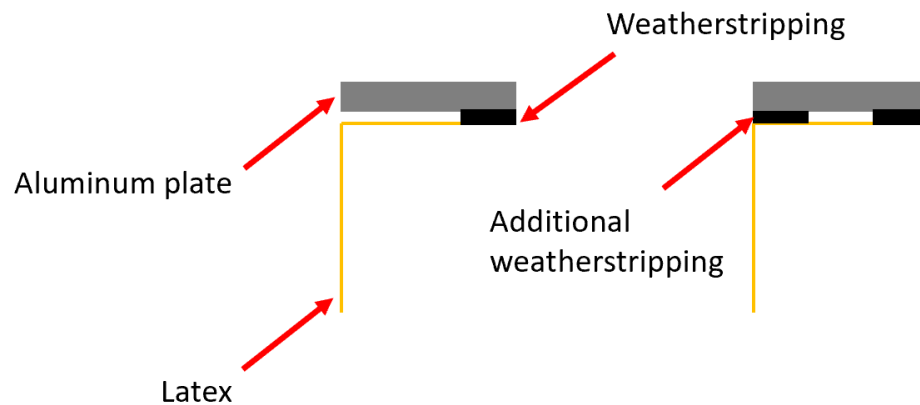


Figure 40. Secondary layer of weatherstripping to ensure engagement with aluminum plate



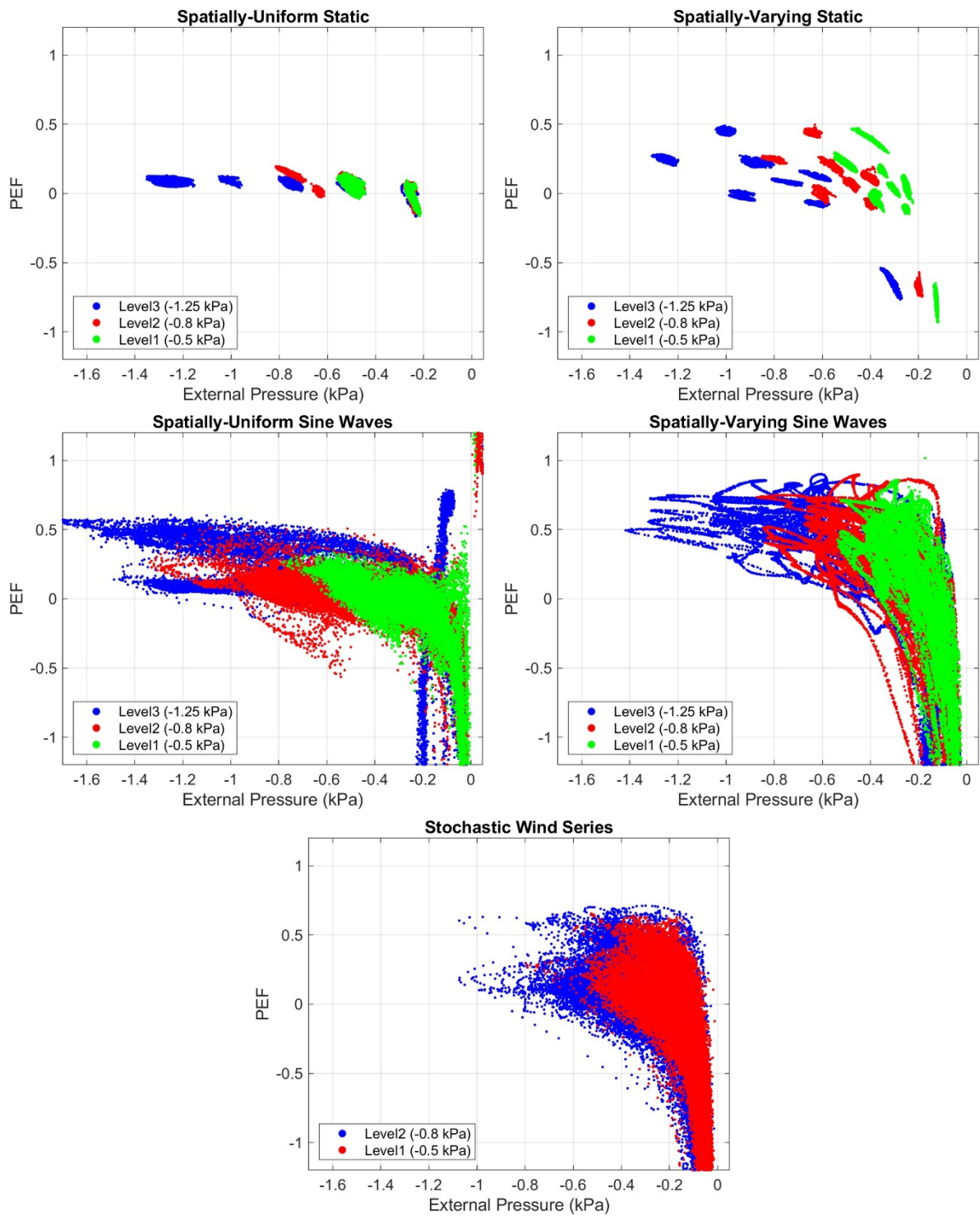


Figure 41. Static, dynamic, and stochastic test results for Specimen 1 (without T).

## Specimen 2- Single Nail Hem

Testing Specimen 2 (July 14 9:00 am – 1:00 pm)

Present:

UF Team:

- Oscar Lafontaine
- Xinyang Wu
- Dmtrii Golovichev
- David O. Prevatt

Advisory Group via Zoom:

- Matt Dobson
- Sara Krompholz
- Fernando Pages

Testing Outcome:

- No failure of the vinyl siding panels was observed during PEF testing
- Pressure Equalization testing was overall successful

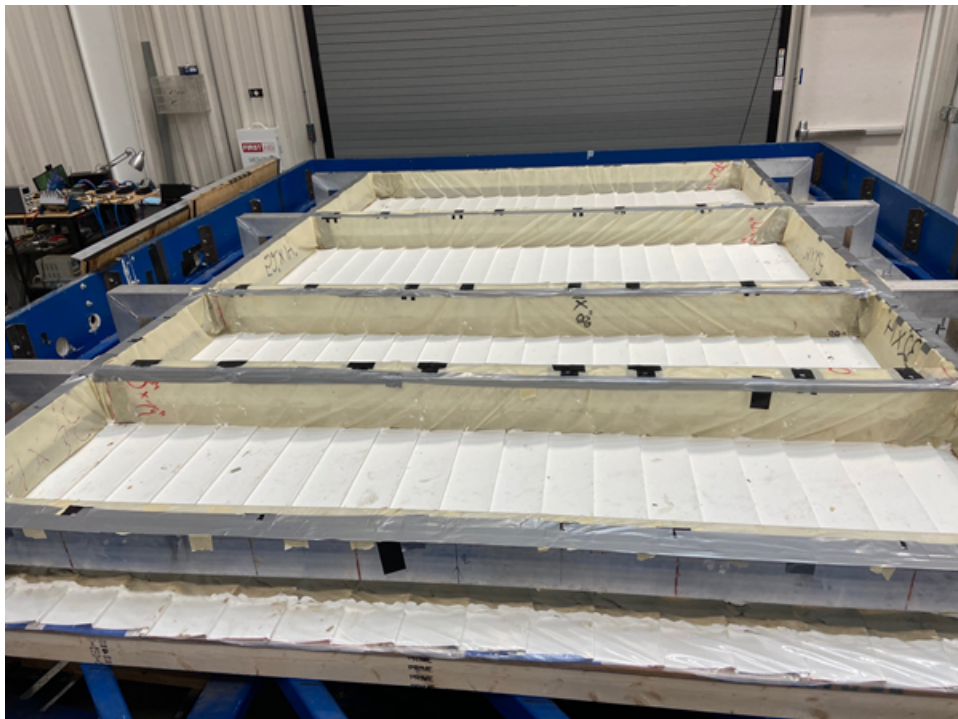


Figure 42. Reinforcement of latex along the frames with duct tape.

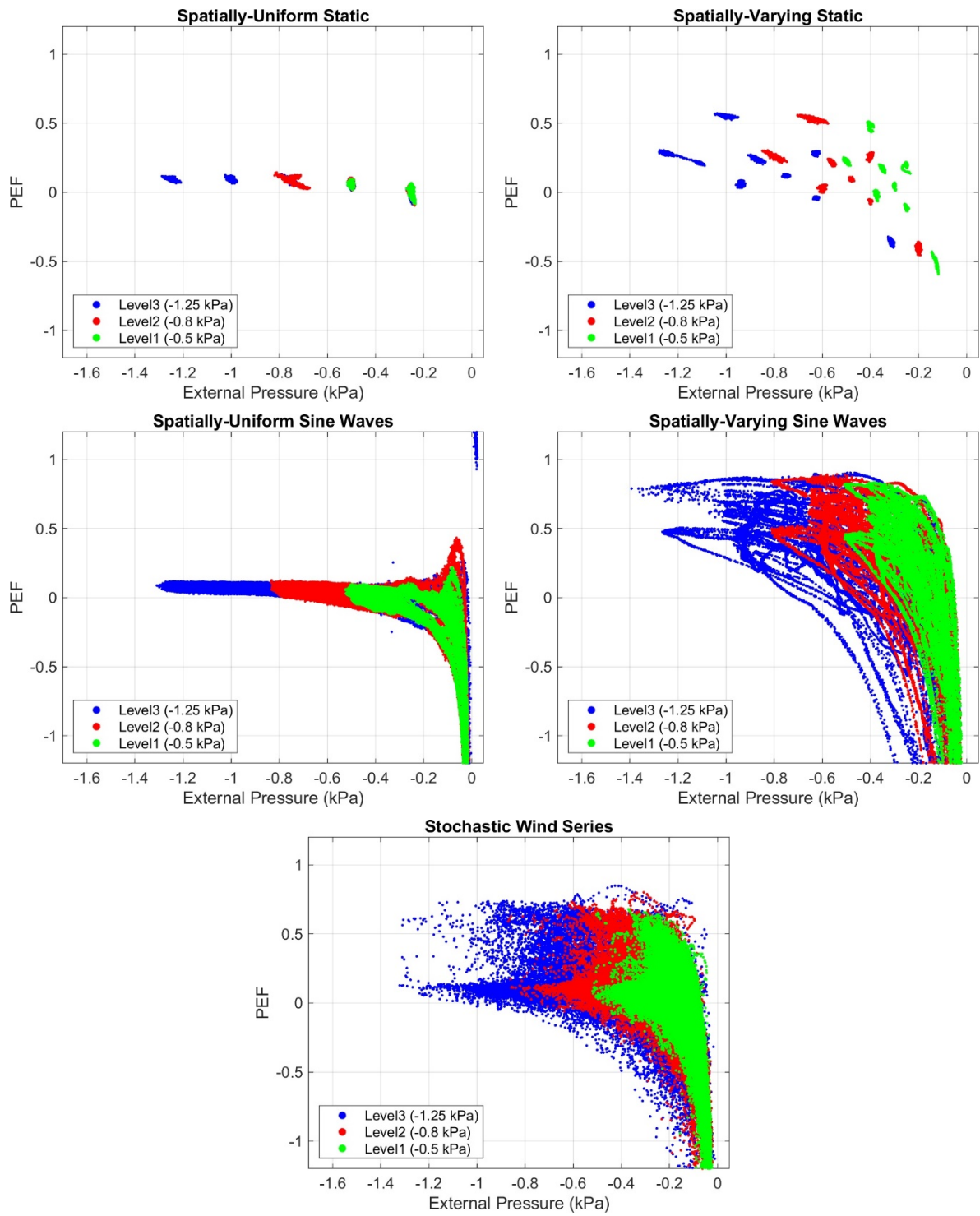


Figure 43. Static, dynamic, and stochastic test results for Specimen 2 without T.

## Specimen 3- Single Nail Hem

**Testing Specimen 3 without T connection (July 16 10:00 am – 2:00 pm)**

Present:

UF Team:

- Oscar Lafontaine
- Xinyang Wu
- Dmtrii Golovichev

Advisory Group via Zoom:

- Matt Dobson
- Sara Krompholz
- James Schock

Testing Outcome:

- Failures of five vinyl siding panels occurred in chamber 3 during spatially varying sine waves (at 1.25 Kpa)
  - Spatially varying sine wave tests show the highest PEFs which mean the panels are subjected to the highest net pressures
  - The failure mechanism has not been yet investigated by verifying under the panels however the same panel deflection heavier was observed as when the fastener slides across the nail hem slot
- Pressure Equalization testing was overall successful

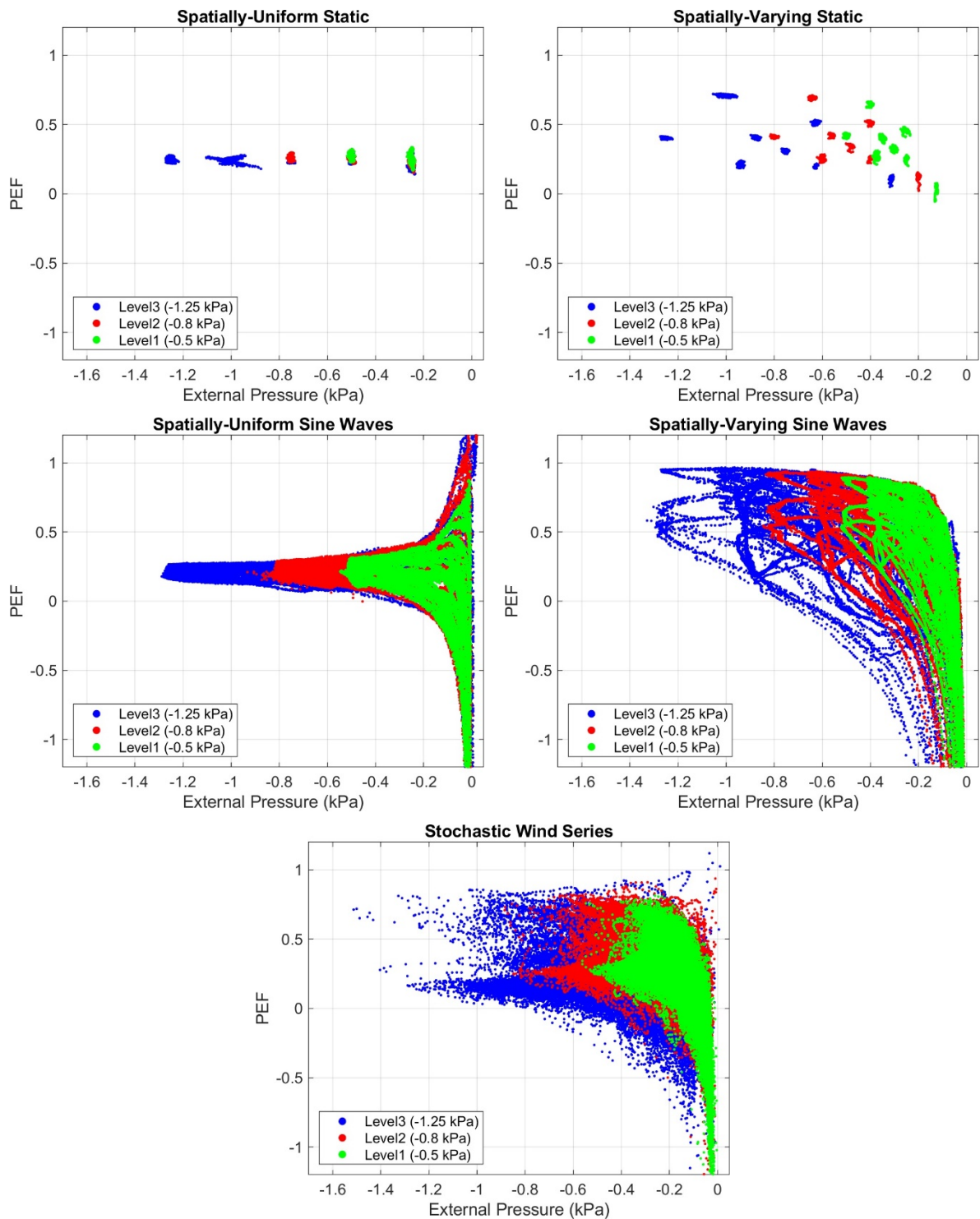


Figure 44. Static, dynamic, and stochastic test results for Specimen 3 without T.

## Specimen 3T- Single Nail Hem

### Testing Specimen 5 with T connection (July 16 5 pm – 7 pm)

Present:

UF Team:

- Oscar Lafontaine

Testing Outcome:

- A T connection was bought after the morning session testing to pressurize all chambers
- The PLA systems were able to apply pressures in all chambers
  - PLA 2 was capable of applying pressures to both Chamber 1 and Chamber 2
- Data for static level 1 and level 2, as well as dynamic and stochastic level 1 was collected to observe the system performance

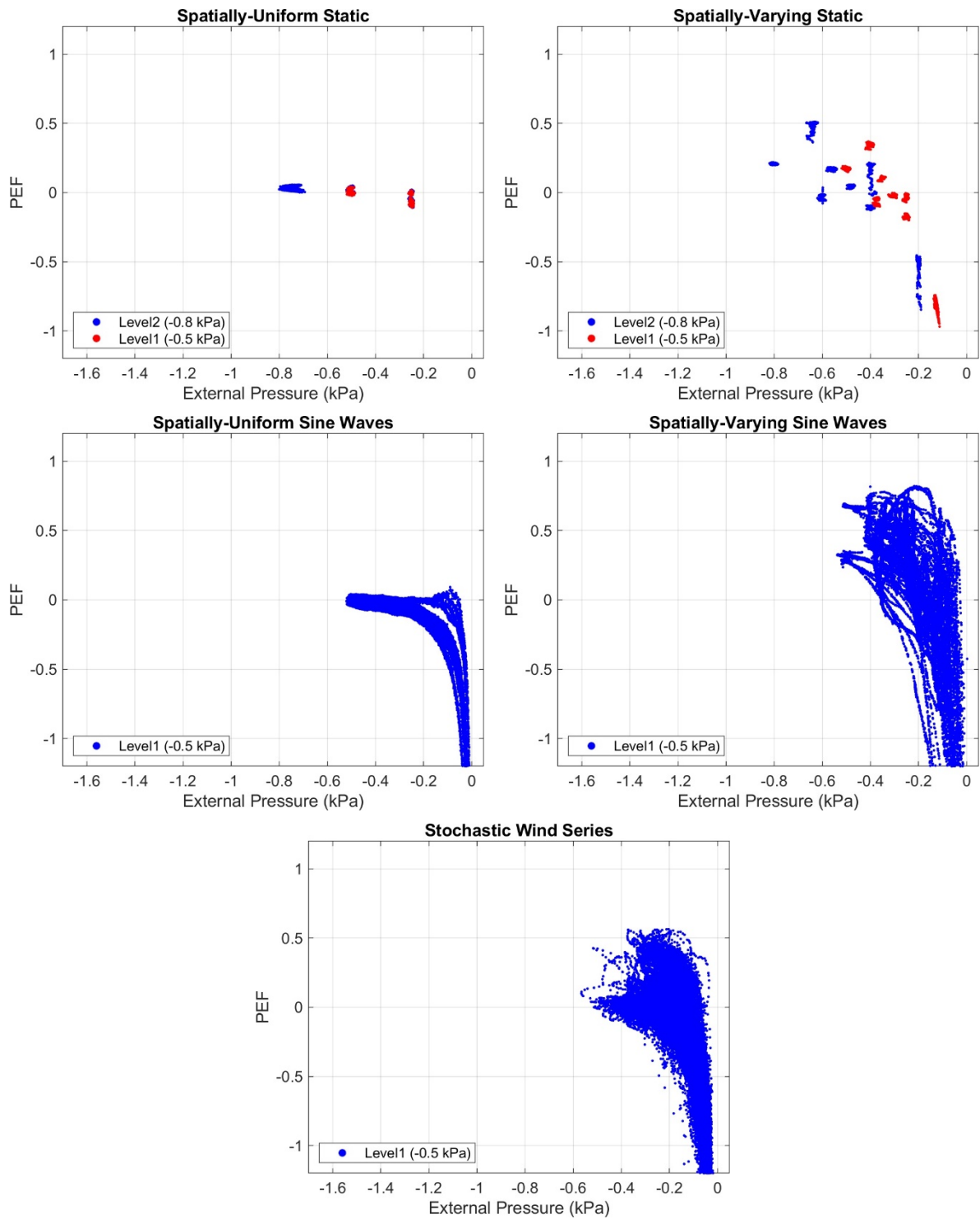


Figure 45. Static, dynamic, and stochastic test results for Specimen 3 with T.

## **Specimen 4- Partially Roll-over Nail Hem**

**Testing Specimen 4 without T connection (July 19 9:00 am – 1:00 pm)**

Present:

UF Team:

- Oscar Lafontaine

Advisory Group via Zoom:

- Matt Dobson

Testing Outcome:

- Pressure Equalization testing was overall successful



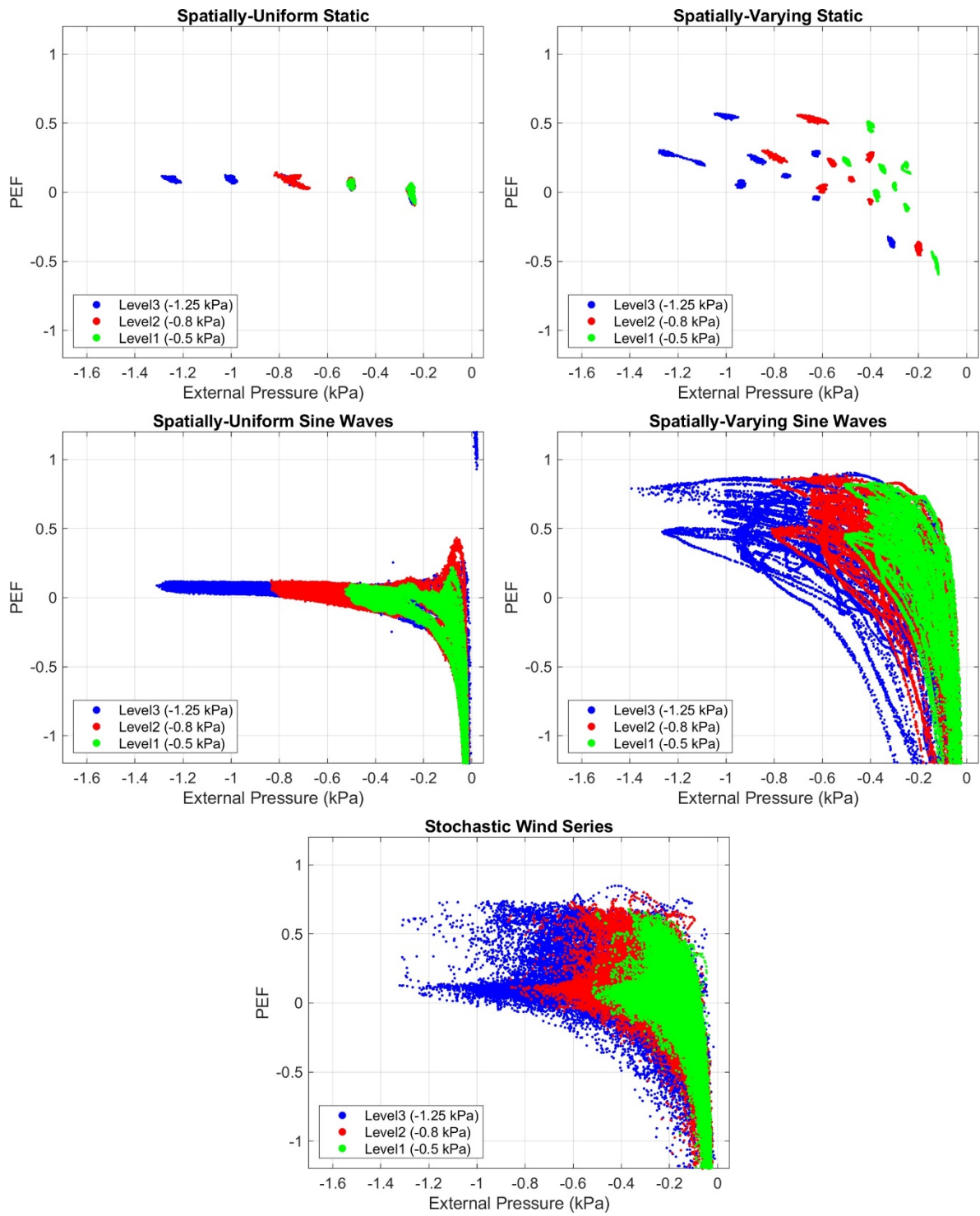


Figure 46. Static, dynamic, and stochastic test results for Specimen 4 without T.

## Specimen 4T- Partially Roll-over Nail Hem

Testing Specimen 4 with T connection (July 20 9:00 am – 12:00 pm)

Present:

UF Team:

- Oscar Lafontaine
- Xinyang Wu
- Dmtrii Golovichev

Testing Outcome:

- Chamber 2 showed brief challenges meeting the target pressure during the spatially varying sine waves while the T connection was installed
- No failure of the vinyl siding panels was observed during PEF testing
- Pressure Equalization testing was overall successful

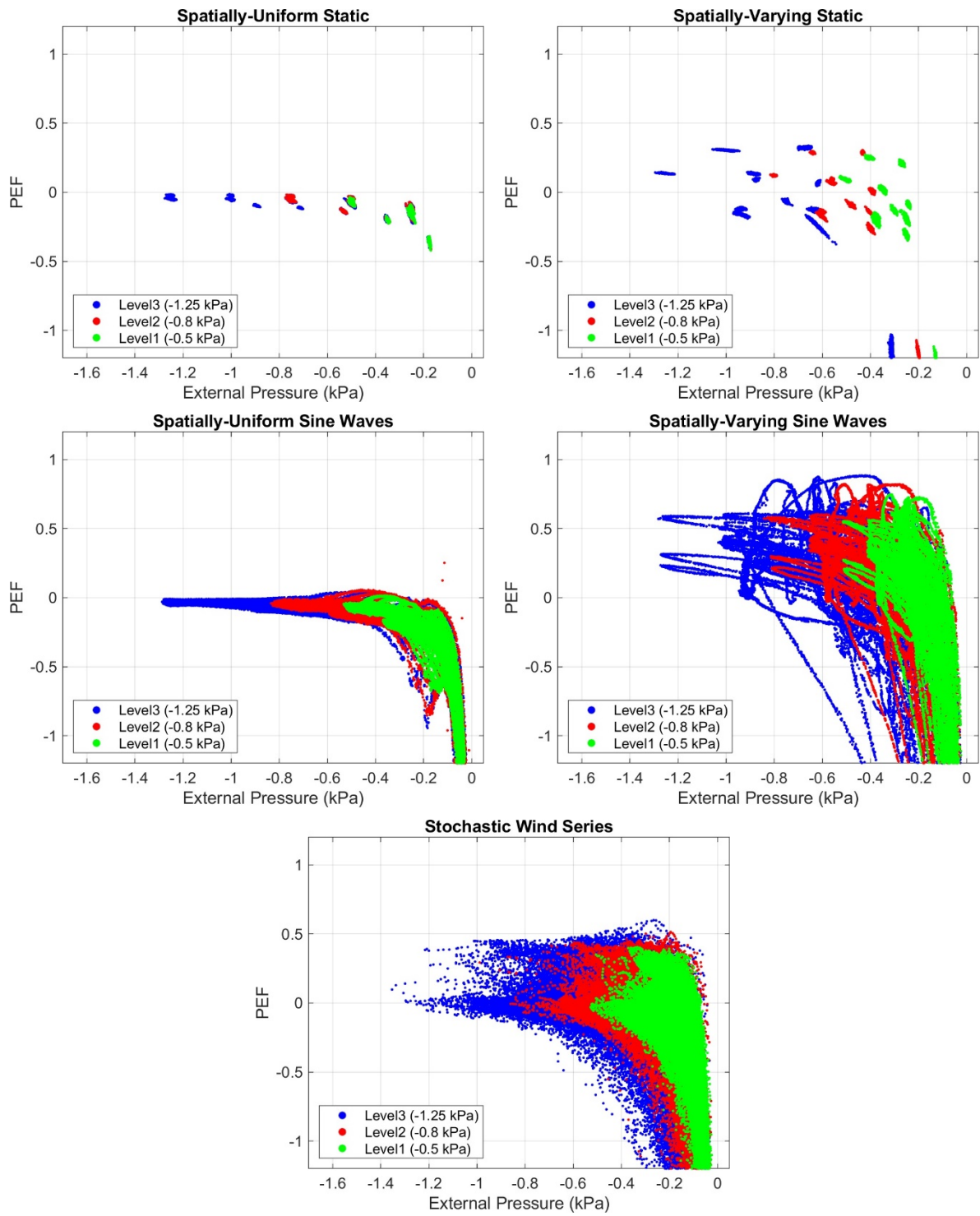


Figure 47. Static, dynamic, and stochastic test results for Specimen 4 with T.

## **Specimen 5- Full Roll-over Nail Hem**

**Testing Specimen 5 without T connection (July 21 5:30 pm – 9:30 pm)**

Present:

UF Team:

- Oscar Lafontaine

Advisory Group via Zoom:

- Matt Dobson
- Fernando Pages

Testing Outcome:

- No failure of the vinyl siding panels was observed during PEF testing
- Pressure Equalization testing was overall successful

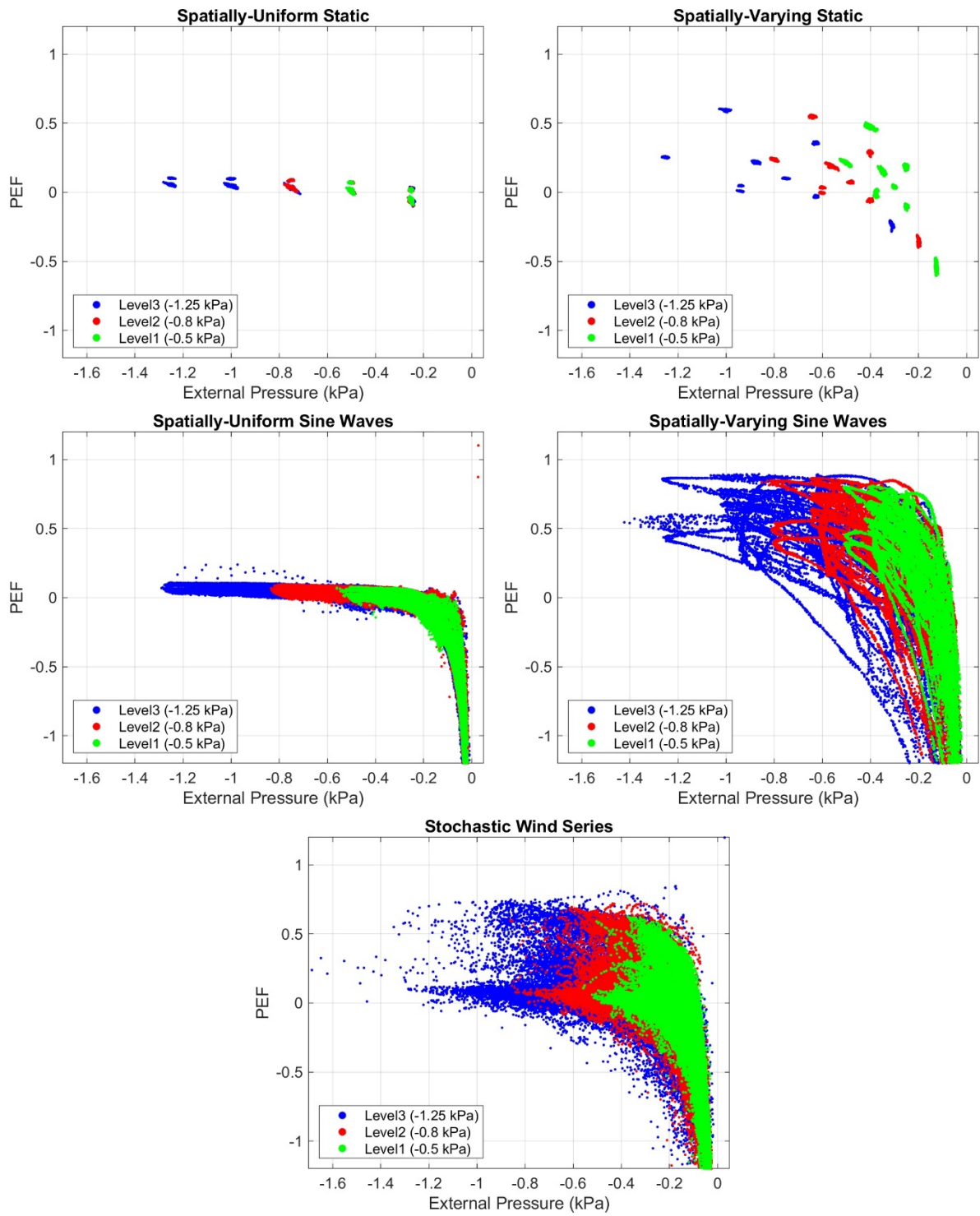


Figure 48. Static, dynamic, and stochastic test results for Specimen 5 without T.

## Specimen 5T-Full Roll-over Nail Hem

Testing Specimen 5 with T connection (July 22 10:00 am – 1:00 pm)

Present:

UF Team:

- Oscar Lafontaine
- Xinyang Wu
- Dmtrii Golovichev

Advisory Group via Zoom:

- Matt Dobson
- Fernando Pages
- Mo Madani

Testing Outcome:

- Chamber 2 showed some challenges meeting the target pressure during the spatially varying sine waves while the T connection was installed
- No failure of the vinyl siding panels was observed during PEF testing
- Pressure Equalization testing was overall successful

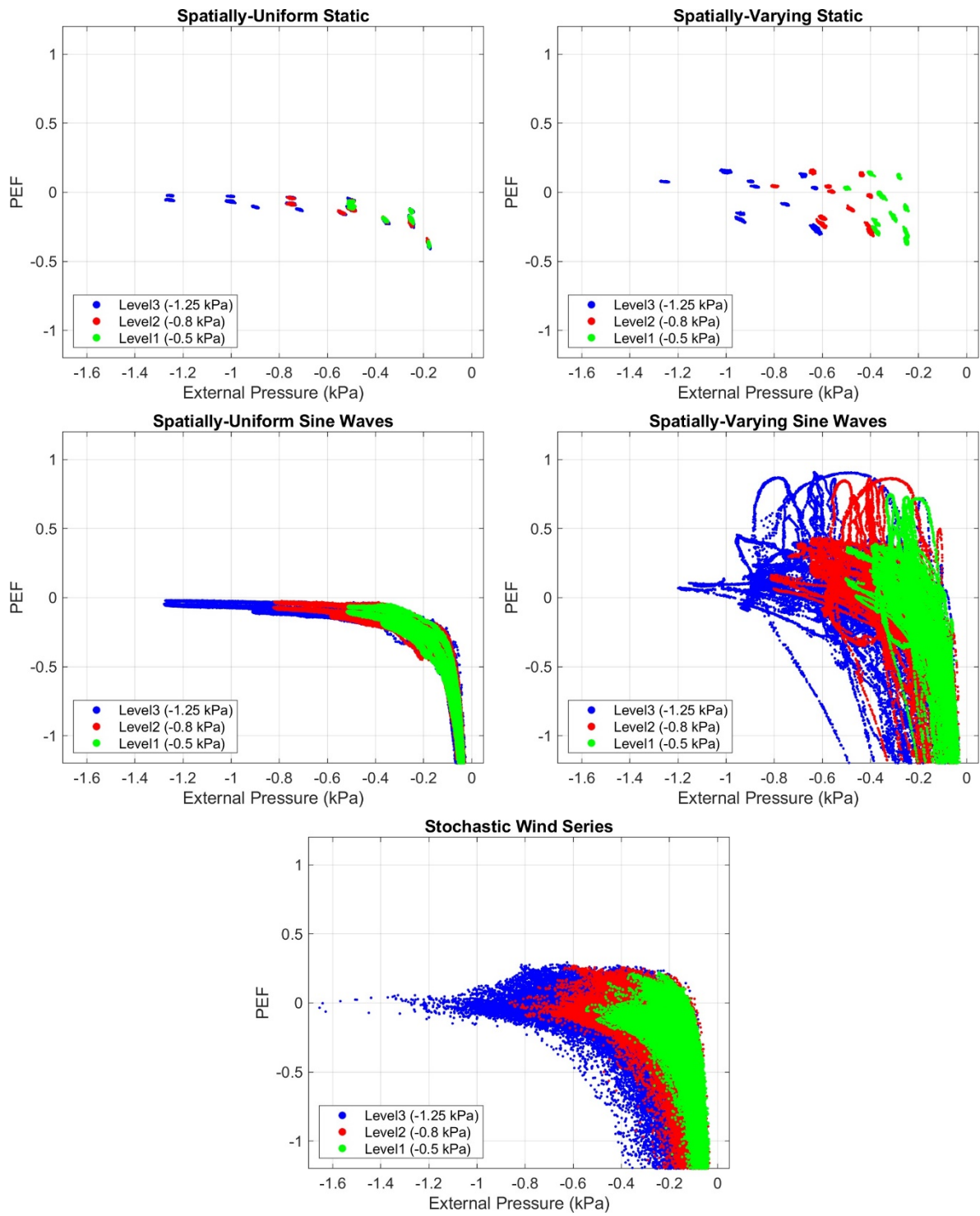


Figure 49. Static, dynamic, and stochastic test results for Specimen 5 with T.

## Appendix B. ASTM D5206 Failure Locations per Specimen

Partial Roll Over Nail Hem Specimen

|  |  |      |       |       |       |       |       |       |
|--|--|------|-------|-------|-------|-------|-------|-------|
|  |  |      |       |       |       |       |       |       |
|  |  | SF-1 | SF-2  | SF-2  | SF-3  | SF-21 | NF-3  | SF-22 |
|  |  |      | SF-4  | SF-5  |       | NF-4  | SF-23 | NF-5  |
|  |  |      |       | SF-6  | SF-7  | NF-6  | NF-7  | SF-24 |
|  |  |      | SF-8  | SF-9  | SF-10 | NF-8  | SF-25 | SF-26 |
|  |  |      | SF-11 | NF-1  | SF-12 | SF-27 | SF-28 | SF-29 |
|  |  |      | SF-13 | NF-2  | SF-14 | NF-9  | SF-30 | SF-31 |
|  |  |      |       | SF-15 | SF-16 | NF-10 | SF-32 | SF-33 |
|  |  |      |       | SF-17 | SF-18 | SF-34 | SF-35 | SF-36 |
|  |  |      |       | SF-19 | SF-20 | SF-37 | SF-38 | SF-39 |
|  |  |      |       |       |       |       |       |       |

Figure 50. Vinyl Siding panel failures in specimen 4 during ASTM D5206. Pressure chambers are indicated by the red boxes, labeled from left to right as Chamber 1, 2, 3, and 4.



Full Roll Over Nail Hem Specimen

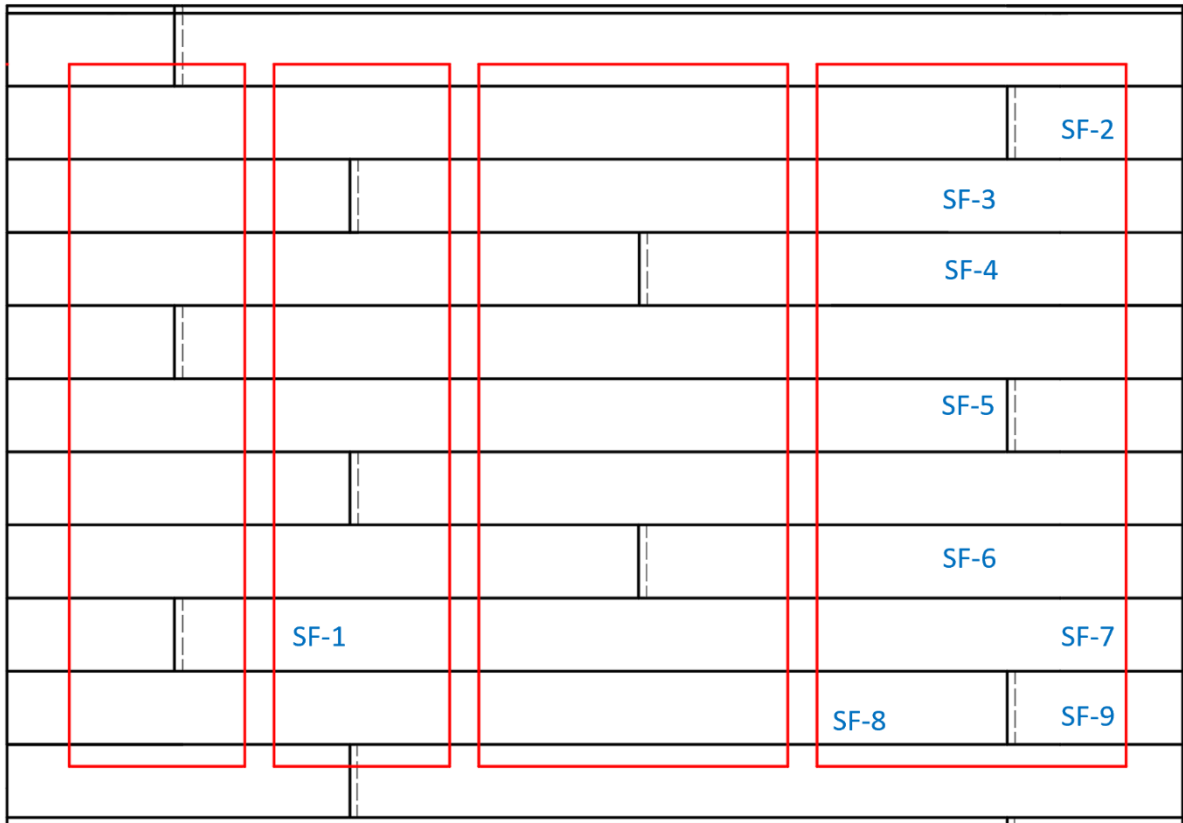


Figure 51. Vinyl Siding panel failures in specimen 5 during ASTM D5206. Pressure chambers are indicated by the red boxes, labeled from left to right as Chamber 1, 2, 3, and 4.



Figure 52. Exploration of failures in vinyl siding panels after ASTM 5206 testing of specimen 4.

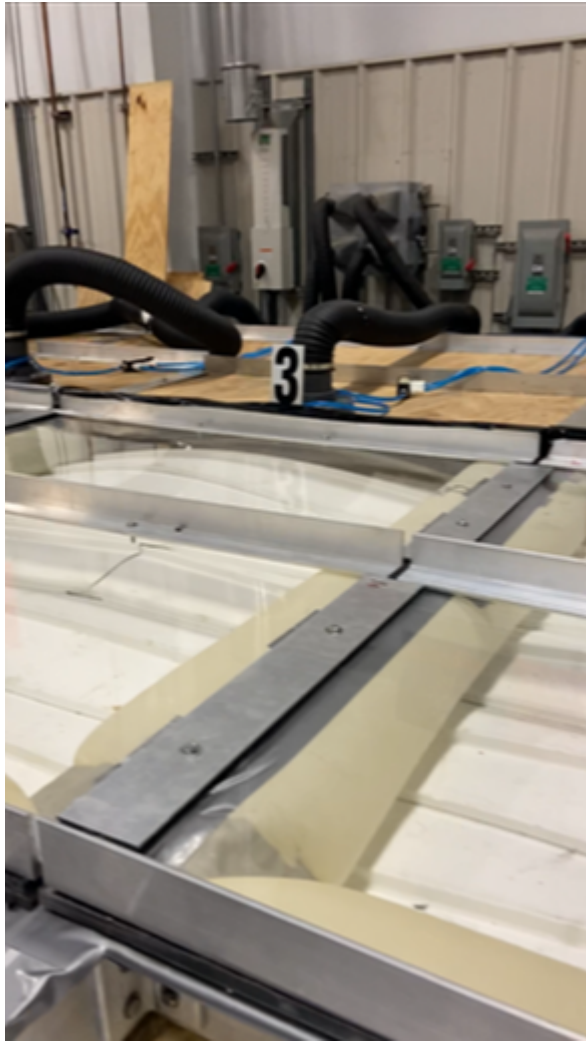


Figure 53. Observed vinyl siding panel deflections during ASTM D5206 testing (Chamber 3)

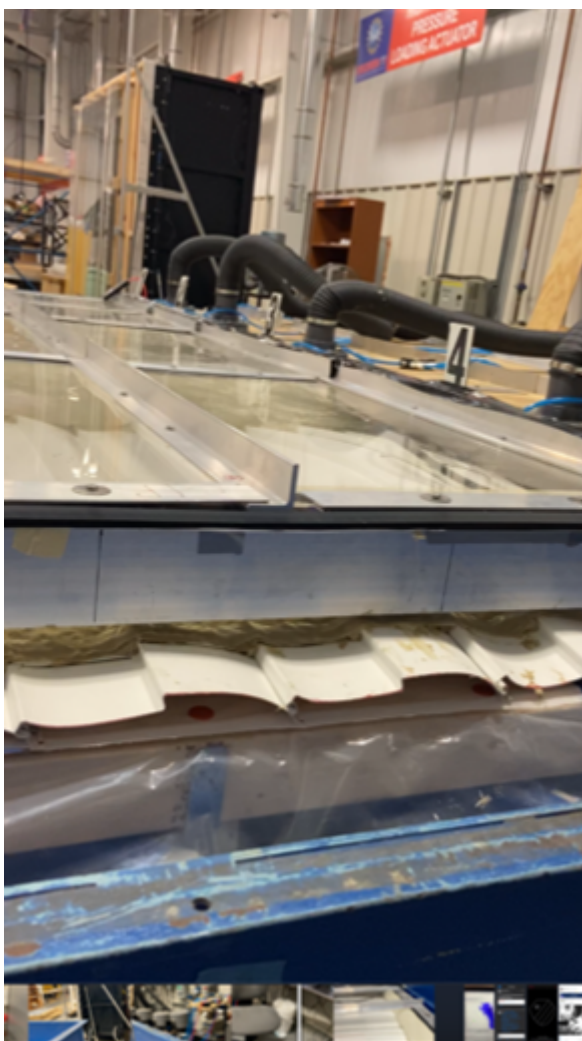


Figure 54. Observed vinyl siding panel deflections during ASTM D5206 testing (Chamber 4)

## Appendix C. Memorandum of First Meeting

**From:** David O. Prevatt, Xinyang Wu  
**To:** Advisory Group Members  
**Date:** 8 February 2020  
**Project:** PHASE II: Experimental Evaluation of Pressure Equalization Factors and Wind Resistance of Vinyl Siding Systems Using a Multi-Chamber Pressure Test Bed  
**Subject:** Notes of Advisory Group Meeting Held on 6 February 2020  
**Attendees:** University of Florida: David O Prevatt (DOP), Oscar La Fontaine (OL), Xinyang Wu (XW); Auburn University: David B Roueche (DBR); Vinyl Siding Institute: Matt Dobson (MD), Stan Hathorn (ST), Sara Krompholz (SK), Neil Sexton (NS); IBHS: Eric Stafford (ES); Western University: Greg Kopp (GK); **ABSENT:** Zach Priest (ZP) PRI

This provides notes of the above meeting. First meeting introducing the project goals, deliverables, review of progress with experimental setup. David O. Prevatt (DOP), David Roueche (DBR) and Oscar Lafontaine (OL) presented slides ([click here for view](#)).

1. Background updates of Phase I of project presented by DOP. DBR presented summary data and case study of previous studies of post Hurricane Irma and Hurricane Michael. Part of broader assessment, using cluster sampling techniques looking broadly at all cladding system types. Relatively high number of vinyl siding failures
  - a. From building damage survey, 87 structures with vinyl siding cladding identified and damage ratios established.
  - b. The complete dataset of 1,200 houses in Hurricane Irma, and 740 in Hurricane Michael. Reports available in Documents folder.
  - c. MD: Suggest the Research Team explains total dataset numbers in their future reports (e.g. total number of houses, number of cladding types, explain damage ratio details etc.)
  - d. DBR showed possible hypothesis of failures on found homes with vinyl siding cladding failure on building surfaces close to adjacent houses (i.e. wind speed up? Venturi effects?)
  - e. GK points out observation of loose house wrap (Tyvek, underlayment) behind siding. Can this change allow interior pressure into gap and the pressure equalization effects assumed?
  - f. MD mentions pattern of vinyl siding failure along soffit line. Information on fasteners are crucial to performance. Fastener length, spacing, fasteners missing. thinks the vinyl siding fasteners information is crucial, like length of fastener and quantity of fastener missing and penetration of fastener 1-1/4 in (min). Basically, some of the encountered failures may be due to installation issues instead of the actual vinyl siding capacity failure.
2. SH: In the slides 15, the Industry-accepted term is nail hem (both single and double nail hem possible)
3. GK: UWO chamber for the(Miller et al. 2017) study used hard exterior sides of pressure chambers (poly-sheet?), and flexible latex material used only for interior walls separating adjacent chambers. Vinyl siding completely enclosed (and not attached to exterior chamber walls.
  - a. DOP: current test setup has vinyl siding sample (and wood wall) extending beyond the exterior chamber walls. UF's specimen then sealed using latex material to top side of vinyl.

4. DBR presented a protested text matrix (see ppt) including 2 repeats. Include ASTM D5206 and Pressure Equalization factors (PEF) test measurement on standard and high-wind vinyl siding systems.
  - a. intermediate testing, developing pressure time histories from the Tokyo Polytechnic University (TPU) wind tunnel pressure database to represent Hurricane Michael orientation of wind direction, on side wall, leeward wall, cornering wind angles leeward wall (45 degree). he proposed two questions:
    - i. Focus: what ultimately is an approach to considers spatial pressure variation, achievable in most standard test laboratories?
    - ii. Can the test rig simulate pressures at failure or observed strengths from Hurricane Michael?
5. GK: For a leaky system requires considerable fan power to achieve failure. UWO experiments utilized up to 3 PLAs on a single pressure box to achieve air flow required at high pressures.
6. Discussion on various available grades of vinyl siding systems in use in Florida and elsewhere.
  - a. Is there a difference between high wind versus builder grade?
  - b. Is 0.04 in thickness a common lower wind grade?
  - c. 0.05 in most strong product but hard to find
  - d. 0.046 in is a solid product available widely, are these both double hems and single hems?
  - e. What is the curl hem vinyl siding?
7. SH: Few single nail hem products meet current Florida FBC requirements. Curl hem and double hem vinyl siding is designed for high-wind rated. Note: current code includes product design requirements using PEFs of 0.5. Previously a PEF of 0.36 was used.
8. ES: According to FEMA/MAT team report for Hurricane Michael, most of vinyl siding installed in Florida were single nail hem, he didn't see any double hem vinyl-siding products.
9. UF will inform Advisory Group prior to testing dates in case others wish to witness tests in person.
10. UF to discuss with SH and MD on particular vinyl siding systems they used previously in IBHS tests as well as at University of Western Ontario and coordinate systems where possible.

## Appendix D. Memorandum of Second Meeting

**From:** Oscar Lafontaine  
**To:** Advisory Group Members  
**Date:** 26 March 2020  
**Project:** PHASE II: Experimental Evaluation of Pressure Equalization Factors and Wind Resistance of Vinyl Siding Systems Using a Multi-Chamber Pressure Test Bed  
**Subject:** Notes of Advisory Group Meeting Held on 24 March 2020  
**Attendees:** University of Florida: David O Prevatt (DOP), Oscar La Fontaine (OL), Xinyang Wu (XW); Auburn University: David B Roueche (DBR); Vinyl Siding Institute: Matt Dobson (MD), Stan Hathorn (ST), Sara Krompholz (SK), Neil Sexton (NS); IBHS: Eric Stafford (ES); Anne Cope (AC) Western University: Greg Kopp (GK); **ABSENT:** Zach Priest (ZP) PRI

This document provides brief notes of the above meeting. David O. Prevatt (DOP), David Roueche (DBR) and Oscar Lafontaine (OL) presented slides ([click here for view](#)) of the experimental work presented in the interim report including preliminary measurements

11. DOP presented a summary of the research focus, rationale for this experimental work, and how the Covid-19 situation could possibly affect our efforts.
12. DOP summarized the key points addressed during the first meeting:
  - a. Meeting held in February 6, 2020
  - b. 10 attendees
  - c. Received feedback on experiment test setup, test matrix, etc.
13. DOP presented and explained the basic functions of the pressure loading actuators (PLAs) and how they are connected to the test bed to each pressure chamber.
14. OLB explained the latex procedure to seal the pressure chamber without restricting the vinyl siding panels deflections.
15. DOP proceeded to provide more insight about the test setup including:
  - a. Chamber size
  - b. Differential pressure transducers
  - c. Specimen construction
16. DOP presented a preliminary data acquisition LabView software used to acquire preliminary measurements.
  - a. The software allowed the manipulation of pressures within each chamber by manual control of the:
    - i. Variable frequency drive voltage (VFD)
    - ii. PLA valve control
  - b. Signal of pressure readings from the pressure transducers are obtained via LabView for:
    - i. Chamber pressures
    - ii. Cavity pressures
17. DOP highlighted where the relevant literature review documents are accessible to the Advisory Group (Task C).
18. DBR presented the approach for preliminary testing performed at UF for gauging the performance characteristics of the test setup.
  - a. Vinyl siding was tested with sealed and unsealed edges.
  - b. Static pressure tests were performed both spatially-uniform and spatially-varying.
  - c. Preliminary measurements of Pressure Equalization Factors (PEFs) were presented.

19. DBR explained the main takeaways from the testing:
  - a. SPLA can generate a range of PEFs on vinyl siding specimens with spatially varying pressures.
  - b. SPLA should be capable of performing destructive tests on vinyl siding panels.
  - c. PEFs are conditioned upon the background leakage to the interior cavity.
20. DBR showed the proposed vinyl siding product types.
  - a. MD and SH provided insight into what specific panels should be ordered and where to buy them.
  - b. There was discussion of how to make sure that the panels installation was not the cause for any observed failures; thus, a Vinyl Siding Institute (VSI) certified installer will be hired to oversee the products installation.
  - c. There was consensus by the Advisory Group and UF Team to not use the products name in any reports or document related to the project.
21. DBR explained the modified test matrix which includes three levels of static uniform, static gradient, dynamic sine waves, dynamic wind traces, and ASTM D5206 up to failure.
22. Matt Dobson expressed he had some concerns about some comments made at the Interim Report which he would share with team.
23. The interim report was accepted.

## Appendix E. Memorandum – Stochastic Wind Traces

**From:** David Roueche, Jinyi Wei (Auburn University)  
**To:** FBC Vinyl Siding Project Team  
**Date:** 25 July 2020  
**Project:** FBC Vinyl Siding Phase II (2019-2020)

**Subject:** Generating Pressure Time Histories from TTU WERFL Building Data

### Introduction

Realistic wind pressure time histories are needed as inputs for the SPLA for initial tuning of the SPLA closed-loop control system and for application to vinyl siding test specimens. The following summarizes the generation of full-scale pressure time histories for four wall pressure zones using full-scale data from the TTU WERFL building.

### Background

The Wind Engineering Research Field Laboratory (WERFL), located at Latitude 33°35'27.23"N and Longitude 101°53'54.39"W, was constructed in Lubbock, Texas on the campus of Texas Tech University in 1989. The facility consists of a 160 ft meteorological tower instrumented at 5 heights and a flat roof test structure with outside dimensions 30'-3" x 45'-3" x 12'-10" high. Omega differential pressure transducers were used to collect differential pressure data at 204 locations on the external surface of the building as well as internal pressures at 2 locations at a sampling frequency of 30 Hz. The exploded view pressure tap layout is shown in Figure 55. Building pressures and anemometric data from the facility are published on DesignSafe and more details can be found in Smith et al. (2018). Two runs, 2071 and 279, are taken out of 16 available runs (each run is 15 minutes long and was taken in nominally neutral conditions, i.e., not a convective storm event). Run 2071 was recorded on 4/16/2003 and had a mean wind speed of 13.4 m/s (30 mph) and longitudinal turbulence intensity of 17% at building roof height with an angle of attack of 355°. Run 279 was recorded on 1/9/2003 and had a mean wind speed of 18.1 mph at roof height, with a longitudinal turbulence intensity at the same height of 17.2% and a wind angle of attack of 10°. In the DesignSafe dataset, pressures are converted to non-dimensional pressure coefficients referenced to the mean building roof height wind speed.

### Analysis

The stochastic wind pressure time histories have the following requirements: 1) represent four adjacent pressure zones; 2) have a time step of 50 ms; 3) contain frequency content no higher than 1 Hz; 4) have a peak pressure equal to predefined pressure levels across all time



histories. To facilitate these requirements, four pressure zones were selected on side walls and leeward walls of the WERFL building for each test run as shown in Figure 55. Pressure taps within each zone were spatially averaged (averaged across each tap at each time step) to create a single time history of pressure coefficients within each zone. A new mean wind velocity was evaluated such that the minimum pressure in any of the four time series is using the following equation:

$$\bar{U}_{reqd} = \sqrt{1.25 \text{ kPa} * (1000) / (0.613 * C_{p_{min}})}$$

The pressure coefficient time histories were then converted to pressures using this required mean wind speed. Because of the scaling laws, the increased wind speed results in a shorter duration pressure time history and increased sampling frequency based on the following relationship:

$$\left(\frac{UT}{L}\right)_1 = \left(\frac{UT}{L}\right)_2$$

As an example, applying the scaling laws with  $U_1 = 13.4 \text{ m/s}$ ,  $T_1 = 15 \text{ min}$ ,  $U_2 = 34 \text{ m/s}$ , and  $L_1 = L_2$  results in  $T_2 = 5.81 \text{ min}$  and a sampling frequency of 77 Hz. In reality, this was an iterative procedure for each pressure level (i.e., Level 1 = -0.5 kPa, Level 2 = -0.8 kPa, Level 3 = -1.25 kPa) to arrive at the wind speed producing the required peak pressure. Ultimately, three minute time series were generated for the side and leeward wall zones for Run 2071, and the side wall zone for Run 279, and a two minute time series was generated for the leeward wall for Run 279, limited due to the scaling laws reducing the duration of the full-scale time series. These data were then resampled to obtain a 50 ms time step (20 Hz sampling frequency), and filtered with a lowpass filter to 1 Hz to produce the final pressure time histories, a sample of which are shown in Figure 56. The pressure time histories were output as tab delimited text files for input into the SPLA Labview software.

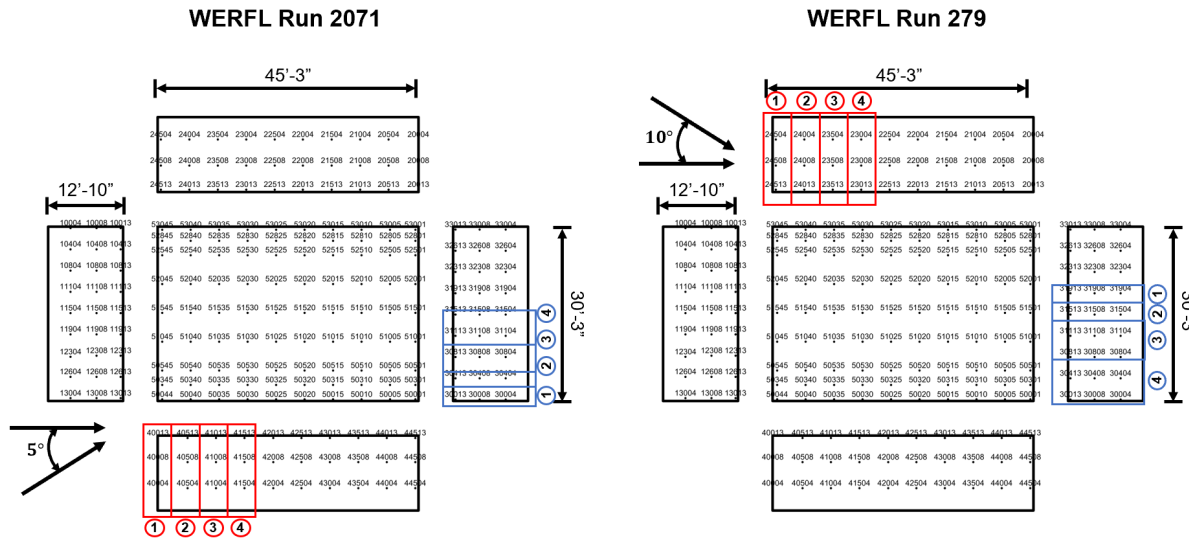


Figure 55. Tap layout and wind angle of attack for the TPU WERFL building, with side wall pressure zones for each test run highlighted.

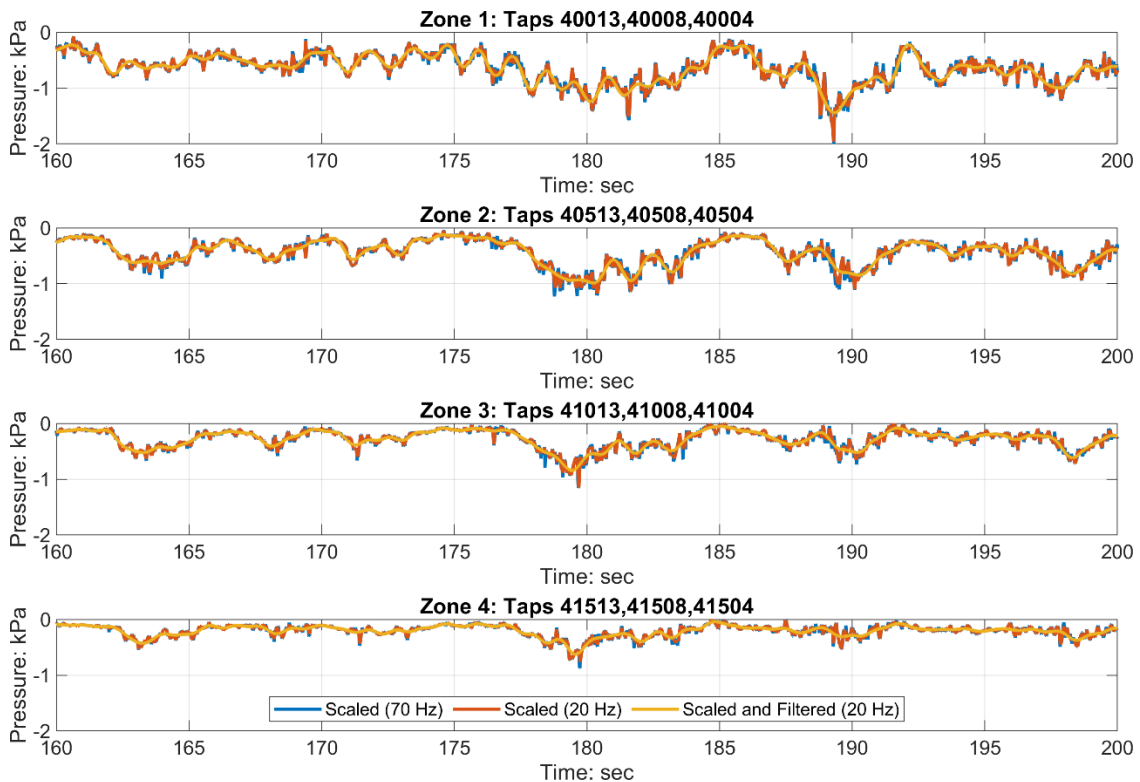


Figure 56. Example time histories for each pressure zone (data taken from Run 2079, side wall case).

## References

Smith, Douglas; Mehta, Kishor; Morse, Stephen, (2018-09-12), "Wind Engineering Research Field Laboratory Selected Data Sets for Comparison to Model-Scale, Full-Scale and Computational Fluid Dynamics Simulations", DesignSafe-CI [publisher], Dataset, doi:10.17603/DS24D68